Torsional Wave Dispersion in a Composite Cylinder with a Functionally Graded Core and an Imperfect Interface

Undergraduate Honors Thesis

Presented in Partial Fulfillment of the Requirements for Graduation with Distinction in the Department of Mechanical Engineering at The Ohio State University

Michael Dean
Spring, 2013

Advisor: Dr. Prasad Mokashi

Abstract

A functionally graded material (FGM) is a kind of composite in which material properties vary continuously as a function of position. FGMs were first proposed in 1984 and have been in use ever since due to advances in manufacturing to suit specific applications in structural mechanics and materials science. The case of a composite cylinder with a radially graded core imperfectly bonded to a homogeneous cladding is the subject of the present work. The goal of this project is to calculate the dispersion relations of this type of composite cylinder subject to guided time-harmonic torsional waves. The methods include determination of proper equation forms for the circumferential displacements in both the core and cladding. Relevant shear stresses are then calculated from these displacements. Boundary conditions are applied so that the stresses in the core and cladding are continuous across the interface. It is also assumed that the outer surface of the cladding is stress free. Imperfect interface conditions are modeled by setting the circumferential displacement jump at the interface radius proportional to the shear stress through a parameter which represents the compliance of the interface. Placing the resulting expressions in matrix form leads to a dimensionless frequency equation that is solved numerically using Maple. Dispersion relations for three cases are plotted in MATLAB and discussed. The effect of interface damage is most easily distinguished in cases of high radial grading of the core, at low wavenumbers with frequencies associated with the third torsional mode.

Acknowledgements

There are many individuals whom I would like to thank for their support and assistance in the completion of this thesis. First, I owe the most sincere gratitude to my advisor, Dr Mokashi, for without your guidance, completion of this project would not have been remotely feasible. Thank you kindly for agreeing to work with me at the beginning of this school year. It has been an exciting whirlwind of a year, and I could not ask for a more fruitful advisor-student relationship than the one that has developed between Dr Mokashi and me. Secondly, I'd like to thank Dr Mendelsohn for agreeing to be on my committee and taking time to help me wrap my brain around the concept of wave dispersion in elastic solids. Thirdly, I appreciate the constructive feedback of Dr Siston in the development of my thesis defense presentation. Outside of school, I would like to express my heartfelt appreciation to my parents, sisters, and Kelsey for your love and support over many years. You've kept me grounded in what is truly important and have never stopped loving me unconditionally; I am forever in your debt. Finally, I send my thanks and praise to God for showering me with the many blessings which I have received throughout my life. I pray that I may always utilize my talents and act in a way that is truly for His greater glory.

Table of Contents

List of Figures

List of Symbols

(r, θ, z) = cylindrical coordinates

t = time

$i = \sqrt{-1}$

a = interface radius/ outer radius of core

b = outer radius of cladding

μ_I = shear modulus of the core

μ_0 = reference shear modulus of the core

μ_{II} = shear modulus of cladding

ρ_I = density of the core

ρ_0 = reference density of the core

ρ_{II} = density of cladding

β = radial grading of the core (/radius)

v = circumferential displacement

τ_{jk} = shear stress on the j plane in the k direction

$R(r)$ = function of r in separation of variables

$Z(z)$ = function of z in separation of variables

ω = dimensional angular frequency

c^2 =phase velocity (μ/ρ)

k = dimensional wavenumber in cylinder

$W(r)$ = modified function of r in Whittaker's Eq.

q_j = relationship of k and ω in core or cladding

κ = transformation parameter in Whittaker's Eq.

γ = transformation parameter in Whittaker's Eq.

ζ = change of variable in Whittaker's Eq.

$M_{\kappa,\gamma}(\zeta)$ = Whittaker function

$M'_{\kappa,\gamma}(\zeta)$ = derivative of Whittaker function with respect to r

${}_1F_1$ = hypergeometric function

D_1 = complex, undetermined coefficient in core stress and displacement equations

D_2 = complex, undetermined coefficient in cladding stress and displacement equations

D_3 = complex, undetermined coefficient in cladding stress and displacement equations

J_n = Bessel function of first kind, order n

Y_n = Bessel function of second kind, order n

I_n = Modified Bessel function of first kind, order n

K_n = Modified Bessel function of second kind, order n

A = dimensional coefficient matrix

η = ratio of cladding to core outer radii (b/a)

λ = ratio of cladding to core shear moduli (μ_{II}/ μ_0)

α = ratio of cladding to core phase velocities (c_2/c_1)

F = scalar interface damage parameter

Ω =dimensionless frequency ($\omega a/c_2$)

ξ = dimensionless wavenumber (ka)

ψ = dimensionless grading of core ($\beta a/2$)

Q_1 = relation of Ω and ξ in the core

Q_2 = relation of Ω and ξ in the cladding

C = relationship between $M'_{\kappa,\gamma}$ and $M_{\kappa,\gamma}$ in simplified, normalized coefficient matrix, $\boldsymbol{A}$

A' = simplified, normalized coefficient matrix

$\boldsymbol{B}$ = det(**A'**). $\boldsymbol{B}$ = 0 is dimensionless frequency equation

CHAPTER 1

Introduction

Since the beginning of recorded history, mankind has constantly sought to improve the materials to which it had access. As civilization developed in ancient Egypt, mud and straw were combined into a composite material in order to make stronger bricks for construction [20]. Thousands of years later in 1984, in response to more demanding aerospace applications a group of Japanese scientists proposed a new type of composite called a functionally graded material (FGM) [12]. FGMs are bi-material composites in which material properties vary as a function of position within the composite [18]. Figure 1.1 illustrates the general idea behind functionally graded materials.

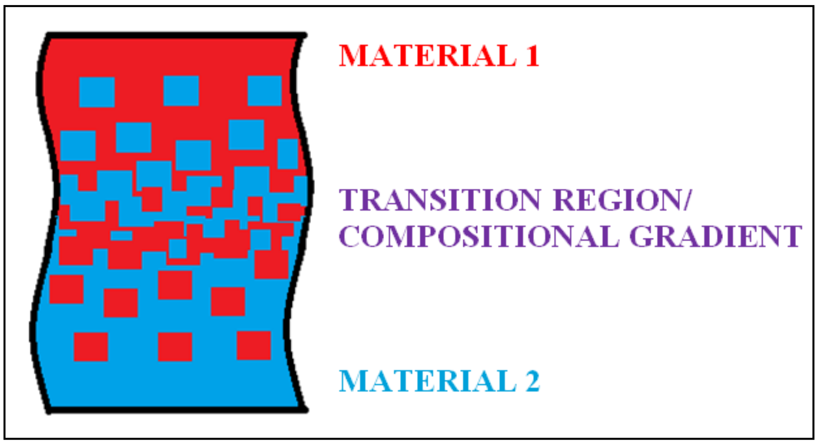

Figure 1.1: General illustration of a functionally graded material

As shown in the figure, an FGM consists of two materials in their unaltered forms at opposite ends of the composite. A continuous transition between the two materials occurs within a region termed the “compositional gradient” [16]. Due to advances in manufacturing, functionally graded materials – the compositional gradient in particular – can be engineered for specific applications in structural mechanics and materials science, the most demanding of which involve service conditions where different surfaces of a material are exposed to dissimilar environments [12]. Functionally graded materials have been proven as suitable alternatives in such applications and are experiencing more wide-spread use as a result.

FGMs improve on two types of existing composites, homogeneous mixtures and laminated composites, in several ways. Traditional composites, illustrated in Figure 1.2 (a), combine two materials as a homogeneous mixture. This has been found to produce an undesirable tradeoff between the desirable properties of both materials [16]. Alternatively, laminated composites, shown in Figure 1.2 (b), stack the different materials in layers. This stacking approach reduces the negative tradeoff between desired material properties found in homogeneous materials since, in laminated composites, the original materials remain unaltered. However, laminated composites contain abrupt transitions in composition, which have been found to result in dangerously large stress concentrations [12]. Meanwhile, in functionally graded materials, the compositional gradient provides a continuous, gradual transition between materials within the composite, allowing for the desirable properties of each component to be utilized to the greatest possible extent [16] while also reducing stress concentrations [12].

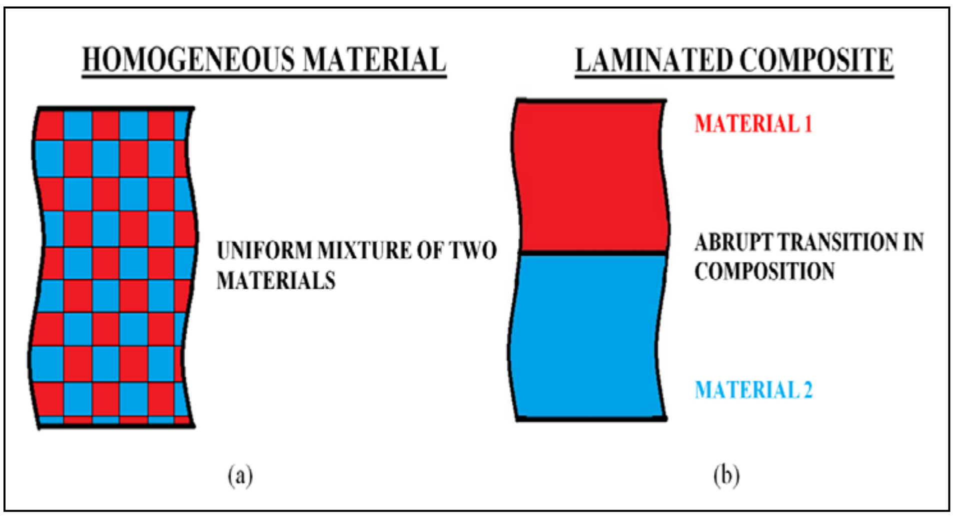

Figure 1.2: General illustrations of other types of composites upon which FGMs improve

Many potential applications exist for functionally graded materials. Towards the beginning of their inception, FGMs consisted mainly of a metal and a ceramic. This combination of materials provides high strength at high temperatures. Previously, these two material properties were considered nearly mutually exclusive. High temperature applications require the use of heat resistant materials like ceramics since they maintain their properties at high temperatures. However, one of the largest drawbacks to using traditional ceramics is that the strength of most ceramics is relatively low, especially compared to the strength of metals. On the other hand, although metals are much stronger than ceramics, metals are adversely affected by high temperatures and can become dangerously ductile. In aerospace applications, this could result in catastrophic failure of the structure subjected to high temperatures. Therefore, high strength materials at high temperatures can be accomplished by combining a ceramic with a metal as a functionally graded material. Doing so allows for the material properties to smoothly transition from the high temperature resistance of the ceramic to the high strength of the metal.

This type of functionally graded material is utilized heavily in the aerospace industry with the ceramic as the outer surface of the aircraft and the metal as the inner surface to provide strength to the structure of the aircraft. As an aircraft travels through the atmosphere at high speeds, it is subjected to extremely high temperatures. Most are familiar with the image of a high temperature “cone” forming around the tip of the spacecraft as it re-enters the atmosphere. With the introduction of FGMs, these spacecraft have become stronger and safer for astronauts in flight.

Many other possible applications of FGMs exist outside of the aerospace industry. For example, functionally graded materials have been increasingly used to manufacture cutting tools with excellent toughness, precision, and life [15]. Additionally, FGMs have been proposed for use as improved bandpass filters and piezoelectric actuators, showing the great potential of FGMs in a wide range of fields [15]. One other potential FGM application of interest and at the heart of this thesis is the use of a functionally graded material as the inner core of a reinforced coaxial cable. Figure 1.3 illustrates this concept.

A coaxial cable can be modeled as an infinitely long composite cylinder. The core, represented on the figure by the colored region, is graded radially. The outer region of the composite cylinder, colored in gray, is termed the “cladding.” The cladding is assumed to be a homogeneous, isotropic material with constant material properties. The functionally graded core and the homogeneous, isotropic cladding are bonded together at their interface by an adhesive. In the case of a “perfect” interface, stresses and displacements are constant and equal across the interface between the core and cladding. Over time, this interface will incur damage and become “imperfect”. As the interface becomes imperfect,

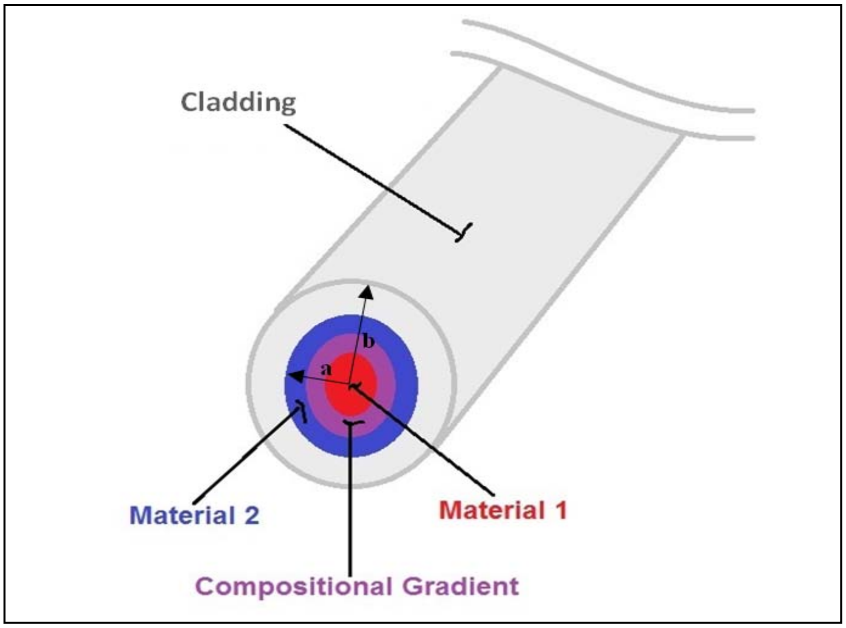

Figure 1.3: Three-dimensional representation of composite cylinder with radially graded core

the adhesive joining the core and cladding is weakened, and there is a slip between the displacements of the core and cladding. The stresses remain continuous and equal across the interface. This type of interface model, called a "flexibly bonded interface," was previously studied in depth by Jones and Whittier [4] [5]. In this thesis, the interface imperfection is modeled by a dimensionless scalar, F, in the fashion of Berger et al [13]. When $F = 0$, the interface is considered perfect. As $F \rightarrow \infty$, the interface is considered completely imperfect, and the bond between the core and cladding is broken. In this case, core and cladding rotate independently of one another.

Wave propagation through different types of elastic media is an important consideration in the field of non-destructive evaluation (NDE). Determining the dispersion relations for the composite cylinder in Figure 1.3 is the subject of this work. Dispersion relations give the relationship between wavenumber and frequency. The wavenumber is mathematically equal to the reciprocal of the wavelength. Wavelength is equal to the distance between individual peak amplitudes within a wave. Therefore, the wavenumber represents the number of peaks in a given wave over a certain *distance*. For this reason, the wavenumber is sometimes referred to as a wave's "spatial frequency," or how frequently a peak in the wave exists in a certain amount of space. Meanwhile, the frequency of the wave equals the number of peak amplitudes in a wave that occur over a period of *time*. For a given wavenumber, there exist specific frequencies that propagate throughout the medium as resonant frequencies. Each of these frequencies at which resonance occurs is called a “wave mode.” The lowest frequency is called the “first mode,” the next highest frequency is the “second mode,” and so on. The purpose of a dispersion relation is to graphically represent a certain mode, for example the second mode, for each wavenumber over a specific range of frequencies.

Dispersion relations of guided torsional waves travelling through a composite cylinder with a perfect interface in which the core and cladding are both homogeneous and isotropic have been studied by Armenàkas [3]. Berger et al [13] and Bhattacharya [8] expanded this work to the case of an imperfect interface. Lai et al [6] further investigated torsional, flexural, longitudinal, and other types of waves in a composite cylinder. Thurston [9] also extensively studied elastic waves in composite rods, which he termed as “clad rods,” focusing much attention on the case of an infinitely thick cladding. More recently, Honarvar et al [18] studied guided ultrasonic waves in a composite cylinder. The focus here is restricted to the case of guided torsional waves since the equation of motion involves only one displacement component and can be solved directly.

The classical torsional wave problem in a homogeneous, isotropic cylinder has been investigated by Kolsky [2], Graff [10], and Achenbach [11]. Torsional waves in functionally graded finite cylinders were studied by Singh et al [18]; their solution utilized Whittaker’s equation, which is a modified form of the hypergeometric equation. Han et al [14] investigated transient waves in a functionally graded cylinder through a hybrid numerical approach. In this approach, the grading of the cylinder was not a continuous function but rather represented by a series of N ring nodes. On the other hand, Elmaimouni et al [17] utilized Legendre polynomials to expand the mechanical components of displacement in calculating guided wave propagation in functionally graded cylinders.

Once dispersion relations are calculated for a specific type of medium, these findings can be used to develop an electronic device that can quickly and effectively test for damage in the structure. These nondestructive material characterization tools are extremely valuable and used in real world applications every day. In the case with which this thesis is concerned, a nondestructive material characterization tool could be used to detect if any damage exists at the interface between the inner and outer sections of a coaxial cable. Such cables could be used as reinforcing, wires or even as electronic lines across which information is transported. Once the dispersion relations are obtained for varying levels of interface imperfection, wavenumbers at which the corresponding frequency changes significantly for increasing damage can be identified. Torsional pulses at these identified wavenumbers would be input into the system at different frequencies. When the frequency becomes equal to a torsional mode, resonance will occur. These detected modes could be cross-referenced to the modes for a brand-new cable with a nearly perfect interface. If there is significant deviation from the modes of the nearly undamaged case, then it could be concluded that interface damage had in fact occurred. If the detected mode was not significantly different from the mode associated with the nearly perfect case, then it could be concluded quickly and cost-effectively that there was no interface damage in the cable.

1.1) Focus of Thesis

The focus of this thesis is to determine the dispersion relations for guided torsional waves in an infinite composite cylinder with a radially graded core and an imperfect interface. The effect of increased radial grading and interface damage is investigated for a limited number of cases. It is assumed that the material properties of the core decay exponentially and continuously in the radial direction until the interface with the cladding. The cladding is assumed to be a homogeneous, isotropic elastic cylinder with constant material properties.

Much focus is given to the methods utilized in determining the displacement equation of the functionally graded core and the frequency equation. The solution for the displacement of the functionally graded core generally follows Singh et al [18]; it is solved through separation of variables and Whittaker's equation. However, slight modifications are made to the solution method and are discussed in Chapter 2. The main purpose of these modifications was to ensure that the units of the displacement and stress equations for the core matched the respective units of the cladding's displacement and stress equations. The solution for the displacement of the cladding of Berger et al [13] is used; this solution is found through Bessel's equation of order zero. The necessary components of stress are determined from the displacement solutions. With the displacement and stress solutions found, three boundary conditions are applied.

For convenience, the outer, curved surface of the cladding is assumed to be stress free. At the interface, the stress in the core and the stress in the cladding are assumed equal. The effect of interface imperfection is present in the displacement interface condition. The difference between displacement of the core and the displacement of the cladding at the interface is directly related to the dimensionless damage scalar F. As F increases, the jump between the two displacements increases.

The three equations that result from these boundary conditions are arranged in matrix form. The determinant of the coefficient matrix is set equal to zero and simplified – this is the frequency equation for the cylinder. Maple is used to solve for the frequency equation in order to obtain the dispersion relations for various levels of grading, interface imperfection, and other parameter ratios such as the ratio of the cladding and core radii. MATLAB is used to plot the dispersion relations which are then presented and discussed in detail.

1.2) Significance of Research

This work contributes to the expansion of the general knowledge base of applied mechanics. Previously, only composite cylinders with imperfect interfaces in which the core and cladding were homogeneous, isotropic materials have been studied. The methods and results of this thesis introduce a functionally graded material into these types of composite cylinders. The calculated dispersion relations may spark further inquiry into this type of scenario. Secondly, the solution approach for the displacement of the functionally graded core is novel since it utilizes Whittaker's equation to solve the equation of motion. Prior research solved the equation of motion using Bessel's equation. This thesis allows for the two solution approaches to be compared, especially if zero grading of the core is assumed, which essentially translates to the core being a homogeneous material. Finally, this research is significant in the fact that it could contribute to the development of a nondestructive material characterization tool meant to test for interface damage in a composite cylinder.

1.3) Overview of Thesis

This thesis consists of four chapters. This first chapter presents the background on functionally graded materials, dispersion relations, and previous research. Chapter 2 provides the mathematical methods utilized in deriving the frequency equation used in calculating the dispersion relations for the composite cylinder. In Chapter 3, the dispersion relations for three main cases are provided and discussed. On each dispersion relation, four damage cases are included. The effects of varying radial grading, interface damage, and core to cladding radius ratio are detailed. Potential application of these findings in the development of a nondestructive material characterization tool is provided as well. Chapter 4 presents the conclusions, contributions of this work, additional applications, a discussion of future work, and a global summary.

Chapter 2

Problem Formulation and Solution Technique

2.1) Problem Statement

Let (r, θ, z) be cylindrical polar coordinates. Consider the infinitely long composite cylinder shown in Figure 2.1. The core, $0 \le r \le a$, is exponentially graded in the radial direction; its radially dependent shear modulus and density are of the form

$$\mu = \mu_I(r) = \mu_0 \exp(-\beta r) \tag{2.1 a}$$

$$\rho = \rho_I(r) = \rho_0 \exp(-\beta r) \tag{2.1 b}$$

where μ_0 is the reference shear modulus, ρ_0 is the reference density, and β is the radial grading parameter. Note that μ_0, ρ_0, and β are all constants. Both shear modulus and density are taken to decay along the radius of the core simply for mathematical convenience.

The cladding, $a \le r \le b$, is an elastic, homogeneous, isotropic material ,whose material properties are constant

$$\mu = \mu_{II} = const \tag{2.2 a}$$

$$\rho = \rho_{II} = const. \tag{2.2 b}$$

Time-harmonic torsional waves travel through the composite cylinder in Figure 2.1 in the z direction. The curved surface of the cladding, $r = b$, is taken to be stress free. The interface between the core and cladding at $r = a$ is assumed thin, and various levels of interface imperfection are considered. This interface is best thought of as an adhesive bond which holds together the core and cladding. There are multiple ways to model interface imperfection mathematically. The model of Berger et al [13] is used to model interface damage. Tractions are taken to be continuous across the interface, and there is a jump in displacement between the core and cladding. These interface conditions are presented in greater detail in Section 2.3.

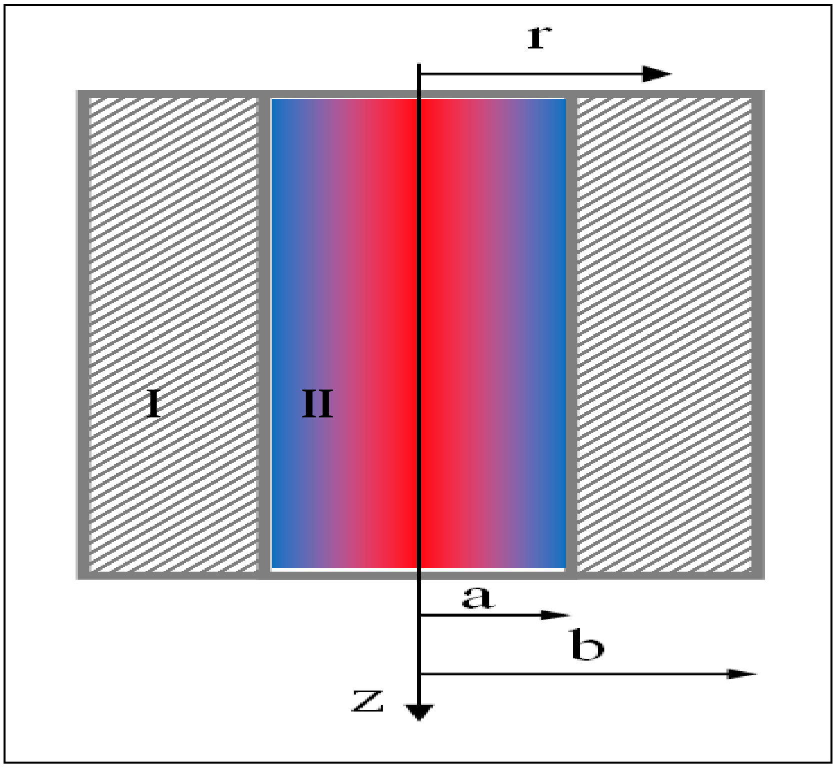

Figure 2.1: Two-dimensional schematic of the infinite composite cylinder under consideration. Colored core is functionally graded material. Gray, hatched area represents homogeneous, isotropic cladding.

In the case of torsion and using cylindrical polar coordinates (r,θ,z), the displacements in the r and z direction are zero and the only non-zero component of displacement is the circumferential, or θ direction, displacement, *v*, which depends only on r, z and t:

$$u = w = 0 \qquad ; \qquad v = v\left(r, z, t\right). \tag{2.3}$$

Shear stresses are written in terms of displacement. The only two non-trivial components of stress are

$$\tau_{r\theta_j} = \mu_j \left(v_{,r_j} - \frac{v_j}{r} \right) \tag{2.4 a}$$

$$\tau_{\theta z_j} = \mu_j \left(v_{,z_j} \right) \tag{2.4 b}$$

where the notation $v_{,r}$ represents partial differentiation of *v* with respect to *r*, etc.

The first step in solving for the dispersion relations associated with this problem is to derive appropriate equations for *v(r,z,t,)* for both the core and cladding. These displacement equations are then used to obtain the shear stresses in (2.4). Boundary conditions on stresses and displacements are then applied to obtain the frequency equation for the system.

2.2) Solutions for Displacement

Functionally Graded Core

The solution for the displacement of the functionally graded core, $0 \le r \le a$, generally follows Singh et al [18]. For convenience, the subscript *I,* which denotes the functionally graded core, has been dropped from the equations in this section. It is understood that all parameters pertain to the core of the composite cylinder until noted. In the case of torsion, the equation of motion can be written as

$$\tau_{r\theta,r} + \tau_{\theta z,z} + \frac{2}{r}\tau_{r\theta} = \rho v_{,tt}. \tag{2.5}$$

These shear stresses and derivatives can be written in terms of *v(r,z,t)*. Substituting in in (2.4) into (2.5) yields

$$v_{,rr} + \frac{1}{r}v_{,r} - \frac{v}{r^2} + \frac{1}{\mu}\left(\mu_{,r}v_{,r} + \mu_{,z}v_{,z}\right) - \frac{v}{\mu r}\mu_{,r} + v_{,zz} = \frac{\rho}{\mu}v_{,tt}. \tag{2.6}$$

Next, the following substitution is made for *v(r,z,t)*

$$v\left(r,z,t\right) = V\left(r,z,t\right)\sqrt{\frac{\mu_0}{\mu}}. \tag{2.7}$$

This approach slightly deviates from Singh et al by introducing a constant factor of $\sqrt{\mu_0}$. Doing so ensures that the units of the core's displacement remain units of length. Displacement of the cladding as given in Berger et al [13] also has units of length. If this additional factor of $\sqrt{\mu_0}$ is not included in this substitution, the resulting units of v_I contain a factor of $\sqrt{stress}^{-1}$, and the displacement equations for the core and cladding become incompatible. Thus, deviating from the general solution of Singh et al [18] is necessary to keep the units of both displacement equations compatible. As a result, (2.6) becomes

$$V_{,rr}+\frac{1}{r}V_{,r}-\frac{V}{r^2}-\frac{3}{2}\frac{V}{\mu r}\mu_{,r}+\frac{V}{4\mu^2}\left(\mu_{,r}^2+\mu_{,z}^2\right)-\frac{V}{2\mu}\left(\mu_{,rr}+\mu_{,zz}\right)+V_{,zz}=\rho\mu^{-1}V_{,tt}\,. \tag{2.8}$$

Note that since $\sqrt{\mu_0}$ is a constant, it drops out from (2.8), and the general form of Singh et al [18] is maintained. It will again become a factor when reverting back to v*(r,z,t)*. *V(r,z,t)* is assumed to be of the form

$$V(r,z,t)=R(r)Z(z)\exp(-i\omega t) \tag{2.9}$$

where *R* is a function of *r* only, Z is a function of *z* only, and ω is angular frequency. The equation of motion then becomes

$$\frac{1}{R}R_{,rr}+\frac{1}{rR}R_{,r}-\frac{1}{r^2}-\frac{3}{2\mu r}\mu_{,r}+\frac{1}{4\mu^2}\left(\mu_{,r}^2+\mu_{,z}^2\right)-\frac{1}{2\mu}\left(\mu_{,rr}+\mu_{,zz}\right)+\frac{1}{Z}Z_{,zz}+\frac{\rho\omega^2}{\mu}=0\,. \tag{2.10}$$

Substituting (2.2) into (2.10) yields

$$\frac{1}{R}R_{,rr}+\frac{1}{rR}R_{,r}-\frac{1}{r^2}+\frac{3\beta}{2r}-\frac{\beta^2}{4}+\frac{1}{Z}Z_{,zz}+\frac{\omega^2}{c_1^2}=0 \tag{2.11}$$

Where $c_1^2=\mu_0/\rho_0$, which represents the shear wave velocity. Equation 2.11 can be solved by separation of variables. Therefore all *R* and *Z* terms are collected on opposite sides of the equation. Each expression is set equal to the square of the separation constant, *k*

$$\frac{1}{R}R_{,rr}+\frac{1}{rR}R_{,r}-\frac{1}{r^2}+\frac{3\beta}{2r}-\frac{\beta^2}{4}+\frac{\omega^2}{c_1^2}=-\frac{1}{Z}Z_{,zz}=k^2\,. \tag{2.12}$$

The separation constant, *k*, represents the wavenumber in the composite cylinder.

What now remains are two ordinary differential equations, one in terms of only *r* and the other in terms of *z*. First, the solution for *R* is considered. Collecting all terms on the left side of the equation and multiplying both sides by *R* gives

$$R_{,rr} + \frac{1}{r} R_{,r} + R\left[-\frac{1}{r^2} + \frac{3\beta}{2r} - \frac{\beta^2}{4} + \frac{\omega^2}{c_1^2} - k^2 \right] = 0 . \qquad (2.13)$$

In order to eliminate $R_{,r}$ from the equation, the following substitution is made

$$R(r) = W(r)\sqrt{\frac{a}{r}} . \qquad (2.14)$$

This is another deviation from the general solution of Singh et al [18]. Similar to the discussion following (2.7), multiplication by a factor of $\sqrt{a}$ ensures compatibility of the units between the displacement equations for the core and cladding. If $\sqrt{a}$ is not included, the units of the core's displacement contain a factor of $\sqrt{length}^{-1}$. Substituting (2.14) into (2.13) results in

$$W_{,rr} + W\left[\frac{\omega^2}{c_1^2} - \frac{\beta^2}{4} - k^2 + \frac{3\beta}{2r} - \frac{3}{4r^2} \right] = 0 . \qquad (2.15)$$

Equation 2.15 has a form similar to Whittaker's equation given by Abramowitz and Stegun [7]

$$W_{,\zeta\zeta} + W\left[-\frac{1}{4} + \frac{\kappa}{\zeta} + \frac{\frac{1}{4} - \chi^2}{\zeta^2} \right] = 0 . \qquad (2.16)$$

Comparing (2.15) and (2.16), the following relations are made

$$-\frac{q_1^2}{4} = \left(\frac{\omega}{c_1}\right)^2 - \left(\frac{\beta}{2}\right)^2 - k^2 ; \qquad \kappa = \frac{3\beta}{2q_1} ; \qquad \chi = 1 ; \qquad \zeta = rq_1 . \qquad (2.17)$$

q_1 represents the relationship between ω and k in the functionally graded core and is given by

$$q_1^2 = 4\left(k^2 + \left(\frac{\beta}{2}\right)^2 - \left(\frac{\omega}{c_1}\right)^2 \right) \qquad (2.18)$$

to include the grading, β.

As a check of the mathematical methods utilized so far, if the core were a homogeneous cylinder, $\beta = 0$, (2.18) reduces to

$$q_1^2 = 4\left(k^2 - \left(\frac{\omega}{c_1}\right)^2\right) \tag{2.19}$$

which is consistent with the classical definition of q [2, 10, 11]. The solution to (2.16) is given by

$$W(\zeta) = AM_{\kappa,\chi}(\zeta) \tag{2.20}$$

where $M_{\kappa,\gamma}(\zeta)$ represents a Whittaker function, and A is an undetermined coefficient. $M_{\kappa,\gamma}(\zeta)$ can be written in terms of the confluent hypergeometric function ${}_1F_1$ as given by Slater [1]

$$M_{\kappa,\chi}(\zeta) = \xi^{\left(\frac{1}{2}+\chi\right)} e^{\left(-\frac{\zeta}{2}\right)} {}_1F_1\left[\frac{1}{2}+\chi-\kappa;1+2\chi;\zeta\right]. \tag{2.21}$$

Slater [1] further defines the confluent hypergeometric function as an infinite series

$${}_1F_1[a,b,x] = \sum_{n=0}^{\infty}\frac{a_n x^n}{b_n n!}\ ; \qquad a_n = a(a+1)(a+2)\cdots(a+n-1). \tag{2.22}$$

Therefore, the solution of R can be written as

$$R(r) = A\sqrt{\frac{a}{r}}M_{\kappa,\chi}(rq_1). \tag{2.23}$$

The solution of Z is next found. Ascertaining the form for Z is much simpler than the solution for R. Recall from (2.12) that the ordinary differential equation for Z is

$$-\frac{1}{Z}Z_{,zz} = k^2. \tag{2.24}$$

Rearranging (2.24) yields

$$Z_{,zz} + k^2 Z = 0. \tag{2.25}$$

The solution of (2.25) is

$$Z(z) = B\exp(ikz) + C\exp(-ikz) \tag{2.26}$$

where B and C are undetermined, complex coefficients. Here, the solution will deviate from the solution of Singh et al [18]. An infinitely long cylinder is considered here, and there is no wave reflection due to interaction with a finite axial boundary. As such, waves travelling in only one axial direction, the + direction, are considered. Consequently, C is set equal to zero, and the solution for Z becomes

$$Z\left(z\right)=B\exp\left(ikz\right). \tag{2.27}$$

With the solutions of R and Z determined, (2.9) and (2.7) are used to obtain the general form of the solution for the circumferential displacement of the functionally graded core

$$v_I(r,z,t)=D_1 a r^{-1/2} M_{\kappa,\chi}(rq_1)\exp\left(\left(\frac{\beta r}{2}\right)+i\left(kz-\omega t\right)\right). \tag{2.28}$$

where D_I is equal to $A\times B$. Note that the subscript I is re-introduced into the equation. Equation 2.28 is dimensionless. The displacement equation for the homogeneous cladding as given by Berger et al [13] has units of length. So, in order to make the displacement equations for the core and cladding compatible, (2.28) is multiplied by an additional factor of the interface radius, a

$$v_I(r,z,t)=\frac{D_1 a^{3/2}}{\sqrt{r}} M_{\kappa,\chi}(rq_1)\exp\left(\left(\frac{\beta r}{2}\right)+i\left(kz-\omega t\right)\right). \tag{2.29}$$

Using (2.4), the shear stresses associated with the case of torsion are determined from the solutions for the circumferential displacement. Thus, the shear stresses in the functionally graded core are

$$\tau_{r\theta_I}=\frac{D_1\mu_0 a^{3/2}}{\sqrt{r}}\left[q_1 M'_{\kappa,\chi}\left(rq_1\right)+M_{\kappa,\chi}(rq_1)\left(\frac{\beta}{2}-\frac{3}{2r}\right)\right]\exp\left(\left(\frac{-\beta r}{2}\right)+i\left(kz-\omega t\right)\right) \tag{2.30}$$

$$\tau_{\theta z_I}=\frac{ikD_1\mu_0 a^{3/2}}{\sqrt{r}} M_{\kappa,\chi}(rq_1)\exp\left(\left(\frac{-\beta r}{2}\right)+i\left(kz-\omega t\right)\right). \tag{2.31}$$

$M'_{\kappa,\gamma}(rq_1)$ represents partial differentiation with respect to r.

Homogeneous, Isotropic Cladding

The displacement of the cladding, v_{II}, is of the form presented in Berger et al [13]. Bessel's equation of order zero is used to determined v_{II}. The solutions of Bessel's equation depend on the relationship between ω, c_2, and k; there are two possible cases.

In the first case, if $\omega^2 > k^2 c_2^{\,2}$, then

$$Z_n = J_n, \quad W_n = Y_n, \quad \text{and} \quad q_2^2 = (\omega/c_2)^2 - k^2 \tag{2.32}$$

where J_n and Y_n are Bessel functions of the first and second kinds of order n respectively.

In the second case, if $\omega^2 < k^2 c_2^{\,2}$, then

$$Z_n = (-1)^n I_n, \quad W_n = K_n, \quad \text{and} \quad q_2^2 = k^2 - (\omega/c_2)^2 \tag{2.33}$$

where I_n and K_n are modified Bessel functions of the first and second kinds of order n respectively. The factor $(-1)^n$ allows for the unified treatment of all frequencies [13].

With this established, the displacement of the cladding is taken to be

$$v_{II}(r,z,t) = \left(\frac{D_2}{q_2} Z_1(q_2 r) + q_2 b^2 D_3 W_1(q_2 r) \right) \exp\left(i\left(kz - \omega t\right)\right) \tag{2.34}$$

where D_2 and D_3 are dimensionless, undetermined coefficients, and b is the outer radius of the cladding. The shear stresses are found by substituting (2.33) into (2.4)

$$\tau_{r\theta_{II}} = -\mu_{II} \left(D_2 Z_2(q_2 r) + (q_2 b)^2 D_3 W_2(q_2 r) \right) \exp\left(i\left(kz - \omega t\right)\right) \tag{2.35}$$

$$\tau_{\theta z_{II}} = i\mu_{II} k \left(\frac{D_2}{q_2} Z_1(q_2 r) + q_2 b^2 D_3 Z_1(q_2 r) \right) \exp\left(i\left(kz - \omega t\right)\right). \tag{2.36}$$

This thesis considers the case presented in (2.33) only. Therefore the cladding's displacement and stresses become

$$v_{II}(r,z,t) = \left(\frac{D_2}{q_2} J_1(q_2 r) + q_2 b^2 D_3 Y_1(q_2 r) \right) \exp\left(i\left(kz - \omega t\right)\right) \tag{2.37}$$

$$\tau_{r\theta_{II}} = -\mu_{II} \left(D_2 J_2(q_2 r) + (q_2 b)^2 D_3 Y_2(q_2 r) \right) \exp\left(i\left(kz - \omega t\right)\right) \tag{2.38}$$

$$\tau_{\theta z_{II}} = i\mu_{II} k \left(\frac{D_2}{q_2} J_1(q_2 r) + q_2 b^2 D_3 Y_1(q_2 r) \right) \exp\left(i\left(kz - \omega t\right)\right). \tag{2.39}$$

Choosing to focus on the case of (2.32) results in a limited range of real angular frequencies over which modes exist for any given wavenumber, k. The upper and lower bounds of ω are given by the definitions of q_1 in (2.18) and q_2 in (2.32) respectively. These limits on ω are affected by both k and the phase velocity in each medium, c_1 and c_2

$$\frac{k^2}{c_2^2} < \omega^2 < \frac{k^2}{c_1^2} + \frac{\beta^2}{2^2} \tag{2.40}$$

The consequences of this restriction in certain cases are presented in detail in Chapter 3, namely a limit on the number of nodes that exist over the range of acceptable frequencies. Future work will involve expanding this thesis to include (2.33) as is discussed in Chapter 4. Now, with the displacement and stress solutions determined, application of the appropriate boundary conditions is considered.

2.3) Boundary Conditions and Frequency Equation

Three boundary conditions are considered in this problem. First, the outer curved surface of the cladding is assumed to be stress free [8, 13]

$$\tau_{r\theta_{II}} = 0 \quad \text{at} \quad r = b. \tag{2.41}$$

Two interface conditions are applied at $r = a$, one in terms of stress and the other in terms of displacement. Tractions across the interface are assumed to be continuous resulting in continuity of $\tau_{r\theta}$ [3, 5, 13]

$$\tau_{r\theta_{II}} = \tau_{r\theta_I} \quad \text{at} \quad r = a. \tag{2.42}$$

Meanwhile, interface imperfection directly affects the displacement interface condition. The difference between displacements of the core and cladding is related to the interface radius, the core's shear modulus, the shear stress at the interface and a dimensionless scalar, F [13]

$$v_{II} - v_I - \left(\frac{a}{\mu_I}\right) F \cdot \tau_{r\theta} = 0 \quad \text{at} \quad r = a. \tag{2.43}$$

F represents the degree to which the interface is damaged. As F increases, the interface is considered more imperfect, and the difference between the cladding and core displacement increases. For the limiting case in which F is increased to infinity, the core and cladding will rotate independently from one another. On the other hand, as F is decreased to zero, the core and cladding displacements are equal, retaining perfect interface conditions.

Equations (2.41), (2.42), and (2.43) are used to determine the frequency equation for the system. These relations result in three homogeneous algebraic equations in the three unknown constants D_1, D_2, D_3, are written in matrix form here

$$\begin{bmatrix} 0 & J_2(q_2 b) & (q_2 b)^2 Y_2(q_2 b) \\ \mu_0\left[q_1 a M'_{\kappa,\chi}(q_1 a) + M_{\kappa,\chi}(q_1 a)\left(\frac{\beta a}{2} - \frac{3}{2}\right)\right]\exp\left(-\frac{\beta a}{2}\right) & \mu_{II} J_2(q_2 a) & \mu_{II}(q_2 b)^2 Y_2(q_2 a) \\ -a\left[M_{\kappa,\chi}(q_1 a) + F\left\{q_1 a M'_{\kappa,\chi}(q_1 a) + M_{\kappa,\chi}(q_1 a)\left(\frac{\beta a}{2} - \frac{3}{2}\right)\right\}\right]\exp\left(\frac{\beta a}{2}\right) & \frac{J_1(q_2 a)}{q_2} & q_2 b^2 Y_1(q_2 a) \end{bmatrix}\begin{bmatrix} D_1 \\ D_2 \\ D_3 \end{bmatrix} = \begin{bmatrix} 0 \\ 0 \\ 0 \end{bmatrix}.$$

(2.44)In order for these equations to have a non-trivial solution the determinant of the coefficient matrix **A** must be equal to zero.

$$\det \boldsymbol{A} = 0. \qquad (2.45)$$

Equation (2.45) is known as the dispersion relation or frequency equation for the system.

2.4) Solution Technique

Matrix Simplification

The frequency equation derived in the previous section is in terms of multiple parameters. Direct numerical solution of (2.45) for ω as a function of k is challenging. Therefore, the elements of the coefficient matrix **A** in (2.45) is rewritten in terms of fewer, dimensionless parameters. This is done by first setting the following ratios of outer radii, shear moduli, and phase velocities

$$\eta = \frac{b}{a}; \qquad \lambda = \frac{\mu_{II}}{\mu_0}; \qquad \alpha = \frac{c_2}{c_1}. \qquad (2.46)$$

Next, $q_2 b$ is eliminated from the coefficient matrix **A** and replaced in terms of $q_2 a$. First, the equation for $q_2$in (2.32) is multiplied by both the interface and cladding's outer radius, a and b respectively

$$\left(q_2 a\right)^2 = \frac{\left(\omega a\right)^2}{c_2^2} - \left(ka\right)^2 \tag{2.47}$$

$$\left(q_2 b\right)^2 = \frac{\left(\omega b\right)^2}{c_2^2} - \left(kb\right)^2 \ . \tag{2.48}$$

Equation (2.48) can be rewritten in terms of η

$$(q_2 b)^2 = \frac{\eta^2 (\omega a)^2}{c_2^2} - \eta^2 (ka)^2. \tag{2.49}$$

Comparing (2.69) with (2.67), it is concluded that

$$\left(q_2 b\right)^2 = \eta^2 \left(q_2 a\right)^2. \tag{2.50}$$

So, $q_2 b$ is eliminated from the coefficient matrix. Meanwhile, the form of $q_1 a$ is found by multiplying (2.18) by a

$$\left(q_1 a\right)^2 = 4\left\{\left(ka\right)^2 + \left(\frac{\beta a}{2}\right)^2 - \left(\frac{\omega a}{c_1}\right)^2\right\}. \tag{2.51}$$

To further simplify the coefficient matrix **A**, $q_1 a$ and $q_2 a$ are replaced by

$$Q_1 = q_1 a; \qquad Q_2 = q_2 a\ . \tag{2.52}$$

The radial grading of the core is replaced by a single parameter. Also, definitions for normalized frequency, Ω, and normalized wavenumber, ξ, are made in order to make the coefficient matrix dimensionless

$$\psi = \frac{\beta a}{2}; \qquad \Omega = \frac{\omega a}{c_2}; \qquad \xi = ka\ . \tag{2.53}$$

As a result, Q_1 and Q_2become

$$Q_1^2 = 4\left(\xi^2 + \psi^2 - \left(\alpha\Omega\right)^2\right); \qquad Q_2^2 = \Omega^2 - \xi^2\ . \tag{2.54}$$

These are the final expressions in terms of the normalized frequency and normalized wavenumber for all of the arguments of the special functions which appear in the numerical solution of the dispersion relations of the composite cylinder.

Since the solution for the displacement of the core contained only one undetermined coefficient, and since the first boundary condition pertains only to the cladding, the presence of the Whittaker functions associated with this problem are contained within coefficients $A_{21}$and A_{31}. In both of these coefficients appears the term

$$C = q_1 a M'_{\kappa,\chi}(q_1 a) + M_{\kappa,\chi}(q_1 a)\left(\frac{\beta a}{2} - \frac{3}{2}\right). \tag{2.55}$$

In terms of the previously identified normalized parameters (2.72???) is

$$C = Q_1 M'_{\kappa,\chi}(Q_1) + M_{\kappa,\chi}(Q_1)\left(\psi - \frac{3}{2}\right). \tag{2.56}$$

$M'_{\kappa,\gamma}(Q_1)$ is evaluated by using the recurrence relation from Eq 2.4.12 in Slater [1]

$$M'_{\kappa,\chi}\left(Q_1\right) = \frac{\tfrac{1}{2} + \chi + \kappa}{Q_1}\left[M_{\kappa+1,\chi}\left(Q_1\right) - \frac{\kappa - \tfrac{Q_1}{2}}{\tfrac{1}{2} + \chi + \kappa} M_{\kappa,\chi}\left(Q_1\right)\right]. \tag{2.57}$$

Recall from (2.17) that $\chi = 1$. Multiplying κ by (*a*/*a*) gives

$$\kappa = \frac{3\psi}{Q_1}. \tag{2.58}$$

The final simplification for $M'_{\kappa,\gamma}(Q_1)$ is

$$M'_{\left(\tfrac{3\psi}{Q_1},1\right)}\left(Q_1\right) = \frac{\tfrac{3}{2} + \tfrac{3\psi}{Q_1}}{Q_1}\left[M_{\left(\tfrac{3\psi}{Q_1}+1,1\right)}\left(Q_1\right) - \frac{\tfrac{3\psi}{Q_1} - \tfrac{Q_1}{2}}{\tfrac{3}{2} + \tfrac{3\psi}{Q_1}} M_{\left(\tfrac{3\psi}{Q_1},1\right)}\left(Q_1\right)\right]. \tag{2.59}$$

Plugging (2.59) into (2.56) yields the final form of *C*.

$$C = \left(\frac{3}{2} + \frac{3\psi}{Q_1}\right) M_{\left(\tfrac{3\psi}{Q_1}+1,1\right)}\left(Q_1\right) + \left(Q_1 - 3\right)\left(\frac{\psi}{Q_1} + \frac{1}{2}\right) M_{\left(\tfrac{3\psi}{Q_1},1\right)}\left(Q_1\right). \tag{2.60}$$

Therefore, the final simplified system of equations is

$$\begin{bmatrix} 0 & J_2\left(\eta Q_2\right) & (\eta Q_2)^2 Y_2\left(\eta Q_2\right) \\ C\exp\left(-\psi\right) & \lambda J_2\left(Q_2\right) & \lambda(\eta Q_2)^2 Y_2\left(Q_2\right) \\ -\dfrac{1}{\eta}\left[M_{\kappa,\chi}(Q_1)+FC\right]\exp(\psi) & \dfrac{J_1\left(Q_2\right)}{\eta Q_2} & \eta Q_2 Y_1\left(Q_2\right) \end{bmatrix} \begin{bmatrix} D_1 \\ D_2 \\ D_3 \end{bmatrix} = \begin{bmatrix} 0 \\ 0 \\ 0 \end{bmatrix}. \tag{2.62}$$

In (2.62), the coefficient matrix is dimensionless and defined as **A'**. Therefore, the normalized frequency equation (dispersion relation) for the cylinder is

$$\det \mathbf{A}' = 0. \tag{2.63}$$

Numerical Solution

Equation (2.63) is solved numerically in Maple. An example Maple worksheet used in the solution of the dispersion relations for the cylinder is included in Appendix B. In Maple, the definitions of Q_1 and Q_2 from (2.54) are first declared. Limits on Ω as given in (2.40) are then set. Equation (2.60) is typed explicitly in order to simplify the coefficient matrix as discussed in the previous section. In the worksheet, the coefficient matrix is declared as **A**. Next, the determinant of **A** is set equal to a variable **B.** Afterwards, values for λ, η, α, ψ, and F are picked.

For a set combination of these parameters, the normalized wavenumber, ξ, is varied from 0 to 1. The goal is to determine the values of Ω for which **B** = 0 for each specific value of ξ. As illustrated in Figure 2.2, **B** can equal zero multiple times for each value of ξ, represented by crossings of the Ω-axis.

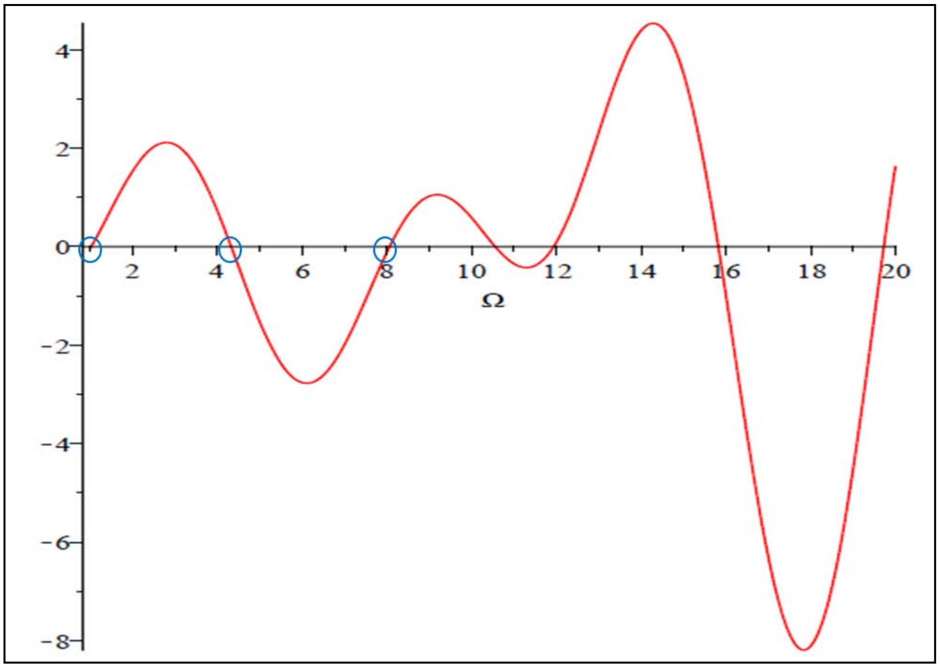

Figure 2.2: Sample plot of det(A) generated in Maple for ξ=0.99, η=1.8, ψ=2, λ=0.01, and α=0.1. First three wave modes are identified by blue circles.

Each value of Ω for which **B** = 0 is called a wave mode; the first crossing is the "first mode," the second crossing is the "second mode," and so on. The number of modes for each value of ξ is directly limited by the definitions of Q_1 and Q_2. The first three modes are sought in this work. As is discussed in Chapter 3, there are certain cases for which multiple modes do not exist over the limited range of wavenumbers and frequencies under consideration. However, for all cases in which three modes did exist within the established range of frequencies, the first three modes are tabulated with their corresponding normalized wavenumber. All data is included in this thesis for reference in Appendix A.

Dispersion curves are directly plotted from this data. The horizontal axis of a dispersion curve is the normalized wavenumber, ξ, and the vertical axis is the normalized frequency, Ω. All dispersion curves are presented and discussed in detail in Chapter 3.

CHAPTER 3

Results

The normalized frequency equation, (2.63), presented in the previous chapter is solved in Maple and plotted with normalized wavenumber, ξ, on the horizontal axis and normalized frequency, Ω, on the vertical axis. Three main cases are presented in this chapter: η = 1.8, 1.25, and 2. The effect of interface imperfection (F = 0, 1, 10, 100) is presented in all three cases. For consistency, phase velocity and shear modulus ratios are constant throughout all cases as α = 0.1 and λ = 0.01, which results in a constant density ratio of 1 between core and cladding materials.

3.1) Case 1

A composite cylinder with an outer radius ratio of η = 1.8 is considered. Radial grading in the core is increased such that ψ = 1, 2, and 3. For each level of grading, the amount of interface imperfection is increased logarithmically, F = 0, 1, 10, and 100. The first three torsional modes are presented.

First Torsional Mode

The effect of increased grading on the first wave mode is first examined. The calculated dispersion curves of the first modes for varying levels of interface imperfection and gradings ψ = 1, 2, and 3 are included as Figures 3.1, 3.2, and 3.3 respectively.

As illustrated in Figures 3.1 – 3.3, increasing the level of radial grading in the core reduces the effect of increased interface damage on the first torsional mode. This is represented on each figure by the four plots converging. In other words, the differences in normalized frequencies for a given normalized wavenumber among the four plots decrease significantly. It is noted that for the first mode, ξ and Ω appear to approach a 1:1 linear relationship as the level of grading increases. As such, detecting interface damage would be difficult, and nondestructive material characterization tools would likely not involve testing for the first torsional mode.

It is important to note that Armenàkas [3] and Berget et al [13] both specify that the first torsional mode is not properly described by Bessel's equation. The approach used in this thesis involves Whittaker's equation, and whether the first torsional mode is properly described by Whittaker's equation remains to be verified. Therefore, the validity of results presented in Figures 3.1 – 3.3 require further investigation.

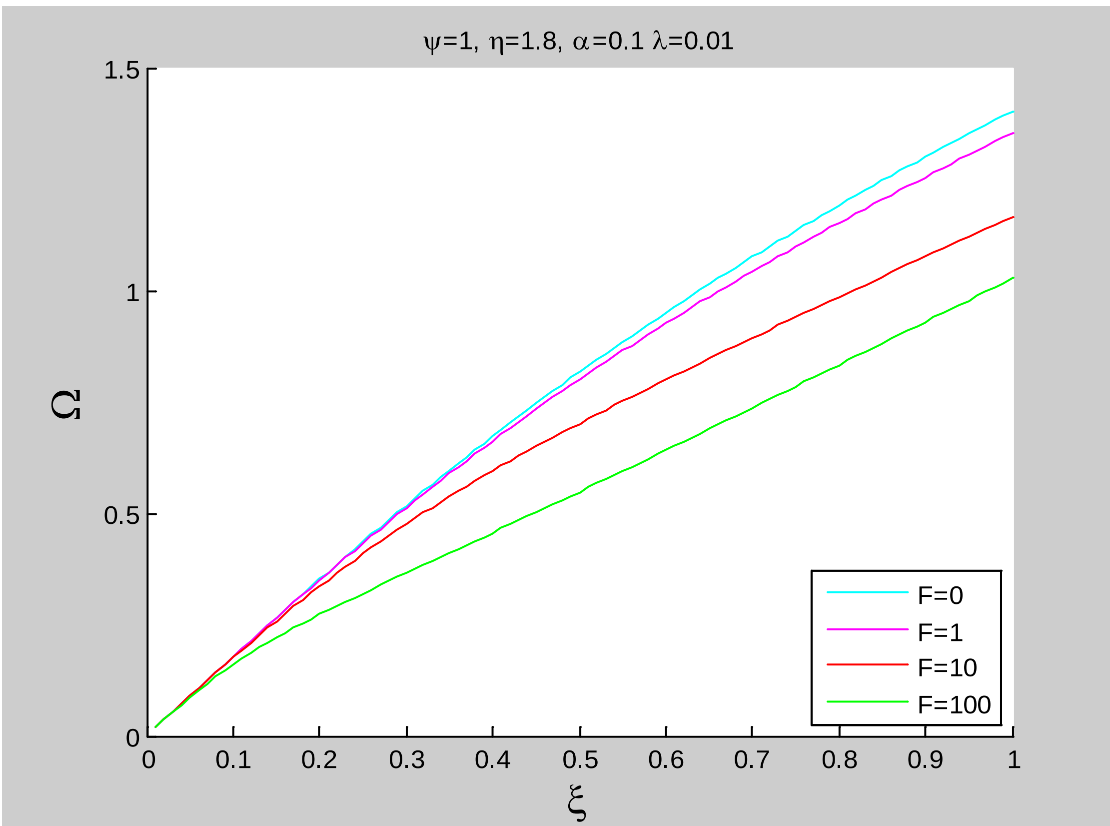

Figure 3.1: First mode for ψ = 1 and η = 1.8

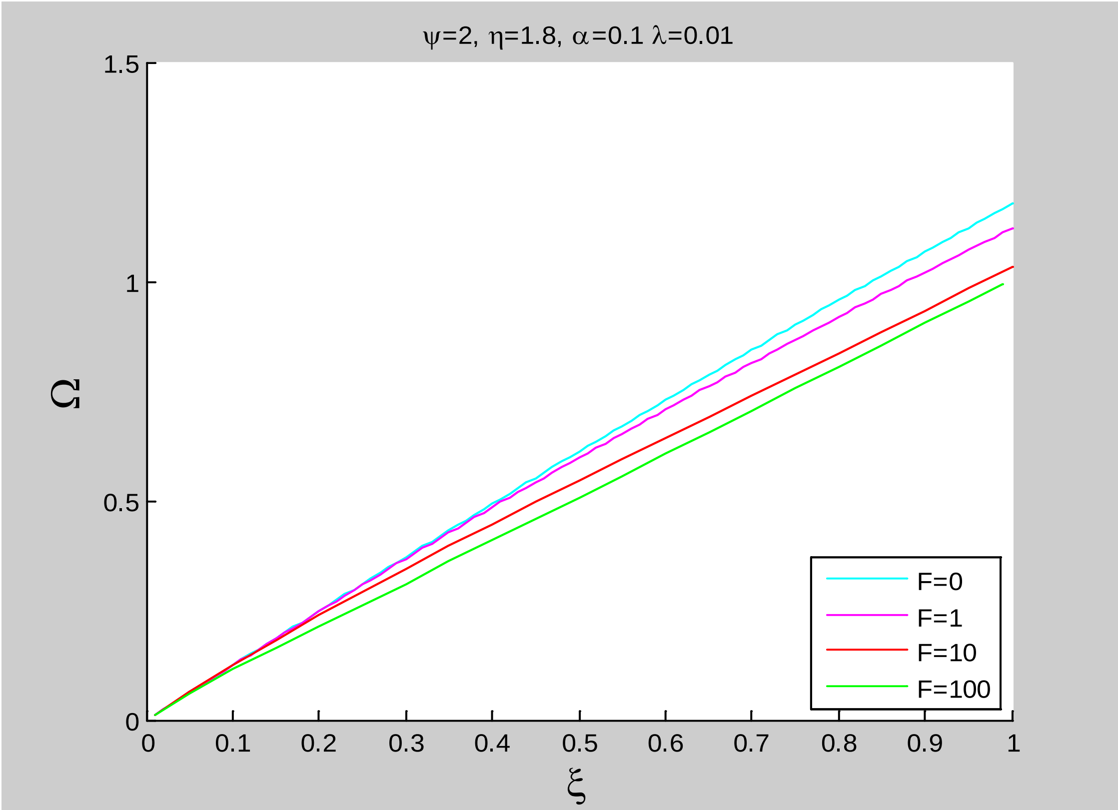

Figure 3.2: First mode for ψ = 2 and η = 1.8

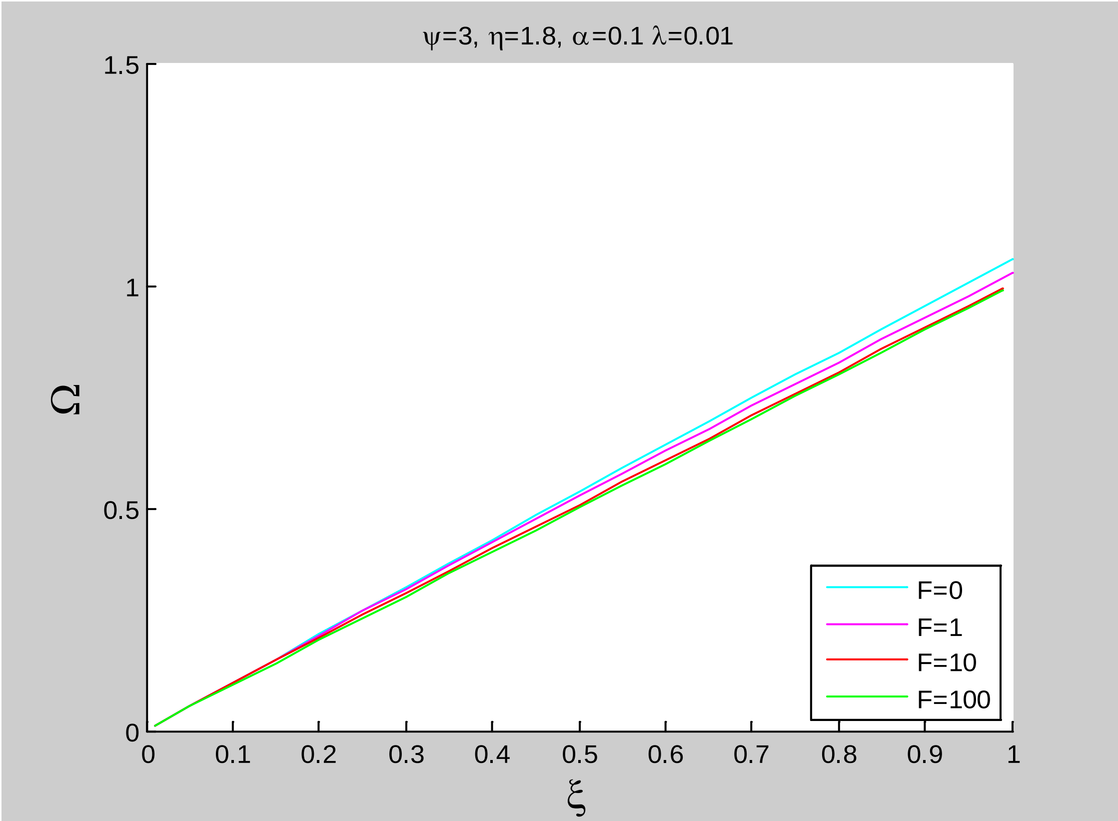

Figure 3.3: First mode for ψ = 3 and η = 1.8

Second Torsional Mode

The effect of increased grading on the second wave mode is next studied. The dispersion curves of the second modes for varying levels of interface imperfection and gradings ψ = 1, 2, and 3 are included as Figures 3.4, 3.5, and 3.6 respectively.

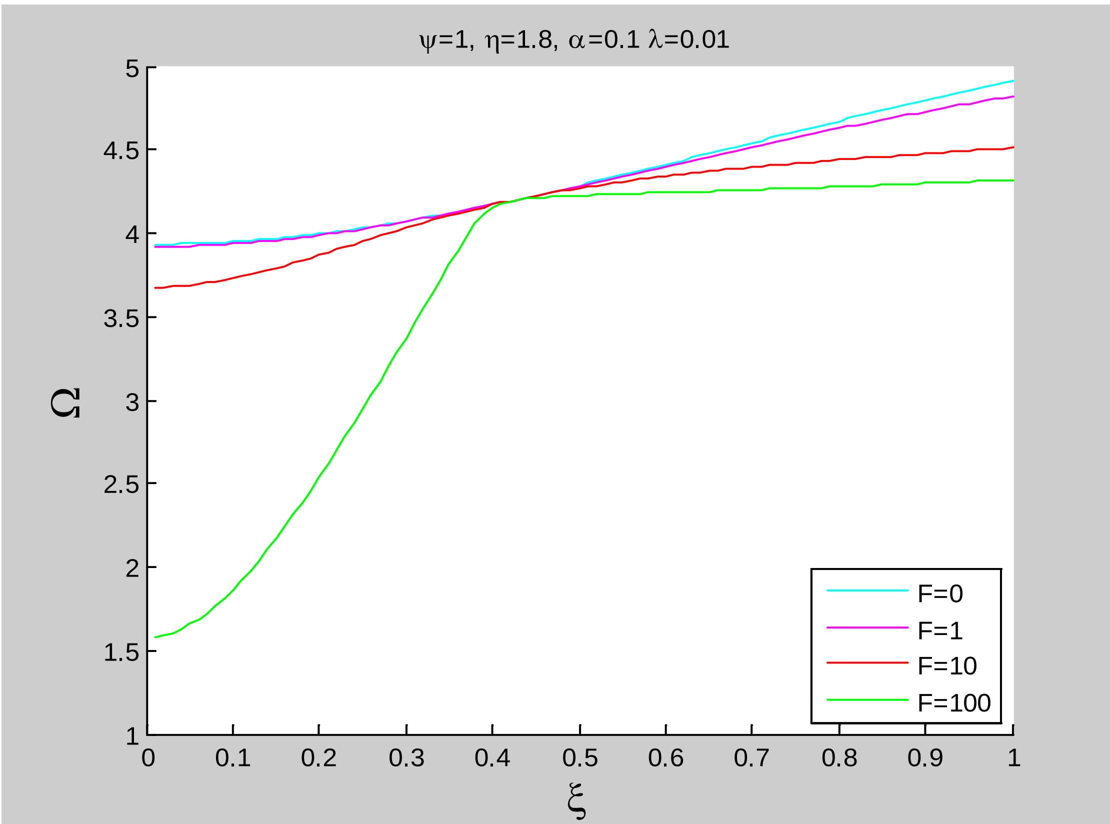

Figure 3.4: Second mode for ψ = 1 and η = 1.8

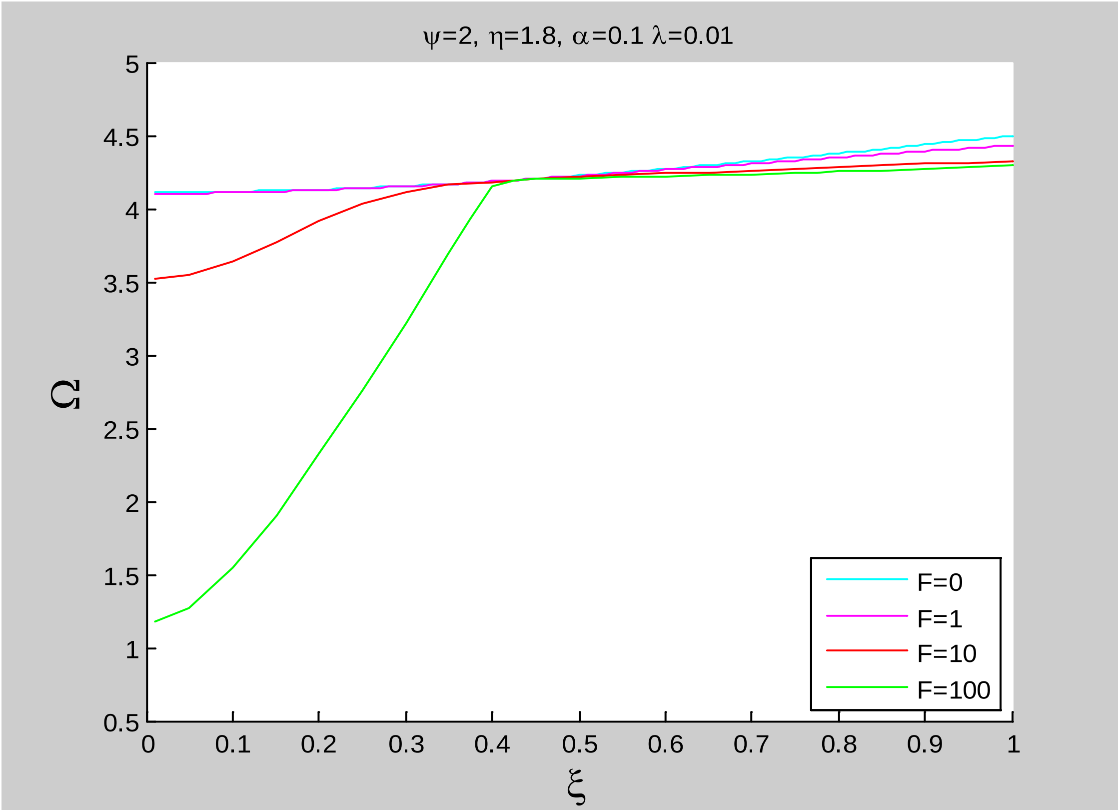

Figure 3.5: Second mode for ψ = 2 and η = 1.8

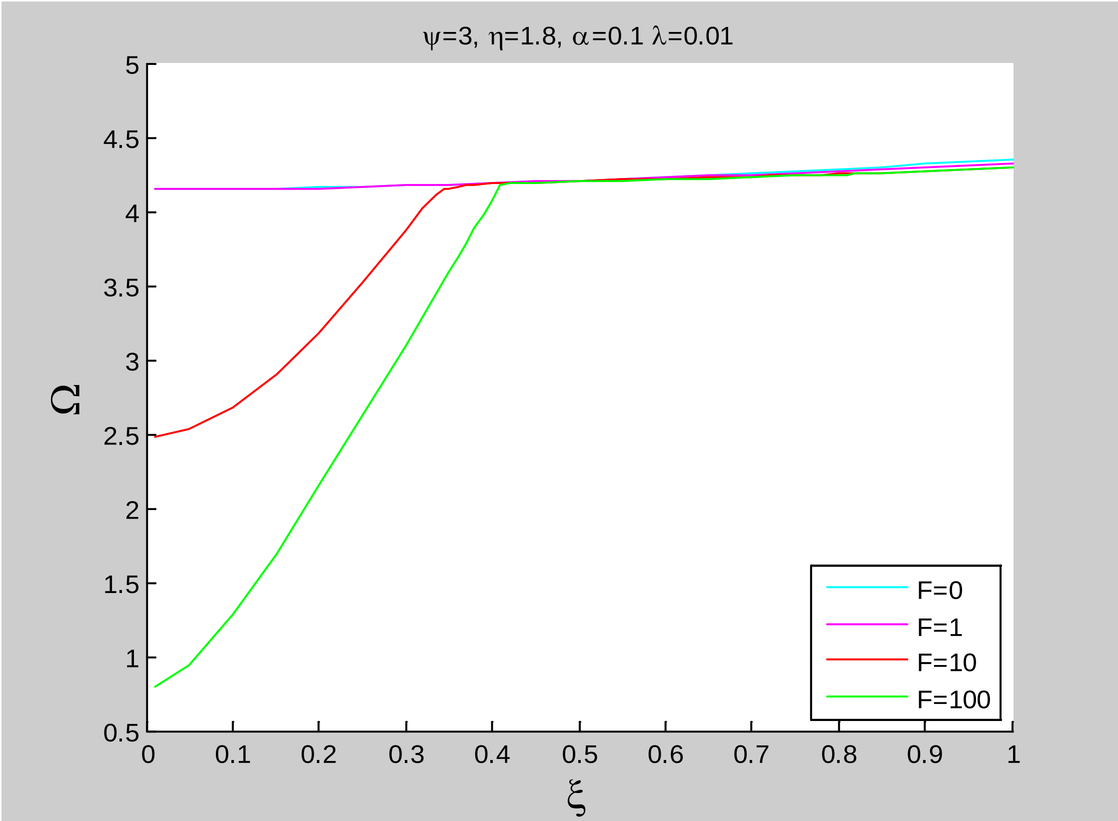

Figure 3.6: Second mode for ψ = 3 and η = 1.8

The general behavior of the dispersion relations in Figures 3.4, 3.5, and 3.6 agree with the findings of Berger et al [13]. At lower wavenumbers, the effect of interface imperfection on the second wave mode is significant. For radial gradings $\psi = 1$ and 2, the largest difference between second torsional mode frequencies at wavenumbers less than $\xi \approx 0.35$ occurs between interface damage $F = 10$ and $F = 100$. At radial grading $\psi = 3$, the difference between these two levels of damage is lessened. For all three levels of grading studied, the second torsional mode values coalesce around $\xi \approx 0.4$. As shown in Figure 3.4, when $\psi = 1$, after the plots converge, they begin to diverge once again as ξ increases to 1. As the plots diverge, the spread amongst them is less than the spread at lower wavenumbers. However, as grading increases to $\psi = 2$ and 3, after the four damage cases converge, the effect of interface imperfection is minimized to an increasing extent. This is a significant result: high grading in the core of a composite cylinder with an imperfect interface greatly minimizes the effect of interface damage on second torsional mode frequencies at higher wavenumbers.

This finding would be valuable in the development of a nondestructive material characterization tool for a composite cylinder with a functionally graded core. Damage testing would be done to determine if the bond between the core and cladding had been weakened. In order to test for this interface damage, pulses at wavenumbers less than $\xi \approx 0.2$ could be input into the system reasonably modeled as a composite cylinder with radius ratio $\eta = 1.8$. When the composite cylinder is first installed into the environment, pulses could be sent into the new, undamaged cylinder to obtain the second torsional mode frequencies for cases of no or low interface damage. Over time, as interface damage is suspected, testing for damage would be simplified. The second torsional mode for the case of a slightly damaged interface, $F = 1$, closely follows that of a perfect interface $F = 0$. So, low levels of interface damage would not be easily discovered. However, a slightly damaged interface is naturally less of a concern than an interface that has been significantly damaged ($F = 10\ldots100$). Therefore, after obtaining baseline values of torsional wave modes for a near perfect interface, if the nondestructive material characterization tool read modal frequencies significantly lower at the same wavenumbers, then it would be easily concluded that the interface had become damaged.

Third Torsional Mode

The effect of increased grading on the third wave mode is the final aspect investigated in Case 1. The dispersion curves of the third modes for varying levels of interface imperfection and gradings $\psi = 1$, 2, and 3 are included as Figures 3.7, 3.8, and 3.9 respectively. Deviation among interface damage cases similar to the deviation in the second torsional mode is discovered. However, this deviation occurs more significantly at lower levels of interface damage and over a larger range of wavenumbers, which would be beneficial in the development of nondestructive material characterization tools as discussed following Figures 3.7 – 3.9.

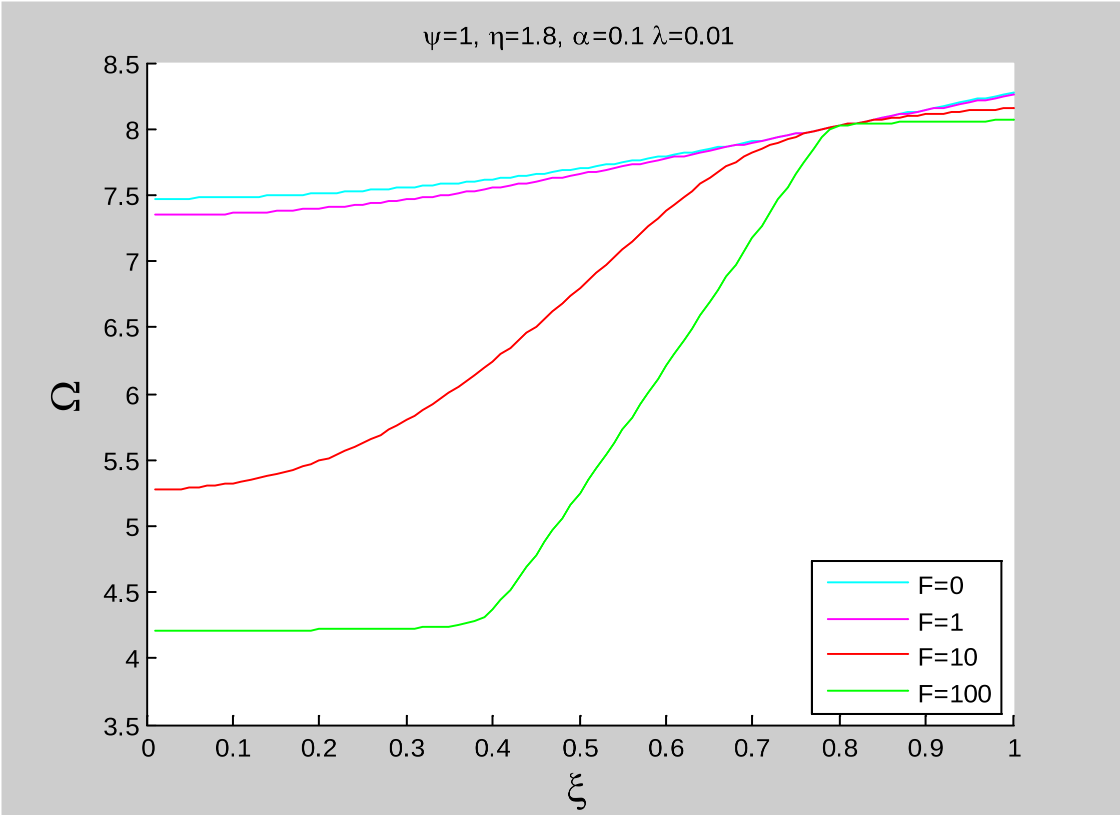

Figure 3.7: Third mode for ψ = 1 and η = 1.8

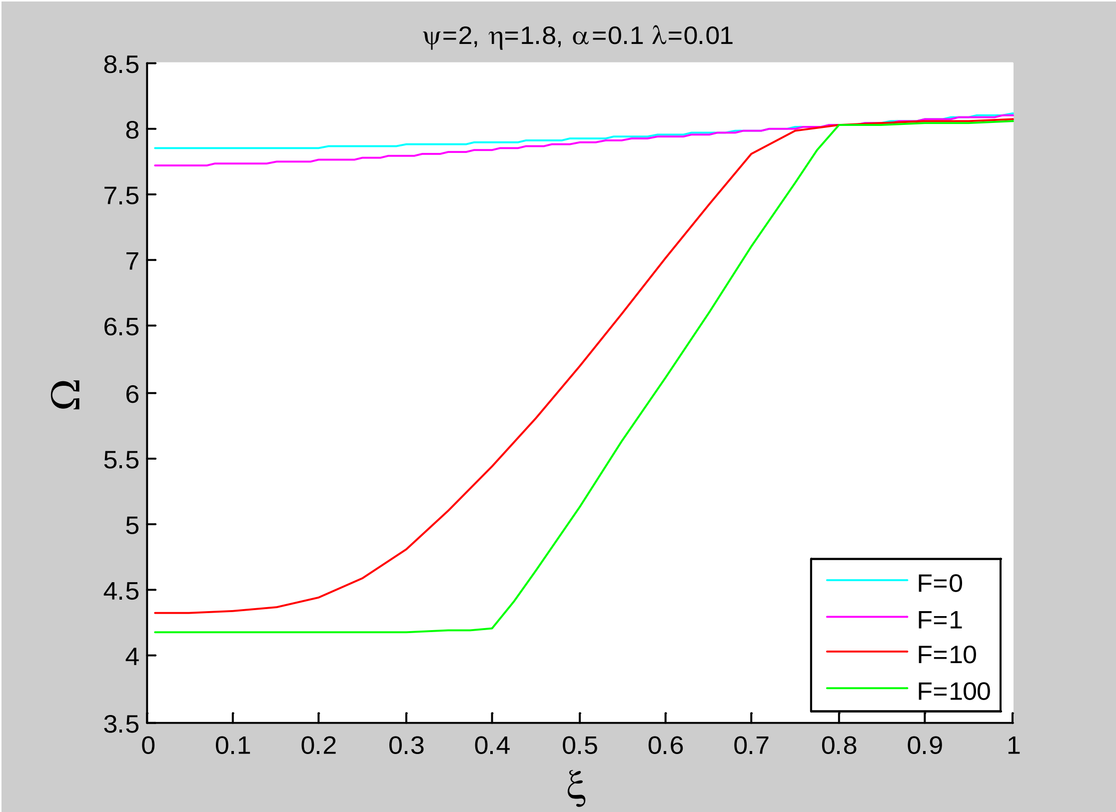

Figure 3.8: Third mode for ψ = 2 and η = 1.8

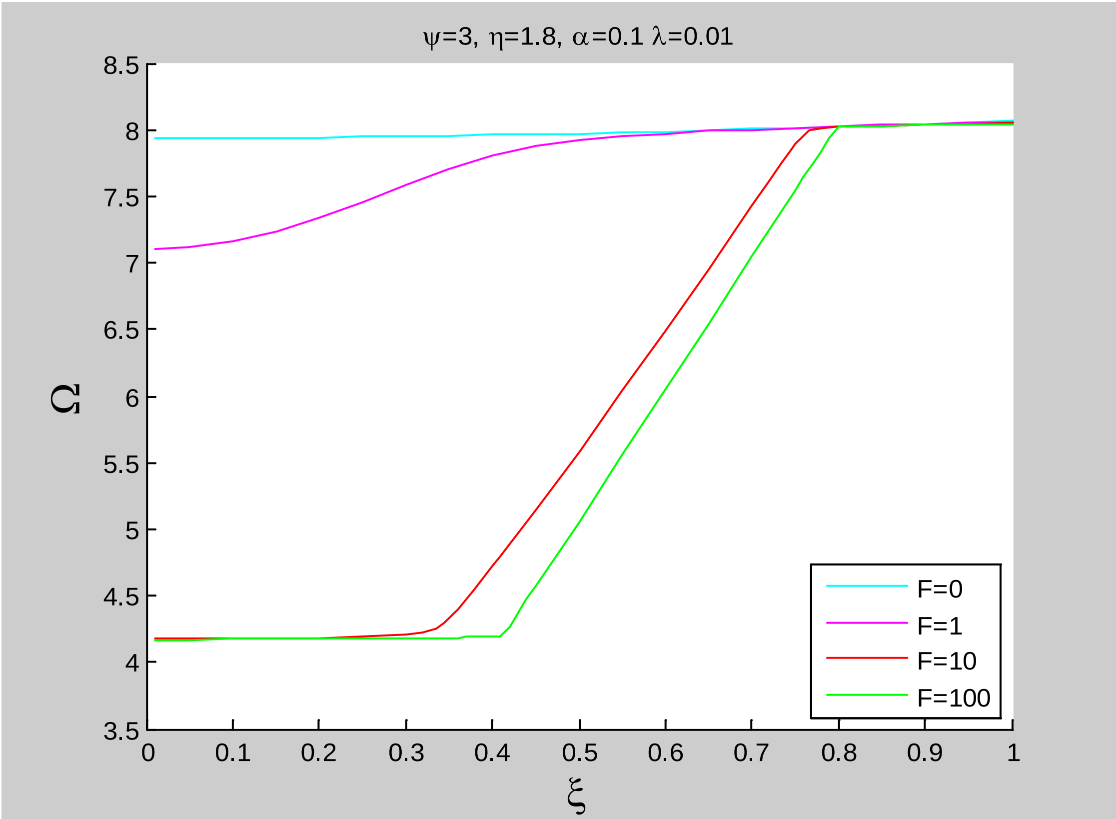

Figure 3.9: Third mode for ψ = 3 and η = 1.8

As is the case for the second torsional mode, there is significant deviation in the values of the third torsional modes for increasing interface damage. For $\psi = 1, 2$, the difference between third torsional mode frequencies for $F = 0$ and 1 is very small. When $\psi = 3$, there is a more noticeable difference at lower wavenumbers between these two damage cases $F = 0$ and 1. Additionally, as the grading increases, the difference in third torsional mode frequencies between damage cases $F = 10, 100$ is noted to decrease for the entire range of wavenumbers. On the other hand, as damage increases from $F = 1$ to $F = 10$, there is a very significant difference in third torsional mode frequencies at wavenumbers lower than $\xi \approx 0.4$. This transition value of the wavenumber is twice as large as it is in the second torsional mode, which is noted to be $\xi \approx 0.2$. Therefore these results for the third torsional mode could be used in the development of a nondestructive material characterization tool that detected smaller levels of interface damage over a larger range of wavenumbers. (Nice!!)

Also, notice the sharp kinks in the dispersion relations at $\xi \approx 0.4$. These kinks are not numerical artifacts. Rather, they are determined by using very small increments of ξ. The sharpness of the kink is noted to increase as the amount of radial grading, ψ, increases.

3.2) Case 2

In Case 2, a cylinder with a thinner cladding such that $\eta = 1.25$ is considered. Radial grading in the core is increased such that $\psi = 0, 1, 2, 3$, and 5. For each level of grading, the amount of interface imperfection is increased logarithmically, F = 0, 1, 10, and 100. Only the first torsional mode is presented since higher order modes are found to exist outside of the investigated range of frequencies set by the restrictions on Ω discussed previously in (2.41). The purpose of Case 2 is to verify that the findings of Case 1 regarding the first torsional mode are consistent for a composite cylinder with a thin cladding.

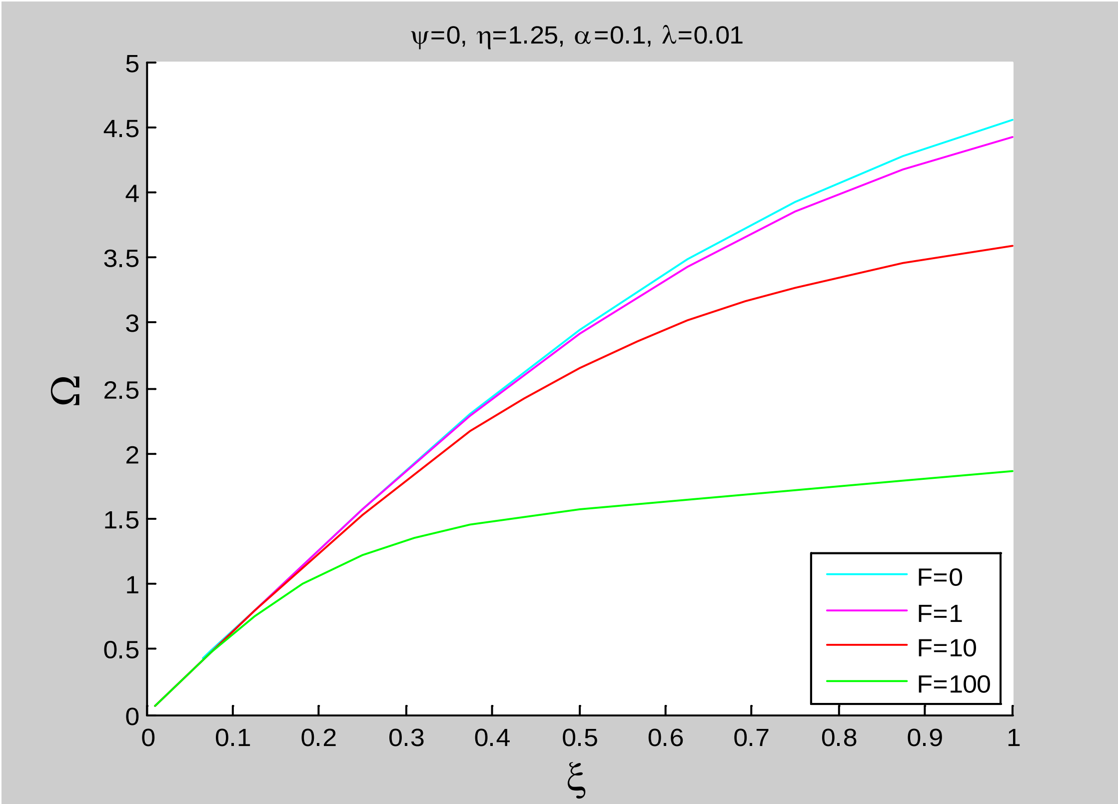

Figure 3.10: First mode for ψ = 0 and η = 1.25

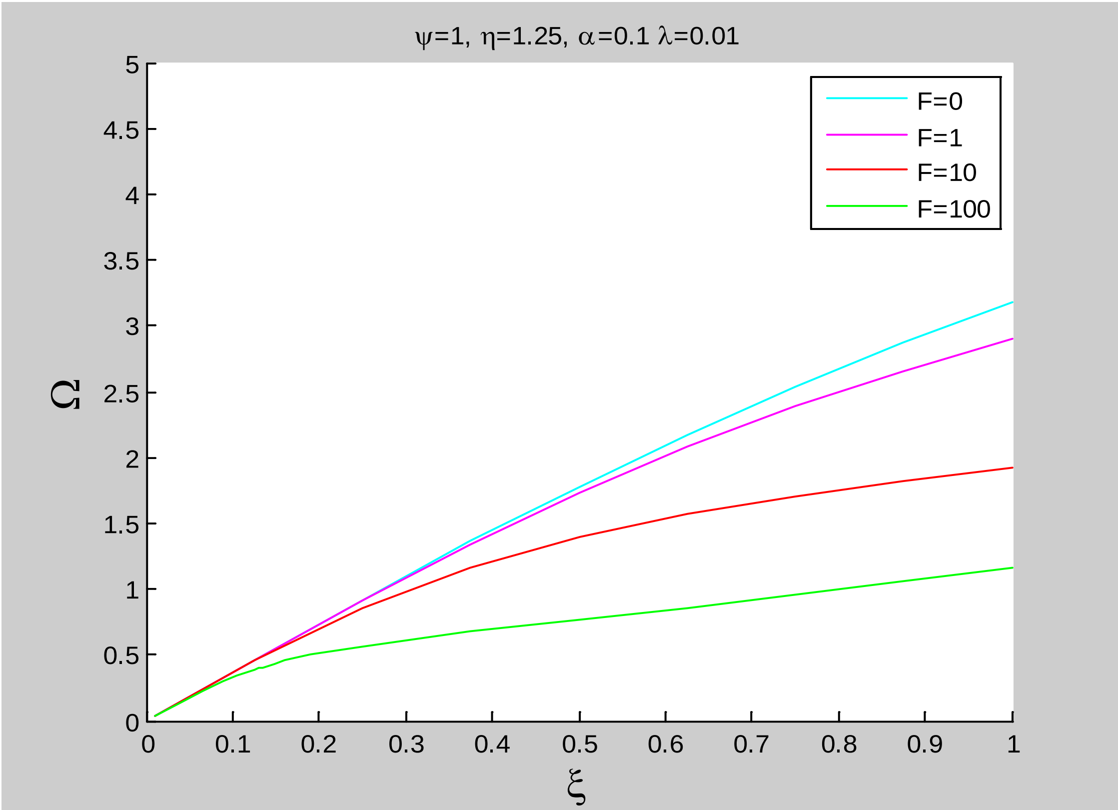

Figure 3.11: First mode for ψ = 1 and η = 1.25

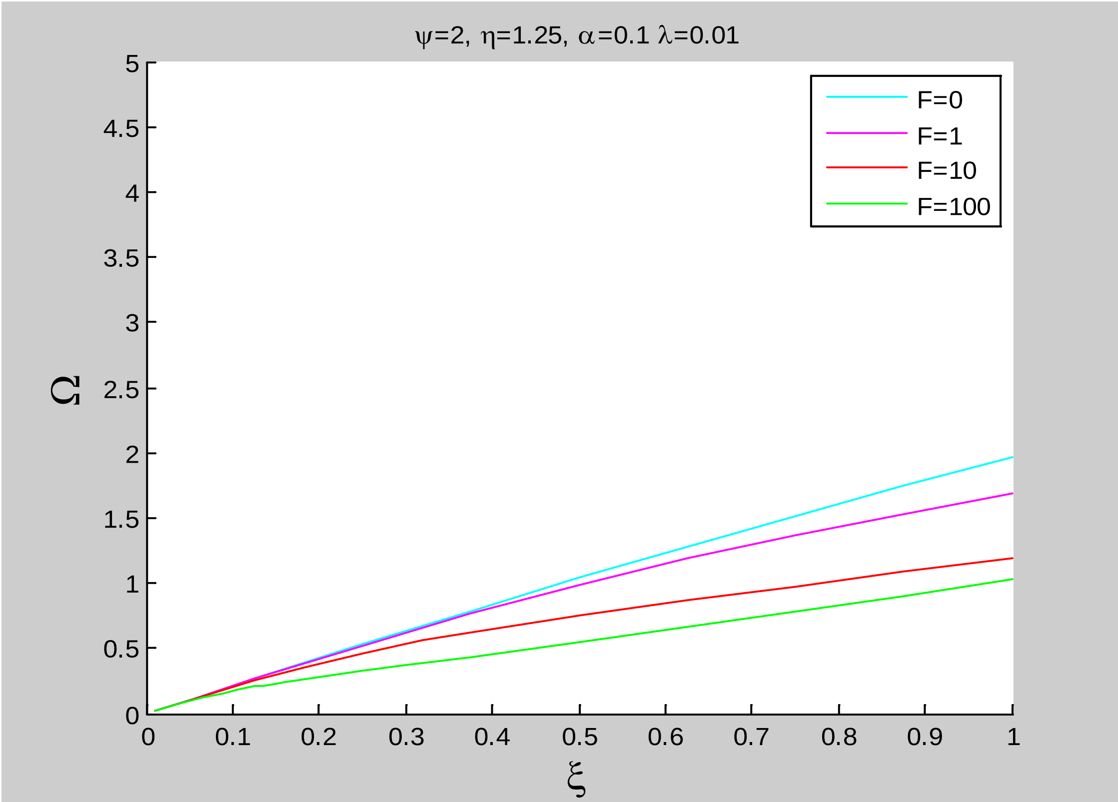

Figure 3.12: First mode for ψ = 2 and η = 1.25

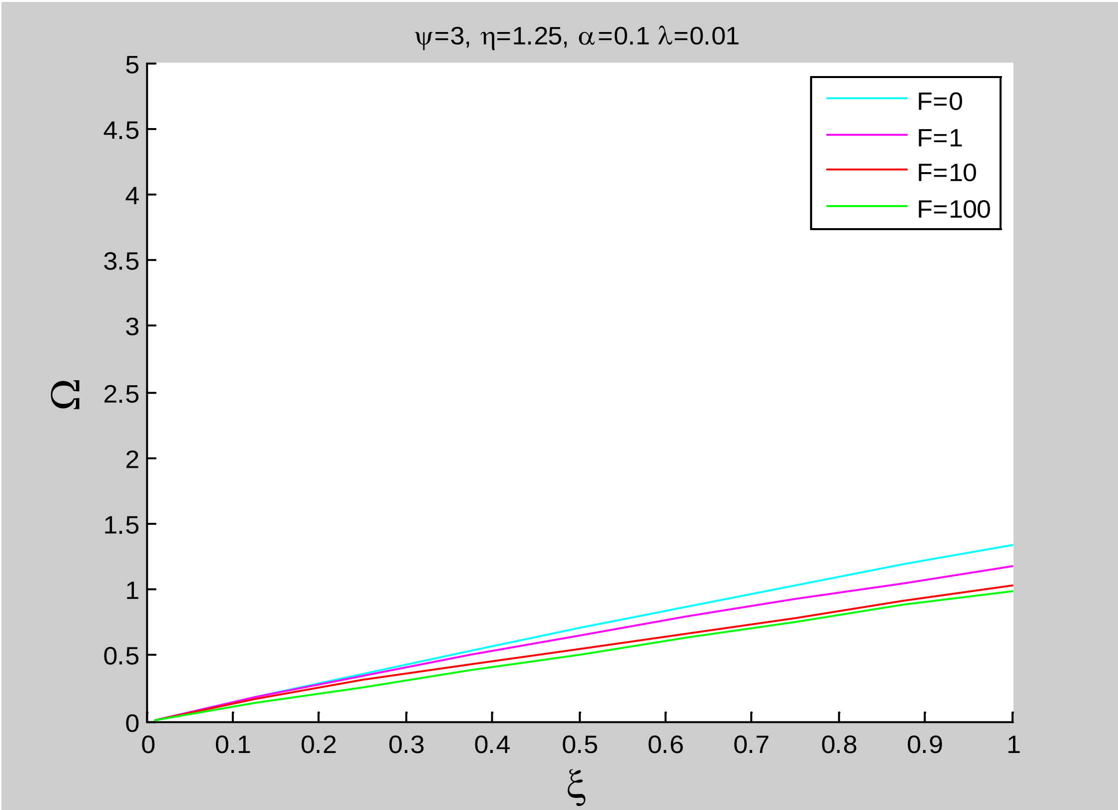

Figure 3.13: First mode for ψ = 3 and η = 1.25

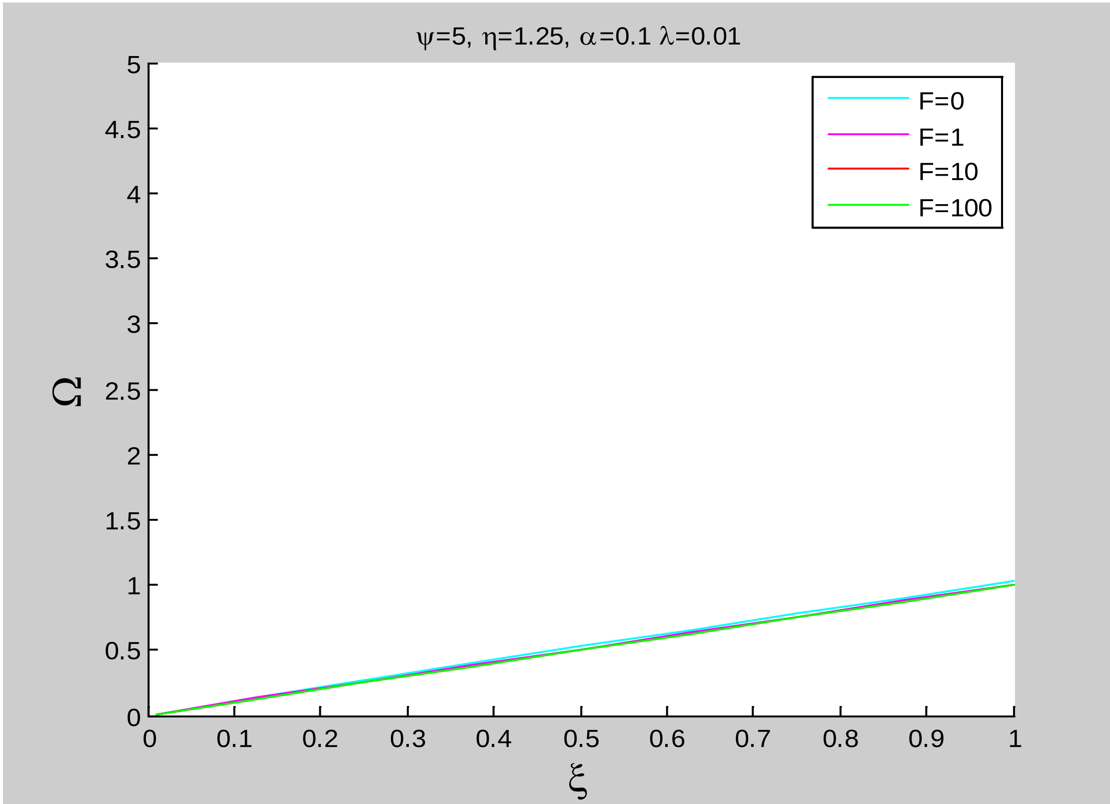

Figure 3.14: First mode for ψ = 5 and η = 1.25

These results confirm that the behavior of the first torsional mode is the same for cylinders η = 1.25 and 1.8. Similar to the first torsional mode of Case 1, the plots for all four damage cases converge to a near 1:1 linear relationship between ξ and Ω as the radial grading increases. In the case of lower radial gradings, the largest spread amongst the plots occurs at wavenumbers near 1. However, the spread among the damage cases for, say, ψ = 1 (as shown in Figure 3.11) is nevertheless rather small.

3.3) Case 3

In Case 3, a cylinder with a larger cladding such that the η = 2 is considered. Radial grading in the core is increased by much smaller increments: ψ = 0.4, 0.8, and 1.2. For each level of grading, the amount of interface imperfection is increased logarithmically, F = 0, 1, 10, and 100. The first three torsional modes are discussed. It is noted that the dispersion relations in Case 3 demonstrate similar behavior to Case 1 for the first three torsional modes. The third torsional mode for ψ = 0.4 is unable to be calculated over the entire range of ξ for the damage cases F = 0, 1, and 10 due to the restrictions placed on

Ω from the definition of q_2 in (2.41). This limitation is discussed at the end of this section following Figure 3.32.

First Torsional Mode

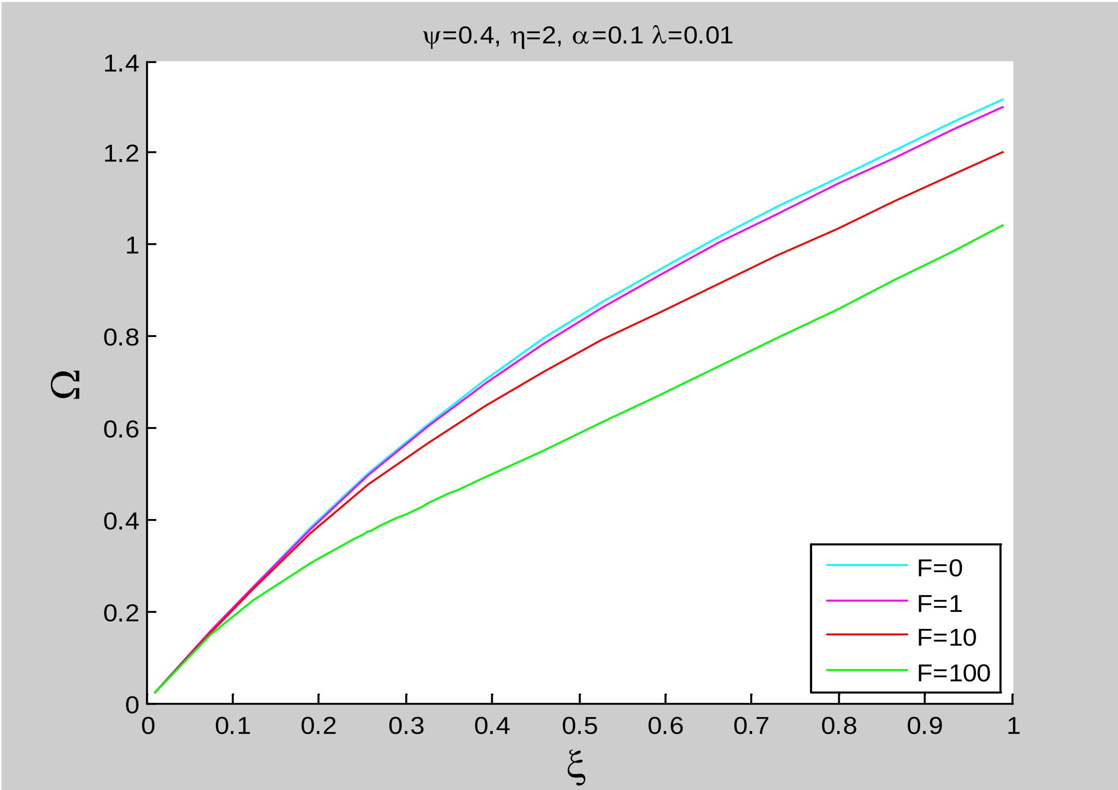

Figure 3.15: First mode for ψ = 0.4 and η = 2

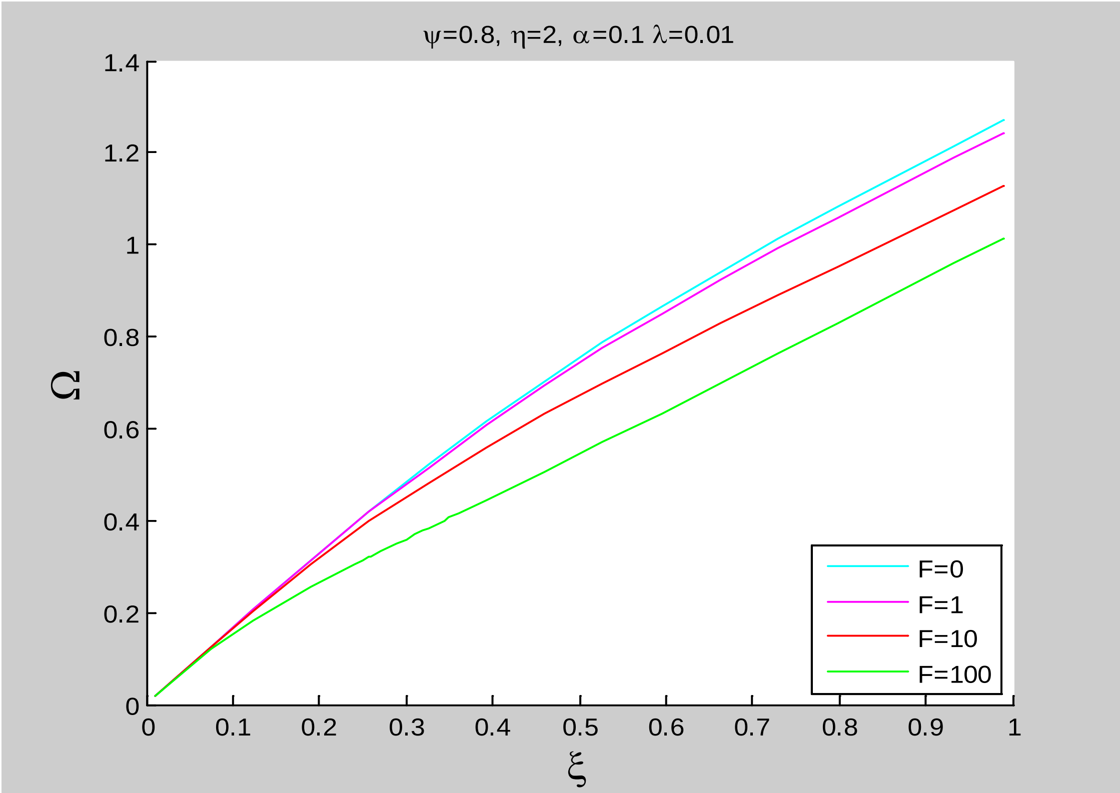

Figure 3.16: First mode for ψ = 0.8 and η = 2

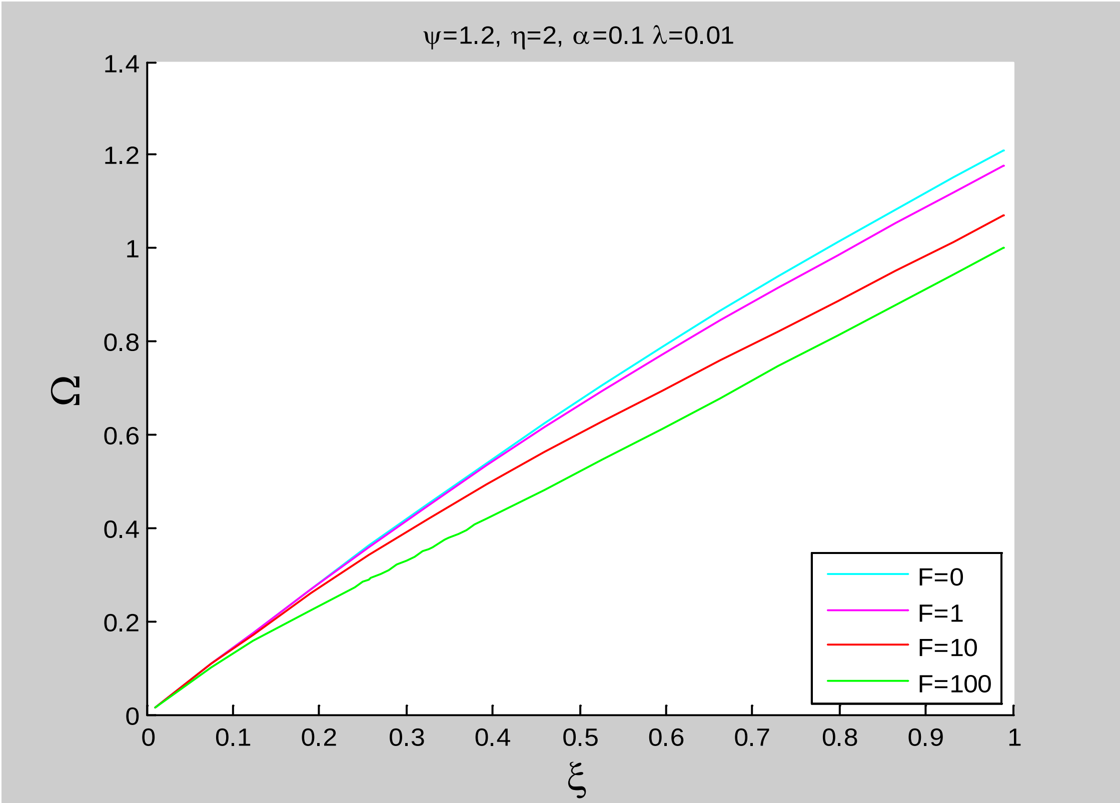

Figure 3.17: First mode for ψ = 1.2 and η = 2

The behavior exhibited in Figures 3.15 – 3.17 is consistent with the previous two cases presented. Since the grading, ψ, is increased by smaller increments in Case 3, spread between the four damage cases on each figure is more apparent than for cases in which the grading is higher. Physically, these lower levels of radial grading in Case 3 are more likely to occur than for the extreme grading cases presented in the previous two sections in Chapter 3. In the functionally graded core, the shear modulus and density decay exponentially by a factor of ψ. Decay by previous values of ψ = 3 or 5, for example, are less likely to occur in reality. Nonetheless, these larger grading values are valuable in the fact that they more vividly illustrate the effect of increased radially grading of the core on the dispersion relations than do small increments of ψ. Again, the validity of the solution methods for the first torsional mode needs to be investigated.

Second Torsional Mode

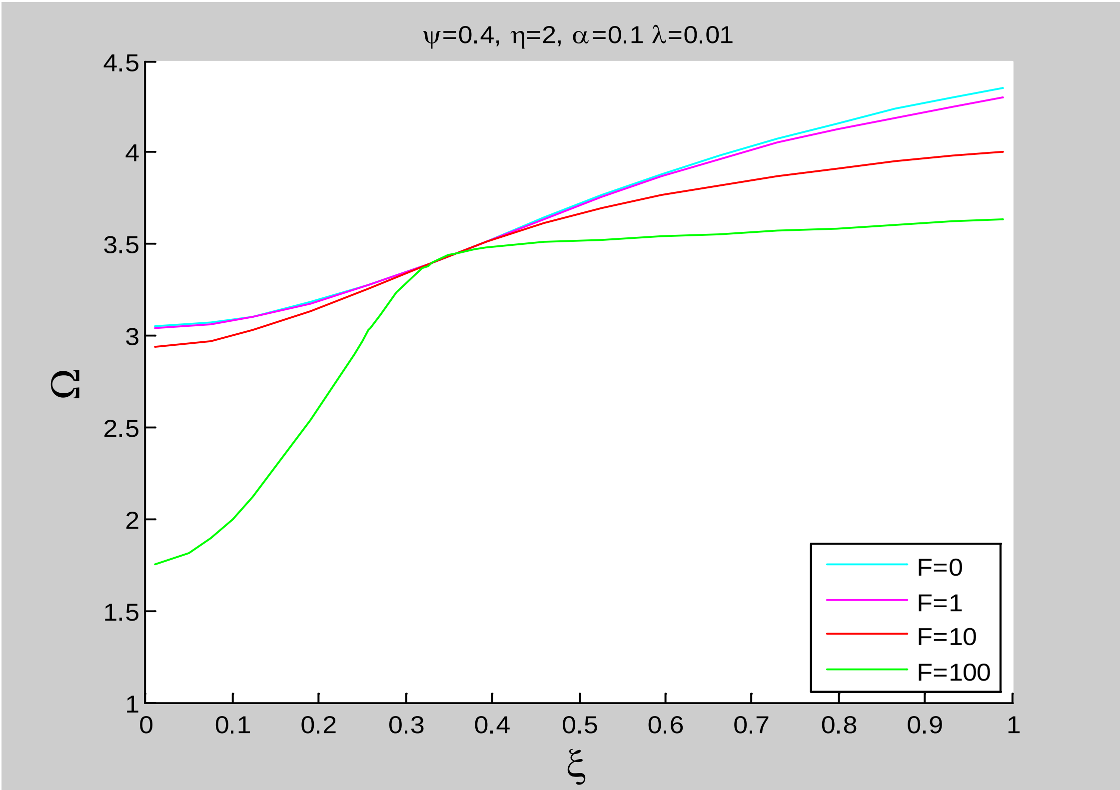

Figure 3.18: Second mode for ψ = 0.4 and η = 2

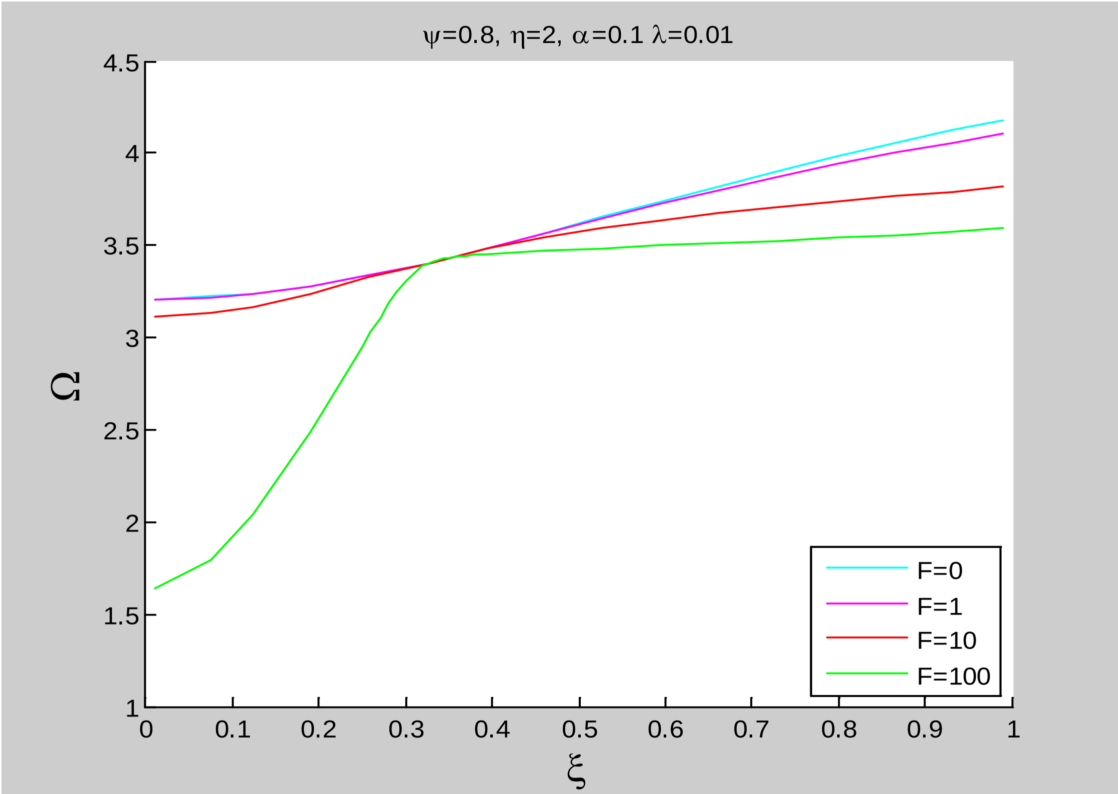

Figure 3.19: Second mode for ψ = 0.8 and η = 2

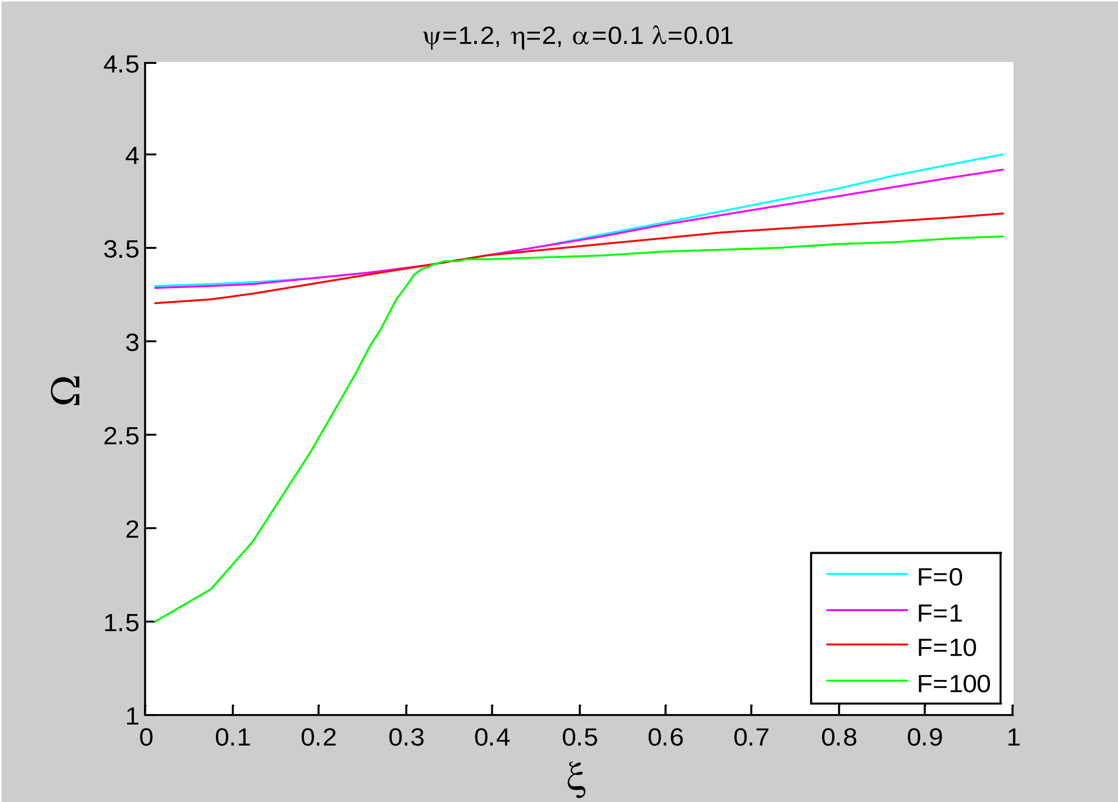

Figure 3.20: Second mode for ψ = 1.2 and η = 2

The effect of interface imperfection is again most pronounced at low wavenumbers for larger level of damage. One effect of an increased radius ratio from η = 1.8 in Case 1 to η = 2 in Case 3 is that the plots of the four damage cases appear to converge at lower wavenumbers. In Case 1, as shown in Figures 3.4 – 3.6, the second torsional modes converge around $\xi \approx 0.4$. Figures 3.18 – 3.20 show that when η = 2, the second torsional modes converge around a lower wavenumber estimated to be around $\xi \approx$ 0.33. At wavenumbers lower than this convergence value, a nondestructive material characterization tool would likely detect high levels of interface damage. However, such a tool would have trouble distinguishing between damage levels F = 0, 1, and 10 since the spread between frequencies at a given wavenumber for these three levels of interface imperfection is small.

Third Torsional Mode

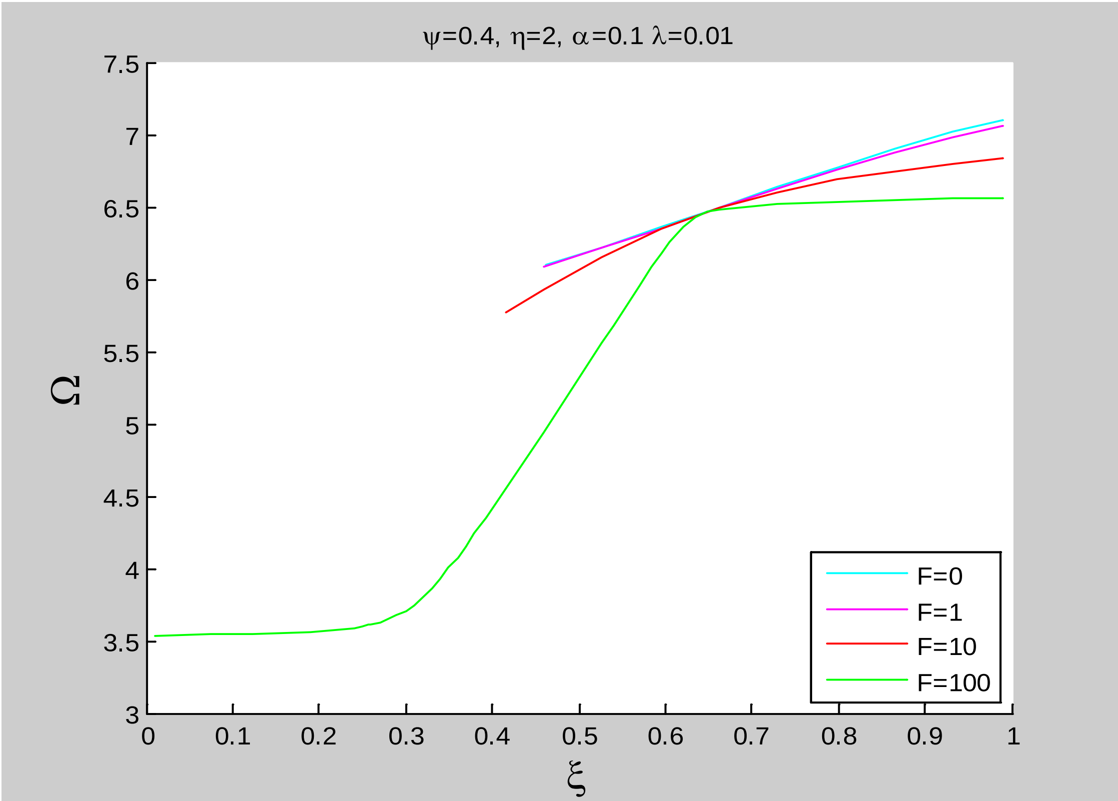

Figure 3.21: Third mode for ψ = 0.4 and η = 2

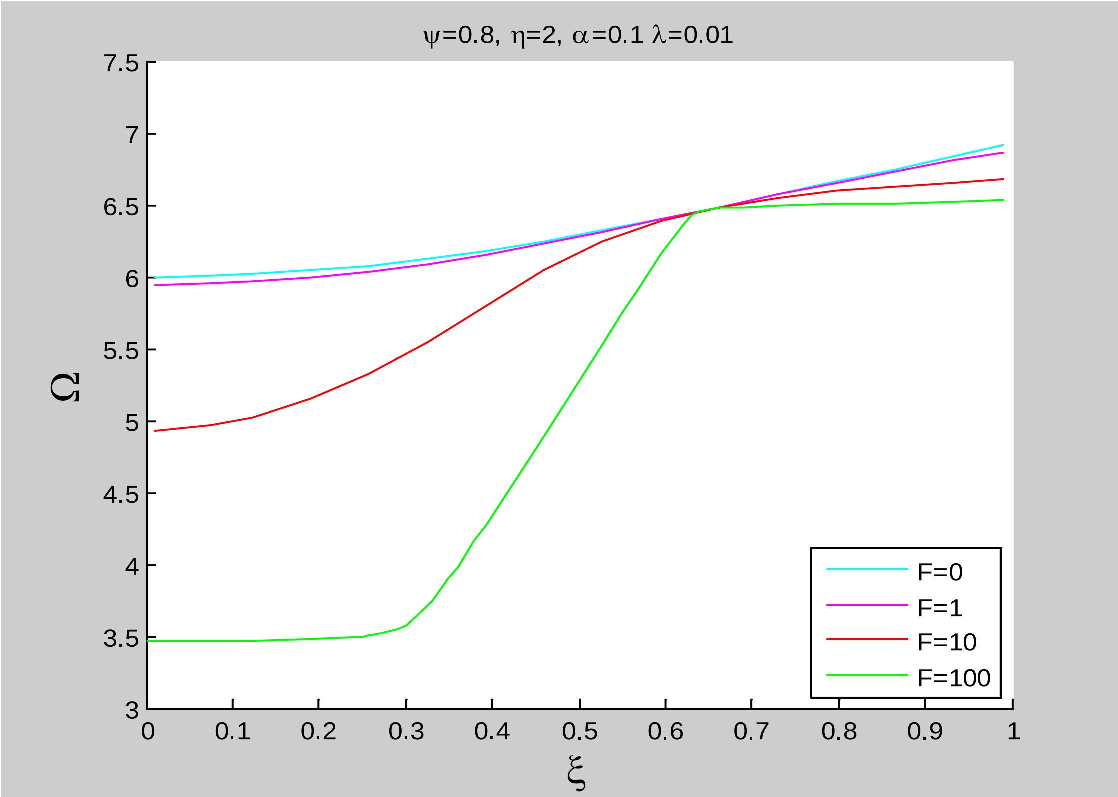

Figure 3.22: Third mode for ψ = 0.8 and η = 2

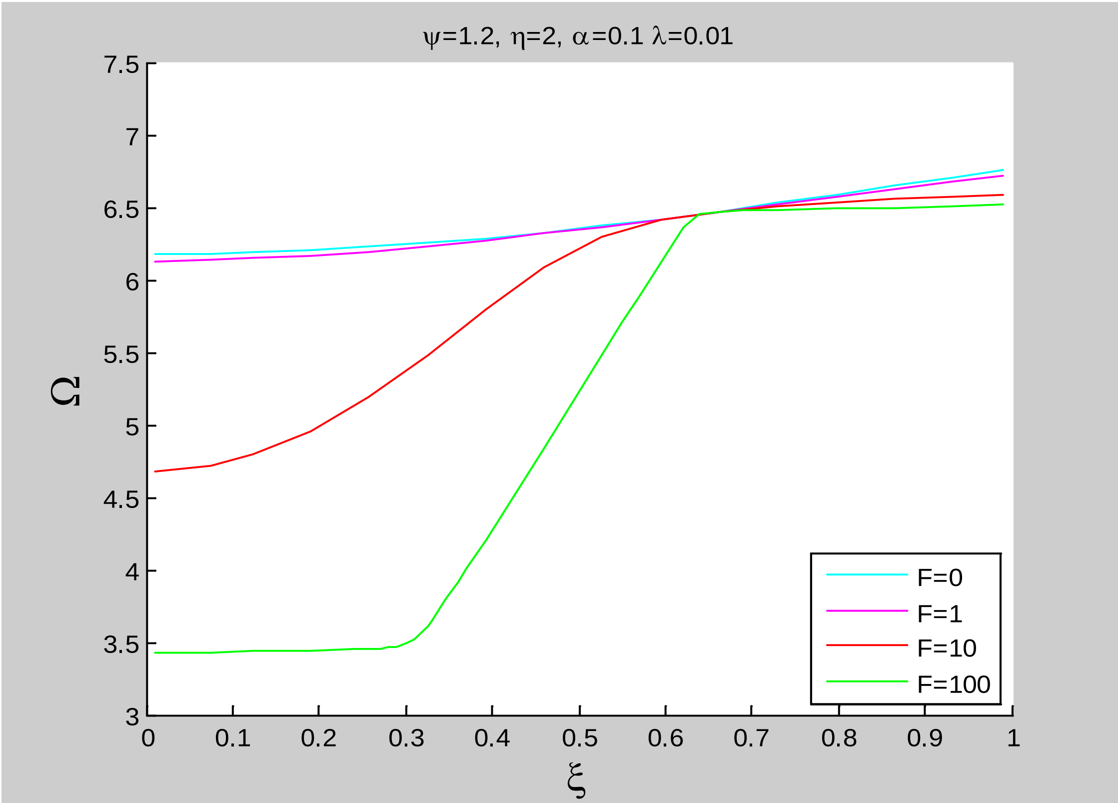

Figure 3.23: Third mode for ψ = 1.2 and η = 2

Confirming the findings demonstrated in Case 1, the propagating frequencies of third torsional mode are more spread apart among the four damage cases than the frequencies of the second torsional mode. Interface imperfection around $F = 10$ is thus more detectible in the range of frequencies associated with the third torsional mode. Again, the effect of increasing η is that the dispersion relations of the third torsional mode converge at a lower wavenumber. In the current case, the dispersion relations converge around $\xi \approx 0.65$, which is a lower wavenumber than Case 1 in which the dispersion relations of the third torsional mode converge at $\xi \approx 0.8$.

As shown in Figure 3.21, the third mode does not exist for lower wavenumbers and damage levels $F = 0$, 1, and 10. The range of Ω is restricted by (2.41). In order to obtain the full dispersion relations of the third torsional mode over the entire range of wavenumbers $\xi = 0$ to 1, the scope of this thesis must be expanded from (2.33) to (2.34). Currently, only combinations of wavenumber and frequency such that $\omega^2 > k^2 c_2^2$ are considered. In Figure 3.21, this limit is apparent. Lower third mode frequencies can be calculated by applying the relations of (2.34) for which $\omega^2 < k^2 c_2^2$. Expanding this thesis to the full range of frequencies is the aim of future work.

Chapter 4

Conclusions

4.1) Contributions

These findings specifically advance the understanding of this type of composite cylinder, albeit in a small way. The frequency equation is written in terms of a combination of Whittaker and Bessel functions. Based on a review of existing literature, this method of solution done not appear to have been previously attempted. Nevertheless, the general shape of the dispersion relations closely follows the behavior of the dispersion relations of Berger et al [13] for the ungraded composite cylinder, which indicates that the methods used in this project are compatible with previous findings. A more careful comparison of the graded and ungraded dispersion relations will be one of the topics addressed in future work.

4.2) Applications

The solution methods presented will serve as a springboard for the expansion of this work to an unrestricted range of frequencies and wavenumbers; this is discussed in the subsequent section. The findings of this thesis and the ensuing expansion of the work could assist in the development of a nondestructive material characterization tool, as detailed throughout this paper. It is seen in the dispersion relations that as interface damage increases, at lower wavenumbers the second and third torsional mode frequencies decrease significantly. Moreover, the amount deviation between dispersion relations for varying levels of interface damage is found to increase as the level of radial grading of the core increases. The numerical solution methods presented in Chapter 2 could be applied to construct and expand a large database containing the dispersion relations for many levels of radial grading for a nearly continuous range of damage levels (as opposed to the few discrete levels of interface damage studied in this thesis). With this database compiled, a damage testing device could be created in which the user would set the radial grading to a desired level via an interface, select a low wavenumber, and increase the frequency of input torsional pulses into the composite cylinder being tested for interface damage. When resonance is detected at a specific frequency, this frequency would be cross-referenced to the existing database of torsional modes to identify the approximate level of interface damage.

4.3) Future Work

Much work remains to be done. The findings of this project are to be expanded to the full range of frequencies by introducing the case of (2.34). Doing so will result in the Bessel functions present in this work being replaced by modified Bessel functions. Recall how in Figure 3.21 the dispersion relations for the third mode are not shown for values of ξ less than about0.4. This is due to the change in sign at this value of ξ of the expressions in the radicals which appear in the arguments of the special functions. Expansion of the solution forms to include these changes in sign would reveal the dispersion relations for wavenumbers between $0 \le \xi \le \xi_0$, where ξ_0 represents the transition value of the wavenumber for a given case. Once the complete dispersion relations are elucidated all of the findings will be published.

It is noted in Chapter 3 that the solutions for the first torsional modes require further investigation. The first torsional mode is not properly described by Bessel's equation, which was employed for both the core and cladding displacement solutions by Armenàkas [3] and Berger et al [13]. It has not been investigated whether or not the approach used in this thesis involving a combination of Whittaker and Bessel functions fails to properly describe the first torsional mode as well. Immediate future work will involve ascertaining the answer to this inquiry through an in-depth investigation of the first torsional mode and the behavior of Whittaker functions.

Further future work could involve determining the dispersion relations of a composite cylinder with a functionally graded cladding and a homogeneous core, or a composite cylinder with a functionally graded core and cladding. It would be interesting to investigate the effect of introducing grading in the cladding on the dispersion relations in a composite cylinder with an imperfect interface. Moreover, this thesis utilized a rather simple model for interface imperfection. Future work could involve using more complex models of interface imperfection to study the effect that this would have on the dispersion relations. Furthermore, since only torsional modes are considered in this thesis, future work could also investigate dispersion of flexural or longitudinal waves in a composite cylinder with a functionally graded core and an imperfect interface.

4.4) Summary

The purpose of this thesis is to determine dispersion relations of torsional waves for a composite cylinder with a functionally graded core and an imperfect interface. This goal was accomplished successfully for three restricted cases. The displacement solutions for the cylinder are derived and used in the development of the frequency equation for the system. This frequency equation is simplified into dimensionless form through use of several ratios of core and cladding properties and then solved numerically to obtain the dispersion relations for three cases. It is concluded that the effect of varying levels of interface imperfection is most apparent in the third mode frequency range at low wavenumbers. Increasing the level of radial grading in the core increases the spread among dispersion relations, and the amount of interface imperfection is more noticeable as a result. The second torsional mode is affected similarly, except that the calculated second torsional mode frequencies are only significantly lower at high levels of interface damage (F = 100). It is noted that the spread among dispersion relations for the second torsional mode for damage cases F = 0, 1, and 10 is considerably less than the spread between F = 10 and F = 100. Therefore, these findings suggest that if a nondestructive material characterization tool were developed to detect interface damage, torsional pulses at low wavenumbers and frequencies in the range of the third mode would best indentify the level of interface imperfection.

References

[1] Slater, L. J. *Confluent Hypergeometric Functions*. London: Cambridge UP, 1960. Print.

[2] Kolsky, H. *Stress Waves in Solids*. New York: Dover Publications, 1963. Print.

[3] Armenàkas, Anthony E. "Torsional Waves in Composite Rods." *The Journal of the Acoustical Society of America* 38.3 (1965): 439-46. Print.

[4] Jones, J. P., and J. S. Whittier. "Waves at a Flexibly Bonded Interface." *Journal of Applied Mechanics* 34 (1967): 905-09. Print.

[5] Whittier, J., and J. Jones. "Axially Symmetric Wave Propagation in a Two-layered Cylinder." *International Journal of Solids and Structures* 3.4 (1967): 657-75. Print.

[6] Lai, Jai-Lue. "Propagation of Harmonic Waves in a Composite Elastic Cylinder." *The Journal of the Acoustical Society of America* 49.1B (1971): 220-28. Print.

[7] Abramowitz, Milton, and Irene A. Stegun. *Handbook of Mathematical Functions: With Formulas, Graphs, and Mathematical Tables*. New York: Dover, 1972. Print.

[8] Bhattacharya, R. C. "On the Torsional Wave Propagation in a Two-layered Circular Cylinder with Imperfect Bonding." *Proc. Indian Natn. Sci. Acad.* 41A.6 (1975): 613-19. Print.

[9] Thurston, R. N. "Elastic Waves in Rods and Clad Rods." *The Journal of the Acoustical Society of America* 64.1 (1978): 1-37. Print.

[10] Graff, Karl F. *Wave Motion in Elastic Solids*. New York: Dover Publications, 1991. Print.

[11] Achenbach, Jan D. *Wave Propagation in Elastic Solids*. Amsterdam: North-Holland, 1993. Print.

[12] Suresh, S., and A. Mortensen. *Fundamentals of Functionally Graded Materials: Processing and Thermomechanical Behaviour of Graded Metals and Metal-ceramic Composites*. London: IOM Communications, 1998. Print.

[13] Berger, J. R., P. A. Martin, and S. J. McCaffery. "Time-harmonic Torsional Waves in a Composite Cylinder with an Imperfect Interface." *The Journal of the Acoustical Society of America* 107.3 (2000): 1161. Print.

[14] Han, X., G. R. Liu, Z. C. Xi, and K. Y. Lam. "Transient Waves in a Functionally Graded Cylinder." *International Journal of Solids and Structures* 38 (2001): 3021-037. Print.

[15] Ichikawa, Kiyoshi. "Activities of the FGM Forum." Functionally Graded Materials in the 21st Century: A Workshop on Trends and Forecasts. Norwell, Massachusetts: Kluwer Academic, 2001. 18. Print.

[16] Ruys, Andrew, and D. Sun. "Functionally Graded Materials (FGM) and Their Production Methods." Azom.com. N.p., 22 Aug. 2002. Web. <http://www.azom.com/article.aspx?ArticleID=1592>.

[17] Elmaimouni, L., J. Lefebvre, V. Zhang, and T. Gryba. "Guided Waves in Radially Graded Cylinders: A Polynomial Approach." *NDT & E International* 38.5 (2005): 344-53. Print.

[18] Singh, B. M., J. Rokne, and R. S. Dhaliwal. "Torsional Vibrations of Functionally Graded Finite Cylinders." *Meccanica* 41.4 (2006): 459-70. Print.

[19] Honarvar, F., E. Enjilela, and A. N. Sinclair. "Guided Ultrasonic Waves in Composite Cylinders." *Mechanics of Composite Materials* 43.3 (2007): 277-88. Print.

[20] "Egyptian Mud Bricks." *Interesting Facts Information Tourism Travel Culture Language Business People RSS*. N.p., 29 Mar. 2010. Web. 08 Jan. 2013.

*Note: References are arranged in chronological order

APPENDIX A

Tables

In Appendix A, all properties relevant to the data presented in each respective table are included in the first row of the table. As such, descriptions are not included in the titles of the tables to avoid redundancy.

Table A1:

F=0	ψ=1	η=1.8	λ=0.01, α=0.1
Wavenumber, ξ	**Mode 1**	**Mode 2**	**Mode 3**
0.010	0.0178448612	3.9333007630	7.4734530780
0.020	0.0356853108	3.9337888960	7.4737295370
0.030	0.0535169449	3.9346020730	7.4741902830
0.040	0.0713353756	3.9357397270	7.4748352900
0.050	0.0891362386	3.9372010660	7.4756645190
0.060	0.1069152010	3.9389850730	7.4766779190
0.070	0.1246679691	3.9410905080	7.4778754290
0.080	0.1423902954	3.9435159050	7.4792569750
0.090	0.1600779866	3.9462595810	7.4808224690
0.100	0.1777269106	3.9493196290	7.4825718110
0.110	0.1953330031	3.9526939300	7.4845048850
0.120	0.2128922748	3.9563801440	7.4866215630
0.130	0.2304008176	3.9603757220	7.4889216980
0.140	0.2478548109	3.9646779050	7.4914051290
0.150	0.2652505278	3.9692837230	7.4940716760
0.160	0.2825843403	3.9741900070	7.4969211390
0.170	0.2998527246	3.9793933850	7.4999533020
0.180	0.3170522666	3.9848902890	7.5031679230
0.190	0.3341796660	3.9906769570	7.5065647410
0.200	0.3512317408	3.9967494400	7.5101434710
0.210	0.3682054310	4.0031036060	7.5139038020
0.220	0.3850978023	4.0097351410	7.5178453980
0.230	0.4019060491	4.0166395620	7.5219678920
0.240	0.4186274975	4.0238122120	7.5262708910
0.250	0.4352596072	4.0312482730	7.5307539690
0.260	0.4517999738	4.0389427730	7.5354166680
0.270	0.4682463303	4.0468905830	7.5402584940
0.280	0.4845965482	4.0550864330	7.5452789180
0.290	0.5008486386	4.0635249150	7.5504773750
0.300	0.5170007522	4.0722004870	7.5558532570
0.310	0.5330511795	4.0811074850	7.5614059160
0.320	0.5489983510	4.0902401260	7.5671346620

0.330	0.5648408357	4.0995925170	7.5730387570
0.340	0.5805773409	4.1091586640	7.5791174200
0.350	0.5962067106	4.1189324760	7.5853698180
0.360	0.6117279236	4.1289077780	7.5917950690
0.370	0.6271400923	4.1390783130	7.5983922390
0.380	0.6424424600	4.1494377550	7.6051603400
0.390	0.6576343986	4.1599797140	7.6120983270
0.400	0.6727154061	4.1706977460	7.6192050990
0.410	0.6876851034	4.1815853600	7.6264794950
0.420	0.7025432316	4.1926360290	7.6339202940
0.430	0.7172896484	4.2038431940	7.6415262130
0.440	0.7319243248	4.2152002760	7.6492959050
0.450	0.7464473415	4.2267006810	7.6572279570
0.460	0.7608588851	4.2383378130	7.6653208900
0.470	0.7751592443	4.2501050760	7.6735731590
0.480	0.7893488059	4.2619958870	7.6819831490
0.490	0.8034280510	4.2740036840	7.6905491740
0.500	0.8173975506	4.2861219270	7.6992694800
0.510	0.8312579617	4.2983441170	7.7081422380
0.520	0.8450100231	4.3106637920	7.7171655510
0.530	0.8586545511	4.3230745420	7.7263374450
0.540	0.8721924355	4.3355700140	7.7356558760
0.550	0.8856246355	4.3481439170	7.7451187250
0.560	0.8989521751	4.3607900320	7.7547238000
0.570	0.9121761398	4.3735022160	7.7644688350
0.580	0.9252976718	4.3862744090	7.7743514910
0.590	0.9383179665	4.3991006400	7.7843693570
0.600	0.9512382682	4.4119750310	7.7945199470
0.610	0.9640598667	4.4248918070	7.8048007060
0.620	0.9767840933	4.4378452970	7.8152090060
0.630	0.9894123172	4.4508299370	7.8257421510
0.640	1.0019459420	4.4638402800	7.8363973750
0.650	1.0143864010	4.4768709970	7.8471718450
0.660	1.0267351580	4.4899168810	7.8580626620
0.670	1.0389936970	4.5029728510	7.8690668640
0.680	1.0511635260	4.5160339530	7.8801814270
0.690	1.0632461720	4.5290953690	7.8914032650
0.700	1.0752431730	4.5421524110	7.9027292360
0.710	1.0871560850	4.5552005300	7.9141561430
0.720	1.0989864690	4.5682353160	7.9256807350
0.730	1.1107358960	4.5812524970	7.9372997100

0.740	1.1224059430	4.5942479450	7.9490097210
0.750	1.1339981860	4.6072176740	7.9608073760
0.760	1.1455142050	4.6201578390	7.9726892420
0.770	1.1569555760	4.6330647430	7.9846518460
0.780	1.1683238750	4.6459348300	7.9966916840
0.790	1.1796206680	4.6587646890	8.0088052190
0.800	1.1908475180	4.6715510510	8.0209888850
0.810	1.2020059780	4.6842907920	8.0332390950
0.820	1.2130975910	4.6969809290	8.0455522410
0.830	1.2241238880	4.7096186210	8.0579246980
0.840	1.2350863880	4.7222011650	8.0703528280
0.850	1.2459865970	4.7347259980	8.0828329880
0.860	1.2568260050	4.7471906930	8.0953615250
0.870	1.2676060850	4.7595929580	8.1079347890
0.880	1.2783282960	4.7719306320	8.1205491320
0.890	1.2889940760	4.7842016890	8.1332009140
0.900	1.2996048470	4.7964042250	8.1458865050
0.910	1.3101620110	4.8085364670	8.1586022910
0.920	1.3206669490	4.8205967630	8.1713446770
0.930	1.3311210240	4.8325835810	8.1841100900
0.940	1.3415255770	4.8444955070	8.1968949830
0.950	1.3518819280	4.8563312430	8.2096958400
0.960	1.3621913750	4.8680896010	8.2225091800
0.970	1.3724551940	4.8797695030	8.2353315580
0.980	1.3826746400	4.8913699750	8.2481595690
0.990	1.3928509440	4.9028901480	8.2609898540
1.000	1.4029853170	4.9143292510	8.2738190990

Table A2:

F=1	ψ=1	η=1.8	λ=0.01, α=0.1
Wavenumber, ξ	**Mode 1**	**Mode 2**	**Mode 3**
0.010	0.0178446318	3.9181766110	7.3465936600
0.020	0.0356834769	3.9187228800	7.3469996030
0.030	0.0535107626	3.9196326490	7.3476760130
0.040	0.0713207443	3.9209049030	7.3486226500
0.050	0.0891077194	3.9225382190	7.3498391730
0.060	0.1068660407	3.9245307790	7.3513251460
0.070	0.1245901302	3.9268803630	7.3530800330
0.080	0.1422744920	3.9295843620	7.3551031970
0.090	0.1599137246	3.9326397790	7.3573939000
0.100	0.1775025336	3.9360432370	7.3599513020

0.110	0.1950357434	3.9397909850	7.3627744590
0.120	0.2125083079	3.9438789080	7.3658623180
0.130	0.2299153215	3.9483025330	7.3692137210
0.140	0.2472520289	3.9530570410	7.3728273980
0.150	0.2645138340	3.9581372760	7.3767019670
0.160	0.2816963089	3.9635377540	7.3808359320
0.170	0.2987952014	3.9692526800	7.3852276800
0.180	0.3158064418	3.9752759540	7.3898754790
0.190	0.3327261497	3.9816011890	7.3947774750
0.200	0.3495506387	3.9882217200	7.3999316920
0.210	0.3662764216	3.9951306250	7.4053360250
0.220	0.3829002138	4.0023207310	7.4109882440
0.230	0.3994189367	4.0097846360	7.4168859850
0.240	0.4158297197	4.0175147210	7.4230267530
0.250	0.4321299014	4.0255031680	7.4294079190
0.260	0.4483170310	4.0337419750	7.4360267150
0.270	0.4643888676	4.0422229750	7.4428802360
0.280	0.4803433797	4.0509378480	7.4499654380
0.290	0.4961787438	4.0598781450	7.4572791330
0.300	0.5118933420	4.0690352980	7.4648179930
0.310	0.5274857599	4.0784006450	7.4725785460
0.320	0.5429547828	4.0879654400	7.4805571780
0.330	0.5582993918	4.0977208760	7.4887501280
0.340	0.5735187601	4.1076580990	7.4971534950
0.350	0.5886122475	4.1177682250	7.5057632330
0.360	0.6035793956	4.1280423600	7.5145751540
0.370	0.6184199222	4.1384716140	7.5235849310
0.380	0.6331337153	4.1490471170	7.5327880960
0.390	0.6477208269	4.1597600370	7.5421800450
0.400	0.6621814667	4.1706015930	7.5517560400
0.410	0.6765159951	4.1815630730	7.5615112130
0.420	0.6907249171	4.1926358450	7.5714405650
0.430	0.7048088746	4.2038113750	7.5815389790
0.440	0.7187686397	4.2150812370	7.5918012130
0.450	0.7326051079	4.2264371270	7.6022219160
0.460	0.7463192905	4.2378708750	7.6127956250
0.470	0.7599123078	4.2493744560	7.6235167760
0.480	0.7733853821	4.2609400030	7.6343797070
0.490	0.7867398307	4.2725598130	7.6453786670
0.500	0.7999770587	4.2842263600	7.6565078220
0.510	0.8130985529	4.2959323010	7.6677612630

0.520	0.8261058743	4.3076704830	7.6791330140
0.530	0.8390006526	4.3194339530	7.6906170370
0.540	0.8517845790	4.3312159630	7.7022072470
0.550	0.8644594007	4.3430099740	7.7138975150
0.560	0.8770269146	4.3548096610	7.7256816790
0.570	0.8894889619	4.3666089190	7.7375535530
0.580	0.9018474223	4.3784018620	7.7495069370
0.590	0.9141042089	4.3901828310	7.7615356250
0.600	0.9262612631	4.4019463910	7.7736334170
0.610	0.9383205498	4.4136873350	7.7857941270
0.620	0.9502840528	4.4254006810	7.7980115900
0.630	0.9621537703	4.4370816780	7.8102796780
0.640	0.9739317111	4.4487257980	7.8225923040
0.650	0.9856198902	4.4603287410	7.8349434320
0.660	0.9972203258	4.4718864270	7.8473270880
0.670	1.0087350350	4.4833950010	7.8597373700
0.680	1.0201660320	4.4948508230	7.8721684530
0.690	1.0315153220	4.5062504690	7.8846145990
0.700	1.0427849040	4.5175907270	7.8970701680
0.710	1.0539767610	4.5288685920	7.9095296210
0.720	1.0650928640	4.5400812620	7.9219875310
0.730	1.0761351660	4.5512261340	7.9344385880
0.740	1.0871056020	4.5623008000	7.9468776070
0.750	1.0980060830	4.5733030370	7.9592995350
0.760	1.1088385030	4.5842308090	7.9716994520
0.770	1.1196047270	4.5950822560	7.9840725830
0.780	1.1303065980	4.6058556910	7.9964142970
0.790	1.1409459290	4.6165495940	8.0087201150
0.800	1.1515245100	4.6271626050	8.0209857110
0.810	1.1620440970	4.6376935200	8.0332069160
0.820	1.1725064220	4.6481412840	8.0453797250
0.830	1.1829131820	4.6585049840	8.0575002900
0.840	1.1932660450	4.6687838450	8.0695649310
0.850	1.2035666500	4.6789772250	8.0815701330
0.860	1.2138166000	4.6890846050	8.0935125450
0.870	1.2240174680	4.6991055880	8.1053889870
0.880	1.2341707970	4.7090398890	8.1171964400
0.890	1.2442780930	4.7188873340	8.1289320550
0.900	1.2543408330	4.7286478500	8.1405931450
0.910	1.2643604590	4.7383214630	8.1521771900
0.920	1.2743383830	4.7479082890	8.1636818290

0.930	1.2842759830	4.7574085340	8.1751048610
0.940	1.2941746050	4.7668224830	8.1864442450
0.950	1.3040355630	4.7761505000	8.1976980910
0.960	1.3138601380	4.7853930200	8.2088646630
0.970	1.3236495820	4.7945505490	8.2199423730
0.980	1.3334051130	4.8036236510	8.2309297800
0.990	1.3431279200	4.8126129520	8.2418255810
1.000	1.352819162	4.821519134	8.252628613

Table A3:

F=10	ψ=1	η=1.8	λ=0.01, α=0.1
Wavenumber, ξ	**Mode 1**	**Mode 2**	**Mode 3**
0.01	0.0178425680	3.6756570640	5.2757270410
0.02	0.0356669925	3.6773728290	5.2772227760
0.03	0.0534552733	3.6802228350	5.2797203070
0.04	0.0711896956	3.6841927390	5.2832265630
0.05	0.0888529654	3.6892625710	5.2877511870
0.06	0.1064283401	3.6954068600	5.2933064720
0.07	0.1238997486	3.7025947800	5.2999072800
0.08	0.1412519014	3.7107903420	5.3075709390
0.09	0.1584703885	3.7199526220	5.3163171090
0.10	0.1755417639	3.7300360260	5.3261676230
0.11	0.1924536162	3.7409906050	5.3371463040
0.12	0.2091946236	3.7527623990	5.3492787360
0.13	0.2257545958	3.7652938340	5.3625920070
0.14	0.2421244996	3.7785241610	5.3771144180
0.15	0.2582964711	3.7923899320	5.3928751490
0.16	0.2742638145	3.8068255170	5.4099038880
0.17	0.2900209882	3.8217636630	5.4282304310
0.18	0.3055635792	3.8371360680	5.4478842460
0.19	0.3208882681	3.8528739980	5.4688940140
0.20	0.3359927841	3.8689089020	5.4912871490
0.21	0.3508758540	3.8851730380	5.5150893100
0.22	0.3655371437	3.9016000940	5.5403239150
0.23	0.3799771960	3.9181257830	5.5670116600
0.24	0.3941973648	3.9346884080	5.5951700730
0.25	0.4081997469	3.9512293800	5.6248130920
0.26	0.4219871131	3.9676936790	5.6559506960
0.27	0.4355628390	3.9840302470	5.6885885900
0.28	0.4489308370	4.0001922960	5.7227279520
0.29	0.4620954898	4.0161375490	5.7583652480

0.30	0.4750615864	4.0318283790	5.7954921200
0.31	0.4878342606	4.0472318740	5.8340953350
0.32	0.5004189331	4.0623198160	5.8741568080
0.33	0.5128212570	4.0770685850	5.9156536730
0.34	0.5250470670	4.0914589960	5.9585584010
0.35	0.5371023328	4.1054760790	6.0028389660
0.36	0.5489931160	4.1191088120	6.0484590120
0.37	0.5607255313	4.1323498170	6.0953780520
0.38	0.5723057111	4.1451950380	6.1435516470
0.39	0.5837397745	4.1576434020	6.1929315690
0.40	0.5950337988	4.1696964730	6.2434659400
0.41	0.6061937958	4.1813581220	6.2950993160
0.42	0.6172256900	4.1926341910	6.3477727250
0.43	0.6281353005	4.2035321930	6.4014236260
0.44	0.6389283253	4.2140610180	6.4559857990
0.45	0.6496103287	4.2242306690	6.5113891410
0.46	0.6601867302	4.2340520230	6.5675593630
0.47	0.6706627961	4.2435366140	6.6244175750
0.48	0.6810436331	4.2526964430	6.6818797530
0.49	0.6913341831	4.2615438150	6.7398560780
0.50	0.7015392199	4.2700911920	6.7982501350
0.51	0.7116633470	4.2783510750	6.8569579750
0.52	0.7217109970	4.2863358980	6.9158670430
0.53	0.7316864317	4.2940579470	6.9748549770
0.54	0.7415937430	4.3015292880	7.0337883290
0.55	0.7514368548	4.3087617140	7.0925212370
0.56	0.7612195258	4.3157666980	7.1508941710
0.57	0.7709453520	4.3225553670	7.2087328790
0.58	0.7806177707	4.3291384720	7.2658477490
0.59	0.7902400643	4.3355263730	7.3220338670
0.60	0.7998153642	4.3417290320	7.3770721270
0.61	0.8093466554	4.3477560070	7.4307317990
0.62	0.8188367813	4.3536164500	7.4827749530
0.63	0.8282884479	4.3593191130	7.5329630220
0.64	0.8377042292	4.3648723550	7.5810655460
0.65	0.8470865714	4.3702841460	7.6268707020
0.66	0.8564377984	4.3755620830	7.6701967400
0.67	0.8657601159	4.3807133970	7.7109029250
0.68	0.8750556169	4.3857449700	7.7488983310
0.69	0.8843262858	4.3906633430	7.7841469760
0.70	0.8935740032	4.3954747330	7.8166683530

0.71	0.9028005506	4.4001850460	7.8465333010
0.72	0.9120076145	4.4047998920	7.8738560540
0.73	0.9211967909	4.4093245960	7.8987839220
0.74	0.9303695894	4.4137642120	7.9214862210
0.75	0.9395274371	4.4181235390	7.9421438480
0.76	0.9486716827	4.4224071290	7.9609404290
0.77	0.9578036001	4.4266193040	7.9780554900
0.78	0.9669243919	4.4307641650	7.9936596590
0.79	0.9760351932	4.4348456030	8.0079116740
0.80	0.9851370747	4.4388673120	8.0209568470
0.81	0.9942310460	4.4428327990	8.0329265860
0.82	1.0033180580	4.4467453930	8.0439386690
0.83	1.0123990090	4.4506082530	8.0540979760
0.84	1.0214747400	4.4544243820	8.0634974730
0.85	1.0305460480	4.4581966300	8.0722193290
0.86	1.0396136780	4.4619277060	8.0803360380
0.87	1.0486783340	4.4656201830	8.0879115080
0.88	1.0577406760	4.4692765070	8.0950020740
0.89	1.0668013240	4.4728990020	8.1016574230
0.90	1.0758608600	4.4764898810	8.1079214180
0.91	1.0849198310	4.4800512460	8.1138328350
0.92	1.0939787480	4.4835850970	8.1194260010
0.93	1.1030380910	4.4870933390	8.1247313640
0.94	1.1120983090	4.4905777830	8.1297759750
0.95	1.1211598230	4.4940401540	8.1345839210
0.96	1.1302230260	4.4974820960	8.1391766900
0.97	1.1392882850	4.5009051740	8.1435734900
0.98	1.1483559430	4.5043108790	8.1477915310
0.99	1.1574263190	4.5077006320	8.1518462600
1.00	1.1664997120	4.5110757890	8.1557515730

Table A4:

F=100	ψ=1	η=1.8	λ=0.01, α=0.1
Wavenumber, ξ	**Mode 1**	**Mode 2**	**Mode 3**
0.01	0.0178219914	1.5827383270	4.2100467230
0.02	0.0355040951	1.5919544800	4.2100930690
0.03	0.0529149034	1.6072070300	4.2101704050
0.04	0.0699389003	1.6283396550	4.2102788690
0.05	0.0864819597	1.6551434750	4.2104186600
0.06	0.1024744650	1.6873659450	4.2105900420
0.07	0.1178720106	1.7247209020	4.2107933460

0.08	0.1326540110	1.7668989450	4.2110289800
0.09	0.1468207744	1.8135774450	4.2112974370
0.10	0.1603896778	1.8644295670	4.2115993060
0.11	0.1733910317	1.9191319360	4.2119352860
0.12	0.1858640957	1.9773707350	4.2123062050
0.13	0.1978535489	2.0388462300	4.2127130400
0.14	0.2094065700	2.1032758440	4.2131569430
0.15	0.2205705706	2.1703959570	4.2136392760
0.16	0.2313915413	2.2399626890	4.2141616580
0.17	0.2419129307	2.3117518730	4.2147260110
0.18	0.2521749581	2.3855584540	4.2153346360
0.19	0.2622142598	2.4611954710	4.2159903030
0.20	0.2720637828	2.5384927700	4.2166963650
0.21	0.2817528478	2.6172955530	4.2174569210
0.22	0.2913073257	2.6974628280	4.2182770180
0.23	0.3007498813	2.7788657960	4.2191629420
0.24	0.3101002509	2.8613861740	4.2201226110
0.25	0.3193755329	2.9449144440	4.2211661300
0.26	0.3285904730	3.0293479350	4.2223065870
0.27	0.3377577372	3.1145886340	4.2235612330
0.28	0.3468881648	3.2005404900	4.2249532400
0.29	0.3559909990	3.2871058390	4.2265144510
0.30	0.3650740953	3.3741802520	4.2282897770
0.31	0.3741441062	3.4616445390	4.2303445220
0.32	0.3832066452	3.5493513990	4.2327771400
0.33	0.3922664300	3.6371015240	4.2357425940
0.34	0.4013274083	3.7245977750	4.2394977110
0.35	0.4103928669	3.8113507410	4.2444951990
0.36	0.4194655261	3.8964700790	4.2515919390
0.37	0.4285476221	3.9781826000	4.2625305610
0.38	0.4376409769	4.0528040190	4.2809674040
0.39	0.4467470601	4.1137007790	4.3135104290
0.40	0.4558670405	4.1548752280	4.3661338060
0.41	0.4650018315	4.1787872370	4.4363560910
0.42	0.4741521299	4.1926179650	4.5169762750
0.43	0.4833184489	4.2013193690	4.6030241070
0.44	0.4925011466	4.2073331630	4.6920409890
0.45	0.5017004504	4.2118325950	4.7828380610
0.46	0.5109164780	4.2154171650	4.8748013710
0.47	0.5201492550	4.2184165240	4.9675878590
0.48	0.5293987307	4.2210243510	5.0609913920

0.49	0.5386647907	4.2233609880	5.1548800340
0.50	0.5479472681	4.2255047910	5.2491646140
0.51	0.5572459536	4.2275088110	5.3437819770
0.52	0.5665606030	4.2294101740	5.4386855310
0.53	0.5758909445	4.2312355980	5.5338396670
0.54	0.5852366844	4.2330047790	5.6292163130
0.55	0.5945975122	4.2347325450	5.7247927230
0.56	0.6039731051	4.2364302640	5.8205500130
0.57	0.6133631311	4.2381067910	5.9164721570
0.58	0.6227672525	4.2397691230	6.0125452730
0.59	0.6321851283	4.2414228600	6.1087571020
0.60	0.6416164161	4.2430725320	6.2050966050
0.61	0.6510607744	4.2447218440	6.3015536480
0.62	0.6605178637	4.2463738530	6.3981187180
0.63	0.6699873479	4.2480311030	6.4947826720
0.64	0.6794688951	4.2496957240	6.5915364690
0.65	0.6889621789	4.2513695170	6.6883708720
0.66	0.6984668785	4.2530540090	6.7852760730
0.67	0.7079826795	4.2547505070	6.8822411870
0.68	0.7175092744	4.2564601310	6.9792535130
0.69	0.7270463626	4.2581838490	7.0762973980
0.70	0.7365936511	4.2599225000	7.1733523790
0.71	0.7461508539	4.2616768120	7.2703899860
0.72	0.7557176930	4.2634474230	7.3673678740
0.73	0.7652938976	4.2652348910	7.4642182390
0.74	0.7748792045	4.2670397070	7.5608228720
0.75	0.7844733583	4.2688623030	7.6569529270
0.76	0.7940761108	4.2707030610	7.7521002520
0.77	0.8036872210	4.2725623190	7.8449020890
0.78	0.8133064555	4.2744403770	7.9307042280
0.79	0.8229335876	4.2763375010	7.9935484260
0.80	0.8325683978	4.2782539290	8.0206361760
0.81	0.8422106733	4.2801898720	8.0308342920
0.82	0.8518602078	4.2821455170	8.0359894730
0.83	0.8615168016	4.2841210340	8.0393034810
0.84	0.8711802613	4.2861165710	8.0417797680
0.85	0.8808503995	4.2881322630	8.0438140330
0.86	0.8905270347	4.2901682280	8.0455908000
0.87	0.9002099913	4.2922245730	8.0472070290
0.88	0.9098990990	4.2943013930	8.0487183530
0.89	0.9195941933	4.2963987710	8.0501589080

0.90	0.9292951145	4.2985167820	8.0515507740
0.91	0.9390017082	4.3006554920	8.0529088560
0.92	0.9487138250	4.3028149590	8.0542435700
0.93	0.9584313199	4.3049952340	8.0555624160
0.94	0.9681540528	4.3071963610	8.0568709250
0.95	0.9778818880	4.3094183800	8.0581732680
0.96	0.9876146937	4.3116613230	8.0594726460
0.97	0.9973523428	4.3139252180	8.0607715580
0.98	1.0070947120	4.3162100890	8.0620719830
0.99	1.0168416810	4.3185159560	8.0633755060
1.00	1.0265931350	4.3208428340	8.0646834130

Table A5:

F=0	ψ=2	η=1.8	λ=0.01, α=0.1
Wavenumber, ξ	**Mode 1**	**Mode 2**	**Mode 3**
0.01	0.0124519952	4.1103976850	7.8440824400
0.02	0.0249034106	4.1105428480	7.8441754380
0.03	0.0373536671	4.1107847370	7.8443304140
0.04	0.0498021862	4.1111232770	7.8445473360
0.05	0.0622483909	4.1115583630	7.8448261580
0.06	0.0746917061	4.1120898610	7.8451668250
0.07	0.0871315589	4.1127176060	7.8455692660
0.08	0.0995673791	4.1134414050	7.8460333980
0.09	0.1119985996	4.1142610350	7.8465591270
0.10	0.1244246568	4.1151762430	7.8471463440
0.11	0.1368449915	4.1161867490	7.8477949300
0.12	0.1492590485	4.1172922430	7.8485047510
0.13	0.1616662777	4.1184923870	7.8492756640
0.14	0.1740661341	4.1197868150	7.8501075110
0.15	0.1864580786	4.1211751320	7.8510001220
0.16	0.1988415779	4.1226569170	7.8519533160
0.17	0.2112161053	4.1242317230	7.8529668990
0.18	0.2235811408	4.1258990730	7.8540406670
0.19	0.2359361717	4.1276584660	7.8551744010
0.20	0.2482806927	4.1295093750	7.8563678730
0.21	0.2606142065	4.1314512470	7.8576208420
0.22	0.2729362238	4.1334835050	7.8589330570
0.23	0.2852462640	4.1356055470	7.8603042540
0.24	0.2975438551	4.1378167460	7.8617341580
0.25	0.3098285344	4.1401164530	7.8632224850
0.26	0.3220998485	4.1425039970	7.8647689370

0.27	0.3343573536	4.1449786820	7.8663732080
0.28	0.3466006158	4.1475397920	7.8680349800
0.29	0.3588292114	4.1501865910	7.8697539240
0.30	0.3710427269	4.1529183190	7.8715297020
0.31	0.3832407595	4.1557342000	7.8733619650
0.32	0.3954229172	4.1586334360	7.8752503560
0.33	0.4075888186	4.1616152120	7.8771945050
0.34	0.4197380936	4.1646786940	7.8791940350
0.35	0.4318703835	4.1678230310	7.8812485600
0.36	0.4439853407	4.1710473560	7.8833576820
0.37	0.4560826291	4.1743507840	7.8855209970
0.38	0.4681619244	4.1777324170	7.8877380900
0.39	0.4802229138	4.1811913410	7.8900085390
0.40	0.4922652964	4.1847266290	7.8923319140
0.41	0.5042887828	4.1883373410	7.8947077750
0.42	0.5162930959	4.1920225230	7.8971356750
0.43	0.5282779703	4.1957812100	7.8996151610
0.44	0.5402431524	4.1996124260	7.9021457700
0.45	0.5521884007	4.2035151860	7.9047270330
0.46	0.5641134856	4.2074884920	7.9073584740
0.47	0.5760181893	4.2115313400	7.9100396100
0.48	0.5879023060	4.2156427170	7.9127699510
0.49	0.5997656417	4.2198216010	7.9155490030
0.50	0.6116080140	4.2240669660	7.9183762640
0.51	0.6234292524	4.2283777770	7.9212512260
0.52	0.6352291979	4.2327529950	7.9241733760
0.53	0.6470077032	4.2371915760	7.9271421960
0.54	0.6587646323	4.2416924720	7.9301571630
0.55	0.6704998604	4.2462546320	7.9332177480
0.56	0.6822132741	4.2508770000	7.9363234210
0.57	0.6939047711	4.2555585200	7.9394736420
0.58	0.7055742599	4.2602981350	7.9426678720
0.59	0.7172216598	4.2650947860	7.9459055670
0.60	0.7288469007	4.2699474140	7.9491861770
0.61	0.7404499232	4.2748549610	7.9525091520
0.62	0.7520306779	4.2798163680	7.9558739370
0.63	0.7635891257	4.2848305800	7.9592799750
0.64	0.7751252375	4.2898965440	7.9627267070
0.65	0.7866389937	4.2950132080	7.9662135700
0.66	0.7981303846	4.3001795260	7.9697400010
0.67	0.8095994097	4.3053944530	7.9733054330

0.68	0.8210460775	4.3106569500	7.9769093010
0.69	0.8324704058	4.3159659840	7.9805510360
0.70	0.8438724208	4.3213205240	7.9842300670
0.71	0.8552521576	4.3267195480	7.9879458260
0.72	0.8666096592	4.3321620400	7.9916977410
0.73	0.8779449771	4.3376469900	7.9954852410
0.74	0.8892581705	4.3431733950	7.9993077560
0.75	0.9005493062	4.3487402600	8.0031647150
0.76	0.9118184584	4.3543465990	8.0070555460
0.77	0.9230657087	4.3599914330	8.0109796810
0.78	0.9342911456	4.3656737930	8.0149365510
0.79	0.9454948642	4.3713927200	8.0189255880
0.80	0.9566769664	4.3771472620	8.0229462250
0.81	0.9678375602	4.3829364800	8.0269978980
0.82	0.9789767597	4.3887594420	8.0310800430
0.83	0.9900946849	4.3946152290	8.0351920990
0.84	1.0011914610	4.4005029320	8.0393335070
0.85	1.0122672200	4.4064216530	8.0435037100
0.86	1.0233220980	4.4123705060	8.0477021540
0.87	1.0343562350	4.4183486150	8.0519282880
0.88	1.0453697780	4.4243551170	8.0561815620
0.89	1.0563628770	4.4303891620	8.0604614330
0.90	1.0673356870	4.4364499090	8.0647673560
0.91	1.0782883670	4.4425365330	8.0690987950
0.92	1.0892210790	4.4486482190	8.0734552130
0.93	1.1001339910	4.4547841660	8.0778360790
0.94	1.1110272720	4.4609435850	8.0822408670
0.95	1.1219010950	4.4671257010	8.0866690520
0.96	1.1327556370	4.4733297500	8.0911201160
0.97	1.1435910780	4.4795549830	8.0955935440
0.98	1.1544075980	4.4858006640	8.1000888250
0.99	1.1652053850	4.4920660700	8.1046054560
1.00	1.1759846230	4.4983504910	8.1091429340

Table A6:

F=1	ψ=2	η=1.8	λ=0.01, α=0.1
[redacted]			
Wavenumber, ξ	**Mode 1**	**Mode 2**	**Mode 3**
0.01	0.0124518383	4.1017944730	7.7205160740
0.02	0.0249021561	4.1019727330	7.7207862160
0.03	0.0373494362	4.1022696090	7.7212359560
0.04	0.0497921675	4.1026847670	7.7218645490

0.05	0.0622288485	4.1032177380	7.7226709580
0.06	0.0746579899	4.1038679260	7.7236538550
0.07	0.0870781182	4.1046346020	7.7248116270
0.08	0.0994877782	4.1055169150	7.7261423800
0.09	0.1118855359	4.1065138850	7.7276439510
0.10	0.1242699816	4.1076244160	7.7293139060
0.11	0.1366397322	4.1088472930	7.7311495610
0.12	0.1489934341	4.1101811860	7.7331479790
0.13	0.1613297654	4.1116246600	7.7353059900
0.14	0.1736474383	4.1131761710	7.7376201980
0.15	0.1859452013	4.1148340790	7.7400869910
0.16	0.1982218412	4.1165966470	7.7427025590
0.17	0.2104761852	4.1184620480	7.7454629000
0.18	0.2227071022	4.1204283720	7.7483638390
0.19	0.2349135047	4.1224936300	7.7514010410
0.20	0.2470943502	4.1246557600	7.7545700230
0.21	0.2592486423	4.1269126340	7.7578661720
0.22	0.2713754318	4.1292620610	7.7612847570
0.23	0.2834738179	4.1317017970	7.7648209470
0.24	0.2955429485	4.1342295460	7.7684698240
0.25	0.3075820210	4.1368429720	7.7722263970
0.26	0.3195902829	4.1395397010	7.7760856240
0.27	0.3315670319	4.1423173250	7.7800424180
0.28	0.3435116160	4.1451734150	7.7840916670
0.29	0.3554234334	4.1481055190	7.7882282500
0.30	0.3673019326	4.1511111730	7.7924470450
0.31	0.3791466118	4.1541879040	7.7967429500
0.32	0.3909570189	4.1573332360	7.8011108900
0.33	0.4027327503	4.1605446950	7.8055458360
0.34	0.4144734507	4.1638198130	7.8100428110
0.35	0.4261788122	4.1671561370	7.8145969060
0.36	0.4378485733	4.1705512260	7.8192032890
0.37	0.4494825181	4.1740026640	7.8238572150
0.38	0.4610804751	4.1775080580	7.8285540380
0.39	0.4726423162	4.1810650430	7.8332892160
0.40	0.4841679551	4.1846712880	7.8380583210
0.41	0.4956573465	4.1883244980	7.8428570470
0.42	0.5071104847	4.1920224160	7.8476812160
0.43	0.5185274016	4.1957628280	7.8525267810
0.44	0.5299081663	4.1995435640	7.8573898350
0.45	0.5412528827	4.2033625010	7.8622666130

0.46	0.5525616887	4.2072175650	7.8671534950
0.47	0.5638347541	4.2111067330	7.8720470090
0.48	0.5750722797	4.2150280380	7.8769438350
0.49	0.5862744952	4.2189795620	7.8818408020
0.50	0.5974416583	4.2229594460	7.8867348940
0.51	0.6085740525	4.2269658870	7.8916232460
0.52	0.6196719860	4.2309971400	7.8965031440
0.53	0.6307357903	4.2350515180	7.9013720260
0.54	0.6417658183	4.2391273900	7.9062274790
0.55	0.6527624433	4.2432231870	7.9110672380
0.56	0.6637260572	4.2473373980	7.9158891810
0.57	0.6746570694	4.2514685690	7.9206913310
0.58	0.6855559050	4.2556153090	7.9254718470
0.59	0.6964230040	4.2597762800	7.9302290260
0.60	0.7072588197	4.2639502050	7.9349612960
0.61	0.7180638174	4.2681358640	7.9396672140
0.62	0.7288384732	4.2723320930	7.9443454590
0.63	0.7395832729	4.2765377840	7.9489948320
0.64	0.7502987108	4.2807518830	7.9536142490
0.65	0.7609852887	4.2849733910	7.9582027370
0.66	0.7716435148	4.2892013600	7.9627594290
0.67	0.7822739023	4.2934348970	7.9672835610
0.68	0.7928769692	4.2976731550	7.9717744660
0.69	0.8034532366	4.3019153400	7.9762315690
0.70	0.8140032285	4.3061607040	7.9806543850
0.71	0.8245274705	4.3104085460	7.9850425110
0.72	0.8350264890	4.3146582110	7.9893956270
0.73	0.8455008109	4.3189090870	7.9937134840
0.74	0.8559509623	4.3231606060	7.9979959060
0.75	0.8663774683	4.3274122380	8.0022427840
0.76	0.8767808521	4.3316634980	8.0064540700
0.77	0.8871616346	4.3359139340	8.0106297770
0.78	0.8975203336	4.3401631340	8.0147699710
0.79	0.9078574638	4.3444107220	8.0188747700
0.80	0.9181735355	4.3486563540	8.0229443400
0.81	0.9284690551	4.3528997210	8.0269788910
0.82	0.9387445238	4.3571405440	8.0309786740
0.83	0.9490004380	4.3613785760	8.0349439770
0.84	0.9592372883	4.3656135960	8.0388751240
0.85	0.9694555599	4.3698454140	8.0427724700
0.86	0.9796557315	4.3740738650	8.0466364000

0.87	0.9898382756	4.3782988070	8.0504673260
0.88	1.0000036580	4.3825201250	8.0542656830
0.89	1.0101523390	4.3867377260	8.0580319270
0.90	1.0202847690	4.3909515370	8.0617665360
0.91	1.0304013940	4.3951615060	8.0654700040
0.92	1.0405026520	4.3993676030	8.0691428410
0.93	1.0505889730	4.4035698130	8.0727855700
0.94	1.0606607800	4.4077681400	8.0763987260
0.95	1.0707184880	4.4119626040	8.0799828550
0.96	1.0807625060	4.4161532400	8.0835385110
0.97	1.0907932330	4.4203400990	8.0870662550
0.98	1.1008110610	4.4245232440	8.0905666560
0.99	1.1108163760	4.4287027510	8.0940402840
1.00	1.1208095530	4.4328787090	8.0974877160

Table A7:

F=10	ψ=2	η=1.8	λ=0.01, α=0.1
Wavenumber, ξ	**Mode 1**	**Mode 2**	**Mode 3**
0.01	0.0124504273	3.5216083770	4.3232095990
0.05	0.0620557453	3.5502237130	4.3276115500
0.10	0.1229616499	3.6359787630	4.3432246430
0.15	0.1819077732	3.7653080620	4.3771914030
0.20	0.2385723577	3.9124554710	4.4481309650
0.25	0.2930522800	4.0369678630	4.5885407060
0.30	0.3456874533	4.1146276280	4.8148798950
0.35	0.3968961402	4.1579265810	5.1076901540
0.40	0.4470718827	4.1841156240	5.4437677680
0.45	0.4965389255	4.2021943620	5.8091464690
0.50	0.5455442922	4.2162500300	6.1955762470
0.55	0.5942669230	4.2282371030	6.5974058160
0.60	0.6428319704	4.2391691910	7.0096121910
0.65	0.6913246183	4.2496123260	7.4241731690
0.70	0.7398014335	4.2599025290	7.8048664700
0.75	0.7882989758	4.2702493580	7.9850886960
0.80	0.8368400472	4.2807887480	8.0229269410
0.85	0.8854381083	4.2916116620	8.0384234800
0.90	0.9341003520	4.3027804480	8.0487536140
0.95	0.9828298198	4.3143385940	8.0573159730
1.00	1.0316268490	4.3263167710	8.0651866210

Table A8:

F=100	ψ=2	η=1.8	λ=0.01, α=0.1
Wavenumber, ξ	**Mode 1**	**Mode 2**	**Mode 3**
0.010	0.0124364065	1.1782469130	4.1757568150
0.050	0.0605616722	1.2755775180	4.1760501460
0.100	0.1149291647	1.5410631520	4.1769678850
0.150	0.1650511645	1.9034179600	4.1785017340
0.200	0.2137589255	2.3176408950	4.1806611520
0.250	0.2622496423	2.7604044200	4.1834698190
0.300	0.3108755620	3.2198360850	4.1870000820
0.350	0.3597048443	3.6893023630	4.1916020690
0.375	-	3.9258337610	4.1950909190
0.400	0.4087244752	4.1507017030	4.2118131010
0.425	-	4.1934925540	4.4119499950
0.450	0.4579036651	4.1979418370	4.6515807910
0.500	0.5072121686	4.2044503370	5.1361191530
0.550	0.5566246656	4.2109610850	5.6237949730
0.600	0.6061210140	4.2179150930	6.1135477550
0.650	0.6556854450	4.2253947600	6.6048501320
0.700	0.7053056352	4.2334249290	7.0973319900
0.750	0.7549719099	4.2420141510	7.5905939230
0.775	-	4.2465192830	7.8369714140
0.800	0.8046766172	4.2511648110	8.0226963620
0.825	-	4.2559506080	8.0281728990
0.850	0.8544136532	4.2608764640	8.0311204890
0.900	0.9041781049	4.2711471700	8.0367654530
0.950	0.9539659828	4.2819740930	8.0425895260
0.990	0.9938109362	-	-
1.000	-	4.2933538090	8.0486852500

Table A9:

F=0	ψ=3	η=1.8	λ=0.01, α=0.1
Wavenumber, ξ	**Mode 1**	**Mode 2**	**Mode 3**
0.01	0.0107868758	4.152298999	7.936586932
0.05	0.0539307392	4.152856411	7.936961473
0.10	0.1078388221	4.154594765	7.938128893
0.15	0.1617020500	4.157480136	7.940064530
0.20	0.2154991198	4.161495060	7.942753630
0.25	0.2692100255	4.166615792	7.946176200
0.30	0.3228164068	4.172812966	7.950307628
0.35	0.3763018329	4.180052382	7.955119410

0.40	0.4296520163	4.188295879	7.960579961
0.45	0.4828549492	4.197502261	7.966655454
0.50	0.5359009679	4.207628221	7.973310665
0.55	0.5887827466	4.218629250	7.980509770
0.60	0.6414952294	4.230460477	7.988217087
0.65	0.6940355103	4.243077428	7.996397726
0.70	0.7464026714	4.256436693	8.005018141
0.75	0.7985975911	4.270496471	8.014046574
0.80	0.8506227323	4.285217012	8.023453389
0.85	0.9024819217	4.300560947	8.033211311
0.90	0.9541801275	4.316493507	8.043295558
0.95	1.0057232440	4.332982657	8.053683906
1.00	1.0571178870	4.349999142	8.064356668

Table A10:

F=1	ψ=3	η=1.8	λ=0.01, α=0.1
Wavenumber, ξ	**Mode 1**	**Mode 2**	**Mode 3**
0.01	0.0107867572	4.144854665	7.105120102
0.05	0.0539159977	4.145669344	7.119654364
0.10	0.1077228675	4.148170200	7.164566177
0.15	0.1613214085	4.152195533	7.237603137
0.20	0.2146304365	4.157559167	7.335601731
0.25	0.2675917600	4.164047001	7.453003173
0.30	0.3201716376	4.171446325	7.580237714
0.35	0.3723591421	4.179567720	7.702254159
0.40	0.4241623918	4.188257291	7.802158762
0.45	0.4756037523	4.197400169	7.872576521
0.50	0.5267149590	4.206917882	7.918902991
0.55	0.5775328026	4.216762444	7.949900674
0.60	0.6280957008	4.226909390	7.971878806
0.65	0.6784412238	4.237351165	7.988529357
0.70	0.7286044859	4.248091554	8.001944347
0.75	0.7786172373	4.259141347	8.013339823
0.80	0.8285074764	4.270515158	8.023452081
0.85	0.8782994171	4.282229214	8.032745905
0.90	0.9280136799	4.294299883	8.041526067
0.95	0.9776676075	4.306742757	8.049999214
1.00	1.0272756360	4.319572118	8.058309587

Table A11:

F=10	ψ=3	η=1.8	λ=0.01, α=0.1

Wavenumber, ξ	**Mode 1**	**Mode 2**	**Mode 3**
0.010	0.010785692	2.481861187	4.180249914
0.050	0.053788136	2.529549733	4.180609079
0.100	0.106815478	2.673095138	4.181752552
0.150	0.158757475	2.896511814	4.183746575
0.200	0.209724618	3.182772360	4.186816166
0.250	0.260005263	3.515685489	4.191711120
0.300	0.309871796	3.878523713	4.202813127
0.320	-	4.022195613	4.216678694
0.335	-	4.111629394	4.247923685
0.345	-	4.147364934	4.293744512
0.350	0.359517458	4.157878452	4.324322148
0.360	-	4.170478757	4.394501739
0.370	-	4.177466403	4.471055096
0.380	-	4.181966728	4.550816473
0.400	0.409061772	4.187799724	4.715520062
0.410	-	4.189962137	4.799563927
0.450	0.458573006	4.196747359	5.143152874
0.500	0.508087872	4.203894220	5.584581917
0.550	0.557624785	4.210910513	6.035597601
0.600	0.607191930	4.218203020	6.493889416
0.650	0.656791935	4.225917228	6.957805454
0.700	0.706424512	4.234116599	7.425772865
0.720	-	4.237539730	7.613410941
0.735	-	4.240162091	7.753543379
0.745	-	4.241936755	7.845630498
0.750	0.756087934	4.242832052	7.890420530
0.765	-	4.245549938	7.995153101
0.780	-	4.248316012	8.017176532
0.800	0.805779849	4.252079437	8.023439573
0.850	0.855497713	4.261866799	8.030823185
0.900	0.905239024	4.272197775	8.036882219
0.950	0.955001432	4.283073330	8.042919502
0.990	0.994825096	-	-
1.000	-	4.294492709	8.049142170

Table A12:

F=100	**ψ=3**	**η=1.8**	**λ=0.01, α=0.1**
Wavenumber, ξ	**Mode 1**	**Mode 2**	**Mode 3**
0.01	0.0107751923	0.8001214139	4.1713686130

0.05	0.0528556562	0.9380370606	4.1716566180
0.10	0.1031334287	1.2765423560	4.1725565740
0.15	0.1526822790	1.6968693440	4.1740563240
0.20	0.2022337679	2.1515682300	4.1761557620
0.25	0.2518832326	2.6228117840	4.1788552600
0.30	0.3016166456	3.1030632930	4.1821572780
0.35	0.3514113379	3.5886888380	4.1860758400
0.36	-	3.6862659470	4.1869389680
0.37	-	3.7839614760	4.1878331240
0.38	-	3.8817589840	4.1887652370
0.39	-	3.9796301310	4.1897550540
0.40	0.4012499337	4.0774797550	4.1908899630
0.41	-	4.1734197490	4.1940510170
0.42	-	4.1918586830	4.2748232280
0.43	-	4.1931809920	4.3728163190
0.44	-	4.1943103580	4.4711012680
0.45	0.4511203916	4.1954153590	4.5695046120
0.50	0.5010144530	4.2011432360	5.0625842770
0.55	0.5509263776	4.2074063210	5.5569392860
0.60	0.6008520951	4.2142429540	6.0522284490
0.65	0.6507886573	4.2216568980	6.5482349300
0.70	0.7007338861	4.2296471220	7.0448042530
0.75	0.7506861412	4.2382111810	7.5418164420
0.76	-	4.2399925900	7.6412606690
0.77	-	4.2417968030	7.7407134960
0.78	-	4.2436237950	7.8401654160
0.79	-	4.2454735360	7.9395646990
0.80	0.8006441670	4.2473459980	8.0231454320
0.81	-	4.2492411540	8.0249189470
0.82	-	4.2511589730	8.0259932860
0.83	-	4.2530994260	8.0270426770
0.84	-	4.2550624830	8.0280940170
0.85	0.8506069867	4.2570481130	8.0291533370
0.90	0.9005738304	4.2673137820	8.0346143450
0.95	0.9505440833	4.2781390250	8.0403733590
0.99	0.9905224034	-	-
1.00	-	4.2895196580	8.0464365980

Table A13:

1st Mode	ψ=0	η=1.25	λ=0.01	α=0.1
Wavenumber, ξ	F=0	F=1	F=10	F=100

0.0100	-	0.064457080	0.064454637	0.064430217
0.0660	0.428636309	-	-	-
0.0750	0.482497715	0.482383300	0.481353934	0.471111049
0.1250	0.801345455	0.800816394	0.796060776	0.749566454
0.1806	-	-	-	0.994400000
0.2500	1.576156079	1.571960908	1.534563897	1.226098157
0.3110	-	-	-	1.356000000
0.3750	2.297692003	2.283897697	2.164110916	1.448407169
0.4367	-	-	2.424000000	-
0.5000	2.94093336	2.910062858	2.655356739	1.565477037
0.5671	-	-	2.863000000	-
0.6250	3.487604906	3.433110925	3.013642173	1.647854343
0.6926	-	-	3.162000000	-
0.7500	3.931873573	3.850649162	3.268646012	1.719730000
0.8750	4.281562023	4.174542117	3.453389591	1.789910815
1.0000	4.553229237	4.423972750	3.593226803	1.861858940

Table A14:

1st Mode	ψ=1	η=1.25	λ=0.01	α=0.1
Wavenumber, ξ	**F=0**	**F=1**	**F=10**	**F=100**
0.010	0.037167143	0.037166631	0.037162023	0.037116034
0.040	-	-	-	0.145448471
0.065	-	-	-	0.228402672
0.088	-	-	-	0.296296706
0.105	-	-	-	0.340757873
0.125	0.463309040	0.462319183	0.453660937	0.386930968
0.130	-	-	-	0.397491624
0.135	-	-	-	0.407680610
0.148	-	-	-	0.432521758
0.160	-	-	-	0.453494588
0.190	-	-	-	0.498948841
0.250	0.918982104	0.911304232	0.849449298	0.568740018
0.375	1.359854673	1.335239230	1.160126642	0.673777305
0.500	1.779681691	1.725349966	1.392057501	0.765774071
0.625	2.173523655	2.076552769	1.566590531	0.859504039
0.750	2.538016191	2.387467036	1.704292819	0.957751386
0.875	2.871470534	2.659767146	1.819910345	1.060443789
1.000	3.173782161	2.897169458	1.922886527	1.166894017

Table A15:

1st Mode	ψ=2	η=1.25	λ=0.01	α=0.1

Wavenumber, ξ	F=0	F=1	F=10	F=100
0.0100	0.021256004	0.021255451	0.021250482	0.021201038
0.0400	-	-	-	0.081746205
0.0550	0.116876315	0.115972140	0.115972140	-
0.0650	-	-	-	0.125655738
0.0880	-	-	-	0.160015356
0.1050	-	-	-	0.182170043
0.1250	0.265318526	0.264254087	0.255382959	0.205483703
0.1300	-	-	-	0.210940108
0.1350	-	-	-	0.216272025
0.1480	-	-	-	0.229629863
0.1600	-	-	-	0.241427779
0.1856	-	-	0.363100000	
0.1900	-	-	-	0.269395973
0.2500	0.528360746	0.520181398	0.464245498	0.322320042
0.3000	-	-	-	0.365853622
0.3194	-	-	0.558000000	-
0.3750	0.786984714	0.761110681	0.623887609	0.432096091
0.5000	1.039301135	0.983031357	0.753420600	0.545873147
0.6250	1.283762545	1.184697228	0.868809962	0.662972130
0.7500	1.519215670	1.367041089	0.978819240	0.782257618
0.8750	1.744915481	1.532322912	1.087583492	0.902978930
1.0000	1.960505171	1.683358363	1.196889569	1.024673307

Table A16:

1st Mode	ψ=3	η=1.25	λ=0.01	α=0.1
Wavenumber, ξ	**F=0**	**F=1**	**F=10**	**F=100**
0.010	0.014380218	0.014379648	0.014374524	0.014323938
0.125	0.179509433	0.178427922	0.170350683	0.143175035
0.250	0.357578256	0.349627488	0.310004070	0.262162694
0.375	0.532902788	0.509340088	0.432676528	0.383655554
0.500	0.704426512	0.656993658	0.551226457	0.506649167
0.625	0.871405482	0.794440629	0.669822433	0.630379850
0.750	1.033423924	0.924344141	0.789364588	0.754511128
0.875	1.190367280	1.049171773	0.909878437	0.878881282
1.000	1.342367240	1.170830264	1.031203931	0.993438312

Table A17:

1st Mode	ψ=5	η=1.25	λ=0.01	α=0.1

Wavenumber, ξ	F=0	F=1	F=10	F=100
0.010	0.010783492	0.010782519	0.010773869	0.010696838
0.125	0.134532292	0.133016251	0.128296750	0.125478649
0.250	0.267644498	0.260377937	0.252204906	0.250248428
0.375	0.398549838	0.384804815	0.376567997	0.375166794
0.500	0.527215162	0.508612098	0.501204137	0.500125407
0.625	0.654062189	0.632483680	0.625974120	0.625100442
0.750	0.779628434	0.756544078	0.750816766	0.750083755
0.875	0.904378998	0.880782360	0.875702711	0.875071817
1.000	1.028653247	1.005173000	1.001224000	1.000592000

Table A18:

F=0	ψ=0.4	η=2	λ=0.01, α=0.1
Wavenumber, ξ	**Mode 1**	**Mode 2**	**Mode 3**
0.0100	0.020952349	3.052316971	-
0.0750	0.156069489	3.072791821	-
0.1225	0.252039199	3.106842334	-
0.1900	0.381557475	3.180187385	-
0.2575	0.500859731	3.277779217	-
0.3250	0.609014131	3.392609376	-
0.3925	0.706417132	3.517015607	-
0.4600	0.794316340	3.643701315	-
0.4609	-	-	6.102474248
0.5275	0.874334458	3.766622346	6.222777079
0.5950	0.948122555	3.881525881	6.355487031
0.6625	1.017165293	3.986049830	6.494347247
0.7300	1.082703292	4.079448580	6.634119608
0.7975	1.145725986	4.162121211	6.769835310
0.8650	1.206998449	4.235126980	6.897499860
0.9325	1.267099746	4.299802853	7.014504097
0.9900	1.317700239	4.349353748	7.104845462

Table A19:

F=1	ψ=0.4	η=2	λ=0.01, α=0.1
Wavenumber, ξ	**Mode 1**	**Mode 2**	**Mode 3**
0.0100	0.020952128	3.042892635	-
0.0750	0.155978871	3.064354223	-
0.1225	0.251662792	3.099931032	-
0.1900	0.380291957	3.176065929	-
0.2575	0.498124617	3.276280292	-

0.3250	0.604379790	3.392539266	-
0.3925	0.699687191	3.516399317	-
0.4585	-	-	6.084139033
0.4600	0.785514491	3.640244617	6.086888767
0.5275	0.863640646	3.758223566	6.216561944
0.5950	0.935801510	3.866658009	6.354268417
0.6625	1.003510090	3.963911881	6.494216705
0.7300	1.067999148	4.049903274	6.630750100
0.7975	1.130230968	4.125513925	6.759248339
0.8650	1.190935657	4.192084903	6.876682120
0.9325	1.250656260	4.251072764	6.981692604
0.9900	1.301054753	4.296378471	7.061326797

Table A20:

F=10	ψ=0.4	η=2	λ=0.01, α=0.1
Wavenumber, ξ	**Mode 1**	**Mode 2**	**Mode 3**
0.0100	0.020950139	2.940778597	-
0.0750	0.155172734	2.973669437	-
0.1225	0.248375269	3.026687645	-
0.1900	0.369642425	3.133795539	-
0.2575	0.476117608	3.261635985	-
0.3250	0.568802037	3.391896529	-
0.3925	0.650297987	3.51115691	-
0.4161	-	-	5.771861446
0.4600	0.723511645	3.613092303	5.92444887
0.5275	0.790976074	3.697171162	6.149246134
0.5950	0.854648777	3.765886112	6.342283511
0.6625	0.915944632	3.822555578	6.49307698
0.7300	0.975846065	3.870231646	6.604822205
0.7975	1.035017251	3.911365042	6.686966581
0.8650	1.093897837	3.947811369	6.748677105
0.9325	1.152772778	3.980942285	6.796711268
0.9900	1.203058059	4.007312888	6.830283857

Table A21:

F=100	ψ=0.4	η=2	λ=0.01, α=0.1
Wavenumber, ξ	**Mode 1**	**Mode 2**	**Mode 3**
0.0100	0.020930292	1.752283985	3.536987939
0.0500	-	1.815633058	-
0.0750	0.147946227	1.895201862	3.539741872

0.1000	-	2.00157045	-
0.1225	0.223079577	2.116887842	3.545002798
0.1900	0.306128514	2.543613852	3.560944382
0.2400	0.356809191	2.902003032	3.589121337
0.2500	0.366317378	2.973758302	3.598829061
0.2575	0.373351373	3.026737124	3.607698942
0.2600	0.375679386	3.044162945	3.611024998
0.2700	0.384916625	3.112238331	3.626600669
0.2800	0.394048077	3.176705787	3.646755358
0.2900	0.403090519	3.236006338	3.672975474
0.3000	0.412058719	3.288511195	3.706823786
0.3100	0.420965659	3.332983426	3.749476461
0.3200	0.429822722	3.369084771	3.801216595
0.3250	0.43423571	3.384178519	3.830296266
0.3300	0.438639859	3.397499678	3.861308906
0.3400	0.447425764	3.419557145	3.9283777
0.3450	0.451809408	3.428662123	3.964054462
0.3500	0.456188001	3.436711847	4.000925386
0.3600	0.464933148	3.450222327	4.077653696
0.3700	0.473666908	3.461057991	4.15755645
0.3800	0.482394212	3.469926195	4.239892158
0.3925	0.493300694	3.479001113	4.34542823
0.4600	0.552382479	3.509034944	4.943661108
0.5275	0.612137259	3.527426729	5.563117803
0.5400	-	-	5.678333759
0.5700	-	-	5.952665974
0.5850	-	-	6.086469909
0.5950	0.672736817	3.542830178	6.172622108
0.6050	-	-	6.254133235
0.6200	-	-	6.359416129
0.6350	-	-	6.430337805
0.6490	-	-	6.46592878
0.6625	0.734164657	3.557610905	6.484530988
0.7300	0.796339055	3.572651606	6.517541753
0.7975	0.859163125	3.588346615	6.531595317
0.8650	0.922544204	3.604892244	6.54286158
0.9325	0.986400344	3.622392265	6.553612348
0.9900	1.041118207	3.638095123	6.56286067

Table A22:

F=0	ψ=0.8	η=2	λ=0.01, α=0.1
[redacted]			

Wavenumber, ξ	Mode 1	Mode 2	Mode 3
0.0100	0.0169370166	3.2105229860	5.9975694300
0.0750	0.1266072641	3.2216925280	6.0041466120
0.1225	0.2056513773	3.2403925880	6.0153037750
0.1900	0.3151569752	3.2812465990	6.0403329090
0.2575	0.4202200055	3.3369835820	6.0760008690
0.3250	0.5200275253	3.4049427600	6.1220357570
0.3925	0.6142489027	3.4820766740	6.1779664050
0.4600	0.7029680754	3.5652290980	6.2430576310
0.5275	0.7865727052	3.6514045340	6.3162646060
0.5950	0.8656346583	3.7379881190	6.3962249660
0.6625	0.9408063004	3.8228873080	6.4813016130
0.7300	1.0127439560	3.9045862420	6.5696771090
0.7975	1.0820594010	3.9821229320	6.6594857440
0.8650	1.1492944610	4.0550122810	6.7489578590
0.9325	1.2149120090	4.1231419990	6.8365476770
0.9900	1.2698234410	4.1775335600	6.9087422250

Table A23:

F=1	ψ=0.8	η=2	λ=0.01, α=0.1
Wavenumber, ξ	**Mode 1**	**Mode 2**	**Mode 3**
0.0100	0.016936785	3.203107229	5.940559132
0.0750	0.126529454	3.215037504	5.948721011
0.1225	0.205322508	3.234918268	5.962521310
0.1900	0.314009742	3.277947837	5.993268778
0.2575	0.417617544	3.335763600	6.036563446
0.3250	0.515364549	3.404884298	6.091496135
0.3925	0.607064127	3.481545777	6.156746791
0.4600	0.692999237	3.562126990	6.230565031
0.5275	0.773757862	3.643492737	6.310825162
0.5950	0.850078202	3.723200714	6.395164967
0.6625	0.922730294	3.799562624	6.481187463
0.7300	0.992440004	3.871586766	6.566679341
0.7975	1.059849075	3.938849233	6.649792883
0.8650	1.125500717	4.001340671	6.729153165
0.9325	1.189840779	4.059322512	6.803880161
0.9900	1.243884907	4.105466792	6.863546820

Table A24:

F=10	ψ=0.8	η=2	λ=0.01, α=0.1

Wavenumber, ξ	Mode 1	Mode 2	Mode 3
0.0100	0.0169350953	3.1091093850	4.9338406180
0.0750	0.1258398189	3.1321626530	4.9663553080
0.1225	0.2024788315	3.1687558450	5.0219962110
0.1900	0.3045803732	3.2406297730	5.1481541080
0.2575	0.3975402658	3.3231564990	5.3278225030
0.3250	0.4818033070	3.4043422090	5.5519906690
0.3925	0.5588564436	3.4771697780	5.8004311720
0.4600	0.6304629935	3.5394199750	6.0412387170
0.5275	0.6982224013	3.5917807140	6.2406854490
0.5950	0.7634083997	3.6360701730	6.3839869610
0.6625	0.8269625065	3.6742288660	6.4802104430
0.7300	0.8895490137	3.7079243150	6.5455600140
0.7975	0.9516218975	3.7384686760	6.5923094210
0.8650	1.0134836970	3.7668552550	6.6278999920
0.9325	1.0753312270	3.7938243190	6.6566459290
0.9900	1.1280996720	3.8160960200	6.6776727970

Table A25:

F=100	ψ=0.8	η=2	λ=0.01, α=0.1
Wavenumber, ξ	**Mode 1**	**Mode 2**	**Mode 3**
0.0100	0.0169182409	1.6405171040	3.4655867720
0.0750	0.1198598312	1.7969619970	3.4672012730
0.1225	0.1821751812	2.0360456070	3.4701964230
0.1900	0.2555381482	2.4906146730	3.4787811940
0.2400	0.3039344259	2.8747659090	3.4934708660
0.2500	0.3133231875	2.9531632170	3.4986953100
0.2575	0.3203249131	3.0116383390	3.5036289670
0.2600	0.3226522633	3.0310017310	3.5055266530
0.2700	0.3319334890	3.1073374990	3.5148264010
0.2800	0.3411770463	3.1806234970	3.5280668460
0.2900	0.3503916722	3.2483317450	3.5477082310
0.3000	0.3595848253	3.3068209520	3.5773303850
0.3100	0.3687628677	3.3525765920	3.6203919530
0.3200	0.3779311911	3.3849318220	3.6775089470
0.3250	0.3825131645	3.3968758770	3.7105319840
0.3300	0.3870943606	3.4066298170	3.7458918400
0.3450	0.4008376837	3.4268554090	3.8618372870
0.3500	0.4054199858	3.4315899800	3.9027538330
0.3600	0.4145883497	3.4392114410	3.9867994710
0.3700	0.4237635414	3.4451215450	4.0730160370

0.3800	0.4329473953	3.4499002260	4.1607935930
0.3925	0.4444416461	3.4548130450	4.2721380830
0.4600	0.5068587173	3.4725411430	4.8911018600
0.5275	0.5699301246	3.4858059430	5.5250635480
0.5500	-	-	5.7376382760
0.5700	-	-	5.9261633290
0.5950	0.6336276894	3.4985649520	6.1583484780
0.6200	-	-	6.3668590080
0.6300	-	-	6.4217534360
0.6400	-	-	6.4506567130
0.6625	0.6978694625	3.5118183970	6.4738532720
0.6900	-	-	6.4839542540
0.7300	0.7625680701	3.5259249410	6.4921589550
0.7975	0.8276457113	3.5410378310	6.5025085050
0.8650	0.8930373577	3.5572278630	6.5121705620
0.9325	0.9586899817	3.5745273090	6.5220525090
0.9900	1.0147897430	3.5901483920	6.5308372340

Table A26:

F=0	**ψ=1.2**	**η=2**	**λ=0.01, α=0.1**
Wavenumber, ξ	**Mode 1**	**Mode 2**	**Mode 3**
0.0100	0.0143009648	3.2974221000	6.1799713050
0.0750	0.1070925666	3.3038024300	6.1839936030
0.1225	0.1744672015	3.3145390850	6.1908060660
0.1900	0.2690721687	3.3382428480	6.2060434530
0.2575	0.3618235307	3.3711632470	6.2276651120
0.3250	0.4522719917	3.4122902170	6.2554492360
0.3925	0.5401192954	3.4604236730	6.2890940310
0.4600	0.6252177272	3.5142505140	6.3282122030
0.5275	0.7075546237	3.5724242810	6.3723290560
0.5950	0.7872271171	3.6336396110	6.4208861740
0.6625	0.8644126997	3.6966946300	6.4732520250
0.7300	0.9393403142	3.7605366650	6.5287396980
0.7975	1.0122651430	3.8242893740	6.5866307320
0.8650	1.0834486690	3.8872621330	6.6462028090
0.9325	1.1531443100	3.9489444890	6.7067582940
0.99	1.2115186750	4.0002068800	6.7586314670

Table A27:

F=1	**ψ=1.2**	**η=2**	**λ=0.01, α=0.1**

Wavenumber, ξ	Mode 1	Mode 2	Mode 3
0.0100	0.0143008086	3.2918795380	6.1305327720
0.0750	0.1070274781	3.2988170270	6.1360517290
0.1225	0.1741894610	3.3104219470	6.1453423000
0.1900	0.2680826770	3.3357391980	6.1658653400
0.2575	0.3595142963	3.3702247330	6.1943829480
0.3250	0.4479907926	3.4122444190	6.2300043840
0.3925	0.5332666942	3.4599981420	6.2716364980
0.4600	0.6153187760	3.5116947630	6.3180458770
0.5275	0.6942975188	3.5656963390	6.3679363500
0.5950	0.7704707338	3.6206154830	6.4200329050
0.6625	0.8441709434	3.6753621770	6.4731599440
0.7300	0.9157530380	3.7291468090	6.5263024970
0.7975	0.9855642276	3.7814520910	6.5786432050
0.8650	1.0539253490	3.8319877000	6.6295737390
0.9325	1.1211211810	3.8806393540	6.6786845240
0.9900	1.1776280560	3.9206047430	6.7189032370

Table A28:

F=10	ψ=1.2	η=2	λ=0.01, α=0.1
Wavenumber, ξ	**Mode 1**	**Mode 2**	**Mode 3**
0.0100	0.0142994033	3.2059636980	4.6777140390
0.0750	0.1064535212	3.2239316530	4.7200947490
0.1225	0.1718188726	3.2517232830	4.7926026520
0.1900	0.2601901844	3.3037995000	4.9566094390
0.2575	0.3426038821	3.3598557860	5.1888022240
0.3250	0.4194855613	3.4118141090	5.4766277890
0.3925	0.4919071844	3.4566144500	5.7931531640
0.4600	0.5610631940	3.4944141300	6.0875191470
0.5275	0.6279931456	3.5266115240	6.2956244510
0.5950	0.6934960498	3.5547542770	6.4102148800
0.6625	0.7581430010	3.5801469720	6.4723894750
0.7300	0.8223235532	3.6037855100	6.5106872150
0.7975	0.8862946304	3.6264002710	6.5377004060
0.8650	0.9502208253	3.6485191410	6.5589556480
0.9325	1.0142043160	3.6705225340	6.5771077730
0.9900	1.0688003600	3.6893833030	6.5911903300

Table A29:

F=100	ψ=1.2	η=2	λ=0.01, α=0.1

Wavenumber, ξ	Mode 1	Mode 2	Mode 3
0.0100	0.0142854010	1.4956145800	3.4325550740
0.0750	0.1016834929	1.6680985010	3.4336537200
0.1225	0.1563689431	1.9265459790	3.4356088700
0.1900	0.2250584719	2.4086196480	3.4406590800
0.2400	0.2731017453	2.8141693830	3.4479322870
0.2500	0.2826066050	2.8978688460	3.4502826410
0.2575	0.2897244643	2.9608614990	3.4524470280
0.2600	0.2920955068	2.9818680750	3.4532708270
0.2700	0.3015738870	3.0657002740	3.4572867520
0.2800	0.3110462371	3.1485144010	3.4631124830
0.2900	0.3205162478	3.2285123780	3.4724839470
0.3000	0.3299869353	3.3015059180	3.4895332450
0.3100	0.3394607374	3.3590067240	3.5226982160
0.3200	0.3489396214	3.3940922860	3.5788554790
0.3250	0.3536814702	3.4046777610	3.6140947010
0.3300	0.3584251502	3.4123154070	3.6524107280
0.3450	0.3726685202	3.4257801950	3.7775361680
0.3500	0.3774207971	3.4286018490	3.8211403800
0.3600	0.3869325854	3.4330112770	3.9099031110
0.3700	0.3964544635	3.4363988360	4.0000915600
0.3800	0.4059867975	3.4391797050	4.0912644230
0.3925	0.4179172865	3.4421352340	4.2062459160
0.4600	0.4826329882	3.4544086540	4.8387451750
0.5275	0.5478055911	3.4655020420	5.4823269450
0.5500	-	-	5.6981934620
0.5700	-	-	5.8902300120
0.5950	0.6133620395	3.4771589000	6.1293997300
0.6200	-	-	6.3584711630
0.6400	-	-	6.4537736260
0.6625	0.6792290755	3.4897838030	6.4680359940
0.6900	-	-	6.4740304240
0.7300	0.7453451986	3.5035121200	6.4799401020
0.7975	0.8116615671	3.5183953320	6.4888182630
0.8650	0.8781400544	3.5344514650	6.4978518070
0.9325	0.9447509588	3.5516827830	6.5073960440
0.9900	1.0015804500	3.5672837790	6.5160020230

APPENDIX B

Maple Worksheet Sample

```
restart : with(plots) : with(linalg) : with(ExcelTools) :
>
```

$> Q_1 := \mathrm{sqrt}\left((2)^2 \cdot \left(\xi^2 + (\psi)^2 - (\alpha \cdot \Omega)^2\right)\right)$;#*relation of omega and k in the core*

$$Q_1 := 2\sqrt{\xi^2 + \psi^2 - \alpha^2\,\Omega^2} \tag{1}$$

$> Q_2 := \mathrm{sqrt}\left((\Omega)^2 - (\xi)^2\right)$;#*realation of omega and k in the cladding*

$$Q_2 := \sqrt{\Omega^2 - \xi^2} \tag{2}$$

$> U := \dfrac{\xi^2 + \psi^2}{\alpha^2} - 0.01$; #*upper bound on omega*

$$U := \frac{\xi^2 + \psi^2}{\alpha^2} - 0.01 \tag{3}$$

$> L := \xi^2 + 0.01$; #*lower bound on omega*

$$L := \xi^2 + 0.01 \tag{4}$$

$> C := \left(\dfrac{3}{2} + \dfrac{3 \cdot \psi}{Q_1}\right) \cdot \mathrm{WhittakerM}\left(\left(\dfrac{3 \cdot \psi}{Q_1} + 1\right), 1, Q_1\right) + (Q_1 - 3) \cdot \left(\dfrac{\psi}{Q_1} + \dfrac{1}{2}\right) \cdot \mathrm{WhittakerM}\left(\left(\dfrac{3 \cdot \psi}{Q_1}\right), 1, Q_1\right)$:

 # simplification of presence of Whittaker function in matrix A

$> A := \Big[\left[0, \mathrm{BesselJ}(2, \eta \cdot Q_2), \left(\eta^2\right) \cdot \left(Q_2^2\right) \cdot \mathrm{BesselY}(2, \eta \cdot Q_2)\right], \left[C \cdot \exp(-\psi), \lambda \cdot \mathrm{BesselJ}(2, Q_2), \lambda \cdot \left(\eta^2\right) \cdot \left(Q_2^2\right) \cdot \mathrm{BesselY}(2, Q_2)\right], \left[-\dfrac{1}{\eta} \cdot \left(\mathrm{WhittakerM}\left(\dfrac{3 \cdot \psi}{Q_1}, 1, Q_1\right) + F \cdot C\right) \cdot \exp(\psi), \dfrac{\mathrm{BesselJ}(1, Q_2)}{\eta \cdot Q_2}, \eta \cdot Q_2 \cdot \mathrm{BesselY}(1, Q_2)\right]\Big]$:

$> B := det(A)$:

$>$ lambda := 0.01; eta := 1.8; α := 0.1; ψ := 1; F := 100;

$$\lambda := 0.01$$

$$\eta := 1.8$$

$$\alpha := 0.1$$

$$\psi := 1$$
$$F := 100 \tag{5}$$

> *ran* := [0.0100000000000000, 0.0200000000000000, 0.0300000000000000,
0.0400000000000000, 0.0500000000000000, 0.0600000000000000, 0.0700000000000000,
0.0800000000000000, 0.0900000000000000, 0.100000000000000, 0.110000000000000,
0.120000000000000, 0.130000000000000, 0.140000000000000, 0.150000000000000,
0.160000000000000, 0.170000000000000, 0.180000000000000, 0.190000000000000,
0.200000000000000, 0.210000000000000, 0.220000000000000, 0.230000000000000,
0.240000000000000, 0.250000000000000, 0.260000000000000, 0.270000000000000,
0.280000000000000, 0.290000000000000, 0.300000000000000, 0.310000000000000,
0.320000000000000, 0.330000000000000, 0.340000000000000, 0.350000000000000,
0.360000000000000, 0.370000000000000, 0.380000000000000, 0.390000000000000,
0.400000000000000, 0.410000000000000, 0.420000000000000, 0.430000000000000,
0.440000000000000, 0.450000000000000, 0.460000000000000, 0.470000000000000,
0.480000000000000, 0.490000000000000, 0.500000000000000, 0.510000000000000,
0.520000000000000, 0.530000000000000, 0.540000000000000, 0.550000000000000,
0.560000000000000, 0.570000000000000, 0.580000000000000, 0.590000000000000,
0.600000000000000, 0.610000000000000, 0.620000000000000, 0.630000000000000,
0.640000000000000, 0.650000000000000, 0.660000000000000, 0.670000000000000,
0.680000000000000, 0.690000000000000, 0.700000000000000, 0.710000000000000,
0.720000000000000, 0.730000000000000, 0.740000000000000, 0.750000000000000,
0.760000000000000, 0.770000000000000, 0.780000000000000, 0.790000000000000,
0.800000000000000, 0.810000000000000, 0.820000000000000, 0.830000000000000,
0.840000000000000, 0.850000000000000, 0.860000000000000, 0.870000000000000,
0.880000000000000, 0.890000000000000, 0.900000000000000, 0.910000000000000,
0.920000000000000, 0.930000000000000, 0.940000000000000, 0.950000000000000,
0.960000000000000, 0.970000000000000, 0.980000000000000, 0.990000000000000, 1] :

> $mode_1$:= [0, 0, 0, 0, 0, 0, 0, 0, 0, 0, 0, 0, 0, 0, 0, 0, 0, 0, 0, 0, 0, 0, 0, 0, 0, 0, 0, 0, 0, 0, 0, 0, 0, 0,
0, 0, 0, 0, 0, 0, 0, 0, 0, 0, 0, 0, 0, 0, 0, 0, 0, 0, 0, 0, 0, 0, 0, 0, 0, 0, 0, 0, 0, 0, 0, 0, 0, 0, 0, 0, 0,
0, 0, 0, 0, 0, 0, 0, 0, 0, 0, 0, 0, 0, 0, 0, 0, 0, 0, 0, 0, 0, 0, 0, 0, 0, 0, 0, 0, 0, 0] :

> $mode_2$:= [0, 0, 0, 0, 0, 0, 0, 0, 0, 0, 0, 0, 0, 0, 0, 0, 0, 0, 0, 0, 0, 0, 0, 0, 0, 0, 0, 0, 0, 0, 0, 0, 0, 0,
0, 0, 0, 0, 0, 0, 0, 0, 0, 0, 0, 0, 0, 0, 0, 0, 0, 0, 0, 0, 0, 0, 0, 0, 0, 0, 0, 0, 0, 0, 0, 0, 0, 0, 0, 0, 0,
0, 0, 0, 0, 0, 0, 0, 0, 0, 0, 0, 0, 0, 0, 0, 0, 0, 0, 0, 0, 0, 0, 0, 0, 0, 0, 0, 0, 0, 0] :

> $mode_3$:= [0, 0, 0, 0, 0, 0, 0, 0, 0, 0, 0, 0, 0, 0, 0, 0, 0, 0, 0, 0, 0, 0, 0, 0, 0, 0, 0, 0, 0, 0, 0, 0, 0, 0,
0, 0, 0, 0, 0, 0, 0, 0, 0, 0, 0, 0, 0, 0, 0, 0, 0, 0, 0, 0, 0, 0, 0, 0, 0, 0, 0, 0, 0, 0, 0, 0, 0, 0, 0, 0, 0,
0, 0, 0, 0, 0, 0, 0, 0, 0, 0, 0, 0, 0, 0, 0, 0, 0, 0, 0, 0, 0, 0, 0, 0, 0, 0, 0, 0, 0, 0] :

> xi := *ran*[1] :

> $mode_1[1]$:= *fsolve*($B = 0$, Omega, L ..3) :

> $mode_2[1]$:= *fsolve*($B = 0$, Omega, 3 ..5) :

> $mode_3[1]$:= *fsolve*($B = 0$, Omega, 5 ..9) :

> xi := *ran*[2] :

> $mode_1[2]$:= *fsolve*($B = 0$, Omega, L ..3) :

> $mode_2[2] := fsolve(B = 0, \text{Omega}, 3..5):$

> $mode_3[2] := fsolve(B = 0, \text{Omega}, 5..9):$

> $\text{xi} := ran[3];$

$$\xi := 0.0300000000000000 \tag{6}$$

> $plot(B, \text{Omega} = L..10)$

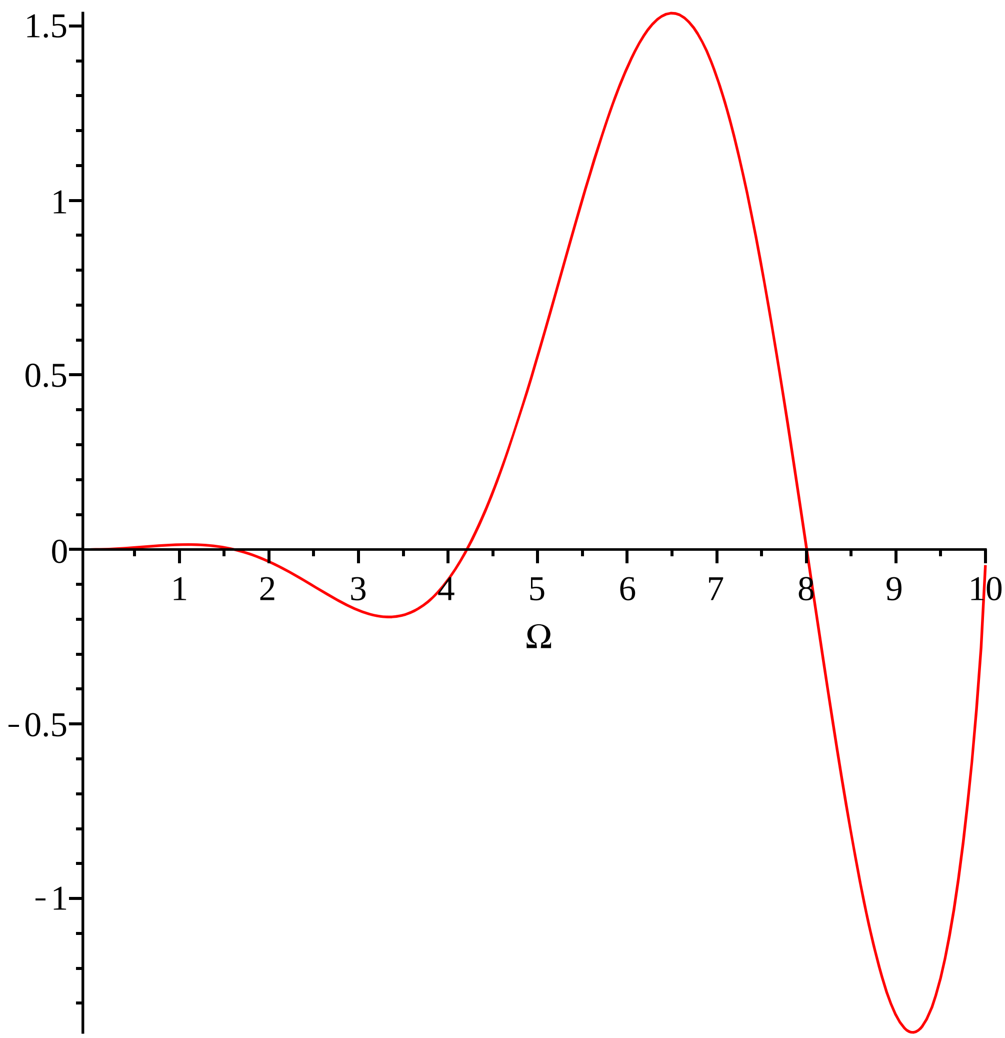

> $mode_1[3] := fsolve(B = 0, \text{Omega}, L..1);$

$$mode_{1_3} := 0.05291490336 \tag{7}$$

> $mode_2[3] := fsolve(B = 0, \text{Omega}, 1..3);$

$$mode_{2_3} := 1.607207030 \tag{8}$$

> $mode_3[3] := fsolve(B = 0, \text{Omega}, 3..8);$

$$mode_{3_3} := 4.210170405 \tag{9}$$

> $\text{xi} := ran[4]:$

```
> mode[1][4] := fsolve(B = 0, Omega, L..3) :
> mode[2][4] := fsolve(B = 0, Omega, 3..5) :
> mode[3][4] := fsolve(B = 0, Omega, 5..9) :

> xi := ran[5] :

> mode[1][5] := fsolve(B = 0, Omega, L..3) :
> mode[2][5] := fsolve(B = 0, Omega, 3..5) :
> mode[3][5] := fsolve(B = 0, Omega, 5..9) :

> xi := ran[6] :

> mode[1][6] := fsolve(B = 0, Omega, L..3) :
> mode[2][6] := fsolve(B = 0, Omega, 3..5) :
> mode[3][6] := fsolve(B = 0, Omega, 5..9) :

> xi := ran[7] :
> mode[1][7] := fsolve(B = 0, Omega, L..3) :
> mode[2][7] := fsolve(B = 0, Omega, 3..5) :
> mode[3][7] := fsolve(B = 0, Omega, 5..9) :

> xi := ran[8] :

> mode[1][8] := fsolve(B = 0, Omega, L..3) :
> mode[2][8] := fsolve(B = 0, Omega, 3..5) :
> mode[3][8] := fsolve(B = 0, Omega, 5..9) :

> xi := ran[9] :

> mode[1][9] := fsolve(B = 0, Omega, L..3) :
> mode[2][9] := fsolve(B = 0, Omega, 3..5) :
> mode[3][9] := fsolve(B = 0, Omega, 5..9) :

> xi := ran[10] :

> mode[1][10] := fsolve(B = 0, Omega, L..3) :
> mode[2][10] := fsolve(B = 0, Omega, 3..5) :
> mode[3][10] := fsolve(B = 0, Omega, 5..9) :

> xi := ran[11] :
```

```
> #plot(B, Omega = L..10);
> mode_1[11] := fsolve(B = 0, Omega, L..3) :
> mode_2[11] := fsolve(B = 0, Omega, 3..5) :
> mode_3[11] := fsolve(B = 0, Omega, 5..8) :

> xi := ran[12] :

> mode_1[12] := fsolve(B = 0, Omega, L..3) :
> mode_2[12] := fsolve(B = 0, Omega, 3..5) :
> mode_3[12] := fsolve(B = 0, Omega, 5..9) :

> xi := ran[13] :

> mode_1[13] := fsolve(B = 0, Omega, L..3) :
> mode_2[13] := fsolve(B = 0, Omega, 3..5) :
> mode_3[13] := fsolve(B = 0, Omega, 5..9) :

> xi := ran[14] :

> mode_1[14] := fsolve(B = 0, Omega, L..3) :
> mode_2[14] := fsolve(B = 0, Omega, 3..5) :
> mode_3[14] := fsolve(B = 0, Omega, 5..9) :

> xi := ran[15] :

> mode_1[15] := fsolve(B = 0, Omega, L..3) :
> mode_2[15] := fsolve(B = 0, Omega, 3..5) :
> mode_3[15] := fsolve(B = 0, Omega, 5..9) :

> xi := ran[16] :

> mode_1[16] := fsolve(B = 0, Omega, L..3) :
> mode_2[16] := fsolve(B = 0, Omega, 3..5) :
> mode_3[16] := fsolve(B = 0, Omega, 5..9) :

> xi := ran[17] :
> mode_1[17] := fsolve(B = 0, Omega, L..3) :
> mode_2[17] := fsolve(B = 0, Omega, 3..5) :
> mode_3[17] := fsolve(B = 0, Omega, 5..9) :
```

> $\mathrm{xi} := ran[18]:$

> $mode_1[18] := fsolve(B = 0, \mathrm{Omega}, L..3):$
> $mode_2[18] := fsolve(B = 0, \mathrm{Omega}, 3..5):$
> $mode_3[18] := fsolve(B = 0, \mathrm{Omega}, 5..9):$

> $\mathrm{xi} := ran[19]:$

> $mode_1[19] := fsolve(B = 0, \mathrm{Omega}, L..3):$
> $mode_2[19] := fsolve(B = 0, \mathrm{Omega}, 3..5):$
> $mode_3[19] := fsolve(B = 0, \mathrm{Omega}, 5..9):$

> $\mathrm{xi} := ran[20]:$

> $mode_1[20] := fsolve(B = 0, \mathrm{Omega}, L..3):$
> $mode_2[20] := fsolve(B = 0, \mathrm{Omega}, 3..5):$
> $mode_3[20] := fsolve(B = 0, \mathrm{Omega}, 5..9):$

> $\mathrm{xi} := ran[21]:$

> $mode_1[21] := fsolve(B = 0, \mathrm{Omega}, L..3):$
> $mode_2[21] := fsolve(B = 0, \mathrm{Omega}, 3..5):$
> $mode_3[21] := fsolve(B = 0, \mathrm{Omega}, 5..9):$

> $\mathrm{xi} := ran[22]:$

> $mode_1[22] := fsolve(B = 0, \mathrm{Omega}, L..3):$
> $mode_2[22] := fsolve(B = 0, \mathrm{Omega}, 3..5):$
> $mode_3[22] := fsolve(B = 0, \mathrm{Omega}, 5..9):$

> $\mathrm{xi} := ran[23]:$

> $mode_1[23] := fsolve(B = 0, \mathrm{Omega}, L..3):$
> $mode_2[23] := fsolve(B = 0, \mathrm{Omega}, 3..5):$
> $mode_3[23] := fsolve(B = 0, \mathrm{Omega}, 5..9):$

> $\mathrm{xi} := ran[24]:$

> $mode_1[24] := fsolve(B = 0, \mathrm{Omega}, L..3):$
> $mode_2[24] := fsolve(B = 0, \mathrm{Omega}, 3..5):$

```
> mode[3][24] := fsolve(B = 0, Omega, 5 ..9) :

> xi := ran[25] :

> mode[1][25] := fsolve(B = 0, Omega, L ..3) :
> mode[2][25] := fsolve(B = 0, Omega, 3 ..5) :
> mode[3][25] := fsolve(B = 0, Omega, 5 ..9) :

> xi := ran[26] :

> mode[1][26] := fsolve(B = 0, Omega, L ..3) :
> mode[2][26] := fsolve(B = 0, Omega, 3 ..5) :
> mode[3][26] := fsolve(B = 0, Omega, 5 ..9) :

> xi := ran[27] :
> mode[1][27] := fsolve(B = 0, Omega, L ..3) :
> mode[2][27] := fsolve(B = 0, Omega, 3 ..5) :
> mode[3][27] := fsolve(B = 0, Omega, 5 ..9) :

> xi := ran[28] :

> mode[1][28] := fsolve(B = 0, Omega, L ..3) :
> mode[2][28] := fsolve(B = 0, Omega, 3 ..5) :
> mode[3][28] := fsolve(B = 0, Omega, 5 ..9) :

> xi := ran[29] :

> mode[1][29] := fsolve(B = 0, Omega, L ..3) :
> mode[2][29] := fsolve(B = 0, Omega, 3 ..5) :
> mode[3][29] := fsolve(B = 0, Omega, 5 ..9) :

> xi := ran[30] :

> mode[1][30] := fsolve(B = 0, Omega, L ..3) :
> mode[2][30] := fsolve(B = 0, Omega, 3 ..5) :
> mode[3][30] := fsolve(B = 0, Omega, 5 ..9) :

> xi := ran[31] :

> mode[1][31] := fsolve(B = 0, Omega, L ..3) :
```

```
> mode[2][31] := fsolve(B = 0, Omega, 3 ..5) :
> mode[3][31] := fsolve(B = 0, Omega, 5 ..9) :

> xi := ran[32] :

> mode[1][32] := fsolve(B = 0, Omega, L ..3) :
> mode[2][32] := fsolve(B = 0, Omega, 3 ..5) :
> mode[3][32] := fsolve(B = 0, Omega, 5 ..9) :

> xi := ran[33] :

> mode[1][33] := fsolve(B = 0, Omega, L ..3) :
> mode[2][33] := fsolve(B = 0, Omega, 3 ..5) :
> mode[3][33] := fsolve(B = 0, Omega, 5 ..7) :

> xi := ran[34] :

> mode[1][34] := fsolve(B = 0, Omega, L ..3) :
> mode[2][34] := fsolve(B = 0, Omega, 3 ..5) :
> mode[3][34] := fsolve(B = 0, Omega, 5 ..9) :

> xi := ran[35] :

> mode[1][35] := fsolve(B = 0, Omega, L ..3) :
> mode[2][35] := fsolve(B = 0, Omega, 3 ..5) :
> mode[3][35] := fsolve(B = 0, Omega, 5 ..9) :

> xi := ran[36] :

> mode[1][36] := fsolve(B = 0, Omega, L ..3) :
> mode[2][36] := fsolve(B = 0, Omega, 3 ..5) :
> mode[3][36] := fsolve(B = 0, Omega, 5 ..9) :

> xi := ran[37] :
> mode[1][37] := fsolve(B = 0, Omega, L ..3) :
> mode[2][37] := fsolve(B = 0, Omega, 3 ..5) :
> mode[3][37] := fsolve(B = 0, Omega, 5 ..9) :

> xi := ran[38] :
```

> $mode_1[38] := fsolve(B = 0, \text{Omega}, L..3)$:
> $mode_2[38] := fsolve(B = 0, \text{Omega}, 3..5)$:
> $mode_3[38] := fsolve(B = 0, \text{Omega}, 5..9)$:

> $\text{xi} := ran[39]$:

> $mode_1[39] := fsolve(B = 0, \text{Omega}, L..3)$:
> $mode_2[39] := fsolve(B = 0, \text{Omega}, 3..5)$:
> $mode_3[39] := fsolve(B = 0, \text{Omega}, 5..9)$:

> $\text{xi} := ran[40]$:

> $mode_1[40] := fsolve(B = 0, \text{Omega}, L..3)$:
> $mode_2[40] := fsolve(B = 0, \text{Omega}, 3..5)$:
> $mode_3[40] := fsolve(B = 0, \text{Omega}, 5..9)$:

> $\text{xi} := ran[41]$:

> $mode_1[41] := fsolve(B = 0, \text{Omega}, L..3)$:
> $mode_2[41] := fsolve(B = 0, \text{Omega}, 3..5)$:
> $mode_3[41] := fsolve(B = 0, \text{Omega}, 5..9)$:

> $\text{xi} := ran[42]$:

> $mode_1[42] := fsolve(B = 0, \text{Omega}, L..3)$:
> $mode_2[42] := fsolve(B = 0, \text{Omega}, 3..5)$:
> $mode_3[42] := fsolve(B = 0, \text{Omega}, 5..9)$:

> $\text{xi} := ran[43]$:

> $mode_1[43] := fsolve(B = 0, \text{Omega}, L..3)$:
> $mode_2[43] := fsolve(B = 0, \text{Omega}, 3..5)$:
> $mode_3[43] := fsolve(B = 0, \text{Omega}, 5..9)$:

> $\text{xi} := ran[44]$:

> $mode_1[44] := fsolve(B = 0, \text{Omega}, L..3)$:
> $mode_2[44] := fsolve(B = 0, \text{Omega}, 3..5)$:
> $mode_3[44] := fsolve(B = 0, \text{Omega}, 5..9)$:

> $\mathrm{xi} := ran[45]:$

> $mode_1[45] := fsolve(B = 0, \mathrm{Omega}, L..3):$
> $mode_2[45] := fsolve(B = 0, \mathrm{Omega}, 3..5):$
> $mode_3[45] := fsolve(B = 0, \mathrm{Omega}, 5..9):$

> $\mathrm{xi} := ran[46]:$

> $mode_1[46] := fsolve(B = 0, \mathrm{Omega}, L..3):$
> $mode_2[46] := fsolve(B = 0, \mathrm{Omega}, 3..5):$
> $mode_3[46] := fsolve(B = 0, \mathrm{Omega}, 5..9):$

> $\mathrm{xi} := ran[47]:$
> $mode_1[47] := fsolve(B = 0, \mathrm{Omega}, L..3):$
> $mode_2[47] := fsolve(B = 0, \mathrm{Omega}, 3..5):$
> $mode_3[47] := fsolve(B = 0, \mathrm{Omega}, 5..9):$

> $\mathrm{xi} := ran[48]:$

> $mode_1[48] := fsolve(B = 0, \mathrm{Omega}, L..3):$
> $mode_2[48] := fsolve(B = 0, \mathrm{Omega}, 3..5):$
> $mode_3[48] := fsolve(B = 0, \mathrm{Omega}, 5..9):$

> $\mathrm{xi} := ran[49];$
> $plot(B, \mathrm{Omega} = L..10)$

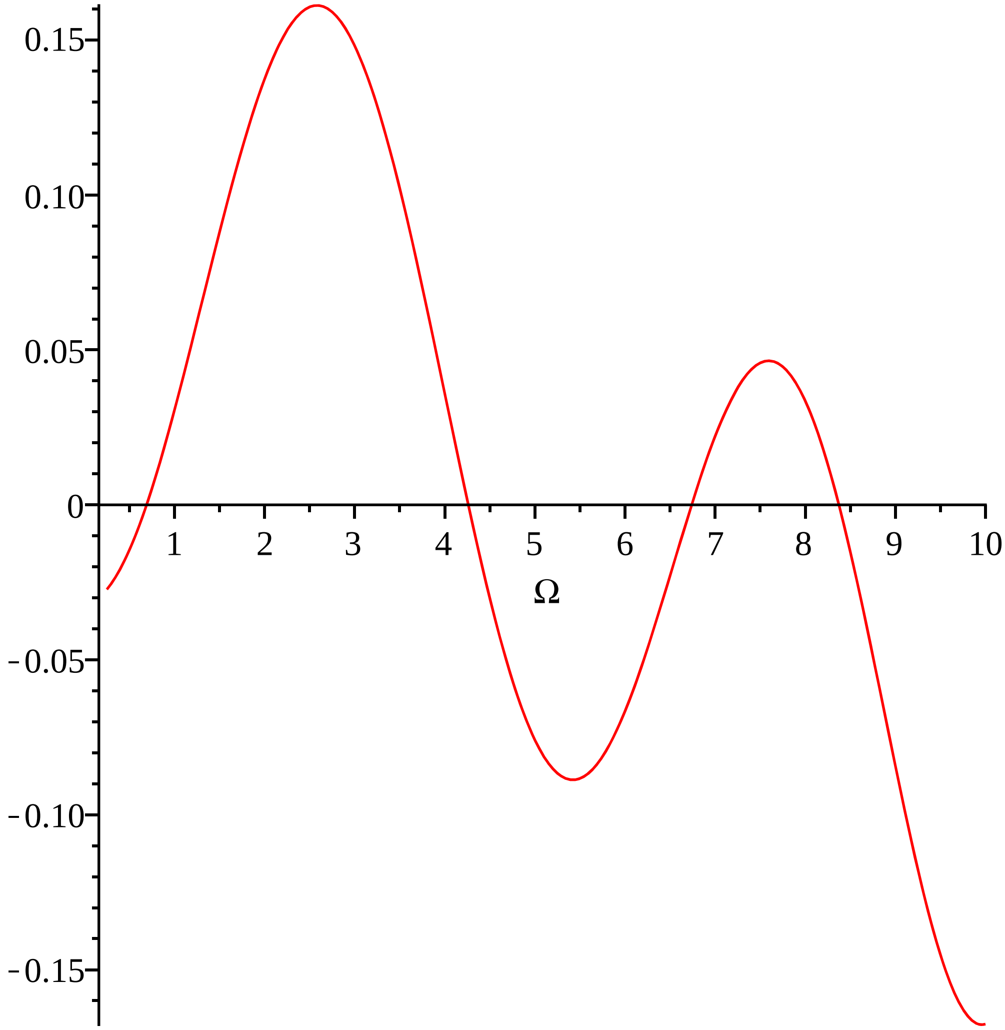

> $mode_1[49] := fsolve(B = 0, \text{Omega}, L..3)$:

> $mode_2[49] := fsolve(B = 0, \text{Omega}, 3..5)$:

> $mode_3[49] := fsolve(B = 0, \text{Omega}, 6..9)$:

> $\text{xi} := ran[50]$:

> $mode_1[50] := fsolve(B = 0, \text{Omega}, L..3)$:

> $mode_2[50] := fsolve(B = 0, \text{Omega}, 3..6)$:

> $mode_3[50] := fsolve(B = 0, \text{Omega}, 6..9)$:

> $\text{xi} := ran[51]$:

> $mode_1[51] := fsolve(B = 0, \text{Omega}, L..3)$:

> $mode_2[51] := fsolve(B = 0, \text{Omega}, 3..6)$:

> $mode_3[51] := fsolve(B = 0, \text{Omega}, 6..9)$:

> $\text{xi} := ran[52]$:

> $mode_1[52] := fsolve(B = 0, \mathrm{Omega}, L..3)$:
> $mode_2[52] := fsolve(B = 0, \mathrm{Omega}, 3..6)$:
> $mode_3[52] := fsolve(B = 0, \mathrm{Omega}, 6..9)$:

> $\mathrm{xi} := ran[53]$:

> $mode_1[53] := fsolve(B = 0, \mathrm{Omega}, L..3)$:
> $mode_2[53] := fsolve(B = 0, \mathrm{Omega}, 3..6)$:
> $mode_3[53] := fsolve(B = 0, \mathrm{Omega}, 6..9)$:

> $\mathrm{xi} := ran[54]$:

> $mode_1[54] := fsolve(B = 0, \mathrm{Omega}, L..3)$:
> $mode_2[54] := fsolve(B = 0, \mathrm{Omega}, 3..6)$:
> $mode_3[54] := fsolve(B = 0, \mathrm{Omega}, 6..9)$:

> $\mathrm{xi} := ran[55]$:

> $mode_1[55] := fsolve(B = 0, \mathrm{Omega}, L..3)$:
> $mode_2[55] := fsolve(B = 0, \mathrm{Omega}, 3..6)$:
> $mode_3[55] := fsolve(B = 0, \mathrm{Omega}, 6..9)$:

> $\mathrm{xi} := ran[56]$:

> $mode_1[56] := fsolve(B = 0, \mathrm{Omega}, L..3)$:
> $mode_2[56] := fsolve(B = 0, \mathrm{Omega}, 3..6)$:
> $mode_3[56] := fsolve(B = 0, \mathrm{Omega}, 6..9)$:

> $\mathrm{xi} := ran[57]$:
> $mode_1[57] := fsolve(B = 0, \mathrm{Omega}, L..3)$:
> $mode_2[57] := fsolve(B = 0, \mathrm{Omega}, 3..6)$:
> $mode_3[57] := fsolve(B = 0, \mathrm{Omega}, 6..9)$:

> $\mathrm{xi} := ran[58]$:

> $mode_1[58] := fsolve(B = 0, \mathrm{Omega}, L..3)$:
> $mode_2[58] := fsolve(B = 0, \mathrm{Omega}, 3..6)$:
> $mode_3[58] := fsolve(B = 0, \mathrm{Omega}, 6..9)$:

> xi := $ran[59]$:

> $mode_1[59] := fsolve(B = 0, \text{Omega}, L..3)$:
> $mode_2[59] := fsolve(B = 0, \text{Omega}, 3..6)$:
> $mode_3[59] := fsolve(B = 0, \text{Omega}, 6..9)$:

> xi := $ran[60]$:

> $mode_1[60] := fsolve(B = 0, \text{Omega}, L..3)$:
> $mode_2[60] := fsolve(B = 0, \text{Omega}, 3..6)$:
> $mode_3[60] := fsolve(B = 0, \text{Omega}, 6..9)$:

> xi := $ran[61]$:

> $mode_1[61] := fsolve(B = 0, \text{Omega}, L..3)$:
> $mode_2[61] := fsolve(B = 0, \text{Omega}, 3..6)$:
> $mode_3[61] := fsolve(B = 0, \text{Omega}, 6..9)$:

> xi := $ran[62]$:

> $mode_1[62] := fsolve(B = 0, \text{Omega}, L..3)$:
> $mode_2[62] := fsolve(B = 0, \text{Omega}, 3..6)$:
> $mode_3[62] := fsolve(B = 0, \text{Omega}, 6..9)$:

> xi := $ran[63]$:

> $mode_1[63] := fsolve(B = 0, \text{Omega}, L..3)$:
> $mode_2[63] := fsolve(B = 0, \text{Omega}, 3..6)$:
> $mode_3[63] := fsolve(B = 0, \text{Omega}, 6..9)$:

> xi := $ran[64]$:

> $mode_1[64] := fsolve(B = 0, \text{Omega}, L..3)$:
> $mode_2[64] := fsolve(B = 0, \text{Omega}, 3..6)$:
> $mode_3[64] := fsolve(B = 0, \text{Omega}, 6..9)$:

> xi := $ran[65]$:

> $mode_1[65] := fsolve(B = 0, \text{Omega}, L..3)$:
> $mode_2[65] := fsolve(B = 0, \text{Omega}, 3..6)$:

```
> mode[3][65] := fsolve(B = 0, Omega, 6..9) :

> xi := ran[66] :

> mode[1][66] := fsolve(B = 0, Omega, L..3) :
> mode[2][66] := fsolve(B = 0, Omega, 3..6) :
> mode[3][66] := fsolve(B = 0, Omega, 6..9) :

> xi := ran[67] :
> mode[1][67] := fsolve(B = 0, Omega, L..3) :
> mode[2][67] := fsolve(B = 0, Omega, 3..6) :
> mode[3][67] := fsolve(B = 0, Omega, 6..9) :

> xi := ran[68] :

> mode[1][68] := fsolve(B = 0, Omega, L..3) :
> mode[2][68] := fsolve(B = 0, Omega, 3..6) :
> mode[3][68] := fsolve(B = 0, Omega, 6..9) :

> xi := ran[69] :

> mode[1][69] := fsolve(B = 0, Omega, L..3) :
> mode[2][69] := fsolve(B = 0, Omega, 3..6) :
> mode[3][69] := fsolve(B = 0, Omega, 6..9) :

> xi := ran[70] :

> mode[1][70] := fsolve(B = 0, Omega, L..3) :
> mode[2][70] := fsolve(B = 0, Omega, 3..6) :
> mode[3][70] := fsolve(B = 0, Omega, 6..9) :

> xi := ran[71] :

> mode[1][71] := fsolve(B = 0, Omega, L..3) :
> mode[2][71] := fsolve(B = 0, Omega, 3..6) :
> mode[3][71] := fsolve(B = 0, Omega, 6..9) :

> xi := ran[72] :

> mode[1][72] := fsolve(B = 0, Omega, L..3) :
```

> $mode_2[72] := fsolve(B = 0, \text{Omega}, 3..6)$:

> $mode_3[72] := fsolve(B = 0, \text{Omega}, 6..9)$:

> $\text{xi} := ran[73]$:

> $mode_1[73] := fsolve(B = 0, \text{Omega}, L..3)$:

> $mode_2[73] := fsolve(B = 0, \text{Omega}, 3..6)$:

> $mode_3[73] := fsolve(B = 0, \text{Omega}, 6..9)$:

> $\text{xi} := ran[74]$:

> $mode_1[74] := fsolve(B = 0, \text{Omega}, L..3)$:

> $mode_2[74] := fsolve(B = 0, \text{Omega}, 3..6)$:

> $mode_3[74] := fsolve(B = 0, \text{Omega}, 6..9)$:

> $\text{xi} := ran[75]$:

> $mode_1[75] := fsolve(B = 0, \text{Omega}, L..3)$:

> $mode_2[75] := fsolve(B = 0, \text{Omega}, 3..6)$:

> $mode_3[75] := fsolve(B = 0, \text{Omega}, 6..9)$:

> $\text{xi} := ran[76]$:

> $mode_1[76] := fsolve(B = 0, \text{Omega}, L..3)$:

> $mode_2[76] := fsolve(B = 0, \text{Omega}, 3..6)$:

> $mode_3[76] := fsolve(B = 0, \text{Omega}, 6..9)$:

> $\text{xi} := ran[77]$:

> $mode_1[77] := fsolve(B = 0, \text{Omega}, L..3)$:

> $mode_2[77] := fsolve(B = 0, \text{Omega}, 3..6)$:

> $mode_3[77] := fsolve(B = 0, \text{Omega}, 6..9)$:

> $\text{xi} := ran[78]$:

> $mode_1[78] := fsolve(B = 0, \text{Omega}, L..3)$:

> $mode_2[78] := fsolve(B = 0, \text{Omega}, 3..6)$:

> $mode_3[78] := fsolve(B = 0, \text{Omega}, 6..9)$:

> $\text{xi} := ran[79]$:

> $mode_1[79] := fsolve(B = 0, \text{Omega}, L..3)$:

> $mode_2[79] := fsolve(B = 0, \text{Omega}, 3..6)$:

> $mode_3[79] := fsolve(B = 0, \text{Omega}, 6..9)$:

> xi := $ran[80]$;

$$\xi := 0.800000000000000 \tag{10}$$

> $plot(B, \text{Omega} = L..10)$

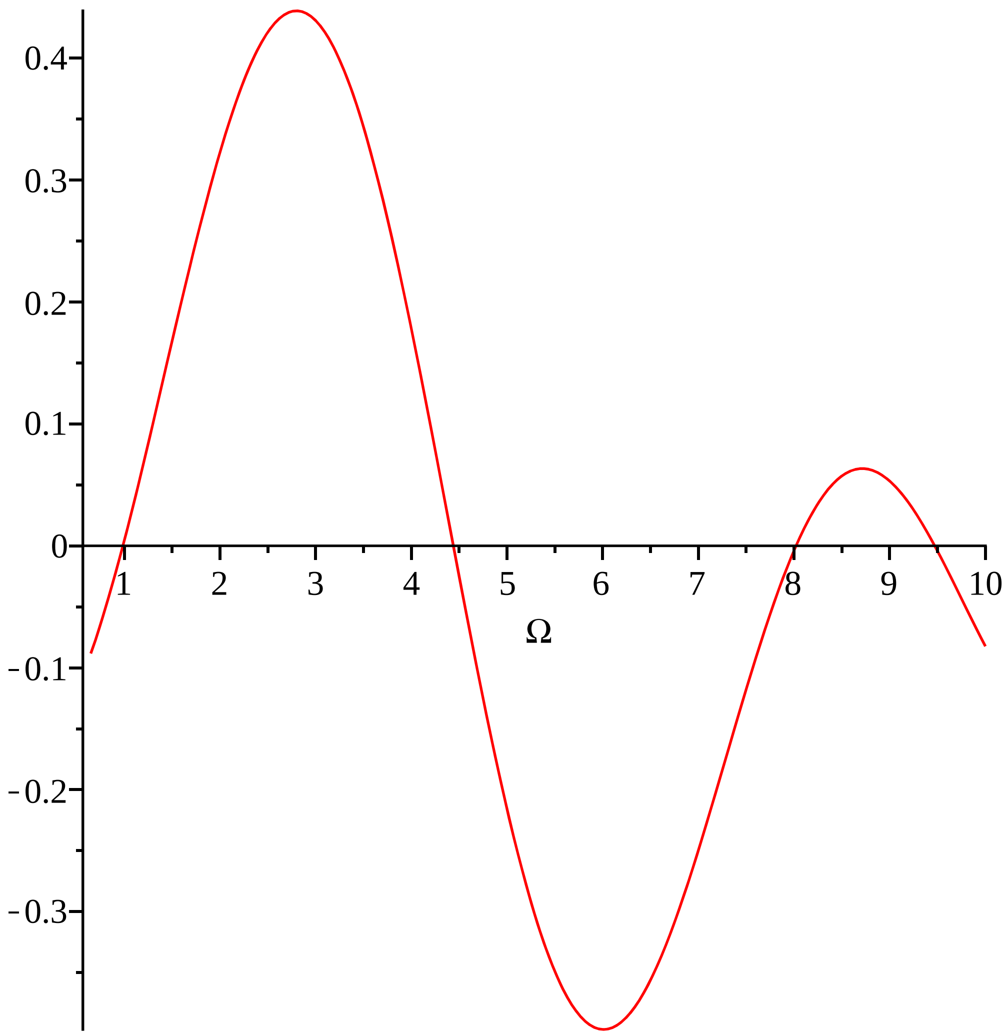

> $mode_1[80] := fsolve(B = 0, \text{Omega}, L..3)$:

> $mode_2[80] := fsolve(B = 0, \text{Omega}, 3..6)$:

> $mode_3[80] := fsolve(B = 0, \text{Omega}, 6..9)$:

> xi := $ran[81]$:

> $mode_1[81] := fsolve(B = 0, \text{Omega}, L..3)$:

> $mode_2[81] := fsolve(B = 0, \text{Omega}, 3..6)$:

> $mode_3[81] := fsolve(B = 0, \text{Omega}, 6..9)$:

```
> xi := ran[82]:

> mode_1[82] := fsolve(B = 0, Omega, L..3) :
> mode_2[82] := fsolve(B = 0, Omega, 3..6) :
> mode_3[82] := fsolve(B = 0, Omega, 6..9) :

> xi := ran[83]:

> mode_1[83] := fsolve(B = 0, Omega, L..3) :
> mode_2[83] := fsolve(B = 0, Omega, 3..6) :
> mode_3[83] := fsolve(B = 0, Omega, 6..9) :

> xi := ran[84]:

> mode_1[84] := fsolve(B = 0, Omega, L..3) :
> mode_2[84] := fsolve(B = 0, Omega, 3..6) :
> mode_3[84] := fsolve(B = 0, Omega, 6..9) :

> xi := ran[85]:

> mode_1[85] := fsolve(B = 0, Omega, L..3) :
> mode_2[85] := fsolve(B = 0, Omega, 3..6) :
> mode_3[85] := fsolve(B = 0, Omega, 6..9) :

> xi := ran[86]:

> mode_1[86] := fsolve(B = 0, Omega, L..3) :
> mode_2[86] := fsolve(B = 0, Omega, 3..6) :
> mode_3[86] := fsolve(B = 0, Omega, 6..9) :

> xi := ran[87]:
> mode_1[87] := fsolve(B = 0, Omega, L..3) :
> mode_2[87] := fsolve(B = 0, Omega, 3..6) :
> mode_3[87] := fsolve(B = 0, Omega, 6..9) :

> xi := ran[88]:

> mode_1[88] := fsolve(B = 0, Omega, L..3) :
> mode_2[88] := fsolve(B = 0, Omega, 3..6) :
```

```
> mode3[88] := fsolve(B = 0, Omega, 6 ..9) :

> xi := ran[89] :

> mode1[89] := fsolve(B = 0, Omega, L ..3) :
> mode2[89] := fsolve(B = 0, Omega, 3 ..6) :
> mode3[89] := fsolve(B = 0, Omega, 6 ..9) :

> xi := ran[90] :
> #plot(B, Omega = L ..20) :
> mode1[90] := fsolve(B = 0, Omega, L ..3) :
> mode2[90] := fsolve(B = 0, Omega, 3 ..6) :
> mode3[90] := fsolve(B = 0, Omega, 6 ..9) :

> xi := ran[91] :
> #plot(B, Omega = L ..20);
> mode1[91] := fsolve(B = 0, Omega, L ..3) :
> mode2[91] := fsolve(B = 0, Omega, 3 ..6) :
> mode3[91] := fsolve(B = 0, Omega, 6 ..9) :

> xi := ran[92] :
> #plot(B, Omega = L ..20);:
> mode1[92] := fsolve(B = 0, Omega, L ..3) :
> mode2[92] := fsolve(B = 0, Omega, 3 ..6) :
> mode3[92] := fsolve(B = 0, Omega, 6 ..9) :

> xi := ran[93] :
> #plot(B, Omega = L ..20);
> mode1[93] := fsolve(B = 0, Omega, L ..3) :
> mode2[93] := fsolve(B = 0, Omega, 3 ..6) :
> mode3[93] := fsolve(B = 0, Omega, 6 ..9) :

> xi := ran[94] :
> #plot(B, Omega = L ..20);
> mode1[94] := fsolve(B = 0, Omega, L ..3) :
> mode2[94] := fsolve(B = 0, Omega, 3 ..6) :
> mode3[94] := fsolve(B = 0, Omega, 6 ..9) :
```

> $\mathrm{xi} := ran[95]:$

> $\#plot(B, \mathrm{Omega} = L..20);$

> $mode_1[95] := fsolve(B = 0, \mathrm{Omega}, L..3):$

> $mode_2[95] := fsolve(B = 0, \mathrm{Omega}, 3..6):$

> $mode_3[95] := fsolve(B = 0, \mathrm{Omega}, 6..9):$

> $\mathrm{xi} := ran[96]:$

> $\#plot(B, \mathrm{Omega} = L..20):$

> $mode_1[96] := fsolve(B = 0, \mathrm{Omega}, L..3):$

> $mode_2[96] := fsolve(B = 0, \mathrm{Omega}, 3..6):$

> $mode_3[96] := fsolve(B = 0, \mathrm{Omega}, 6..9):$

> $\mathrm{xi} := ran[97]:$

> $mode_1[97] := fsolve(B = 0, \mathrm{Omega}, L..3):$

> $mode_2[97] := fsolve(B = 0, \mathrm{Omega}, 3..6):$

> $mode_3[97] := fsolve(B = 0, \mathrm{Omega}, 6..9):$

> $\mathrm{xi} := ran[98]:$

> $\#plot(B, \mathrm{Omega} = L..20):$

> $mode_1[98] := fsolve(B = 0, \mathrm{Omega}, L..3):$

> $mode_2[98] := fsolve(B = 0, \mathrm{Omega}, 3..6):$

> $mode_3[98] := fsolve(B = 0, \mathrm{Omega}, 6..9):$

> $\mathrm{xi} := ran[99]:$

> $plot(B, \mathrm{Omega} = L..20);$

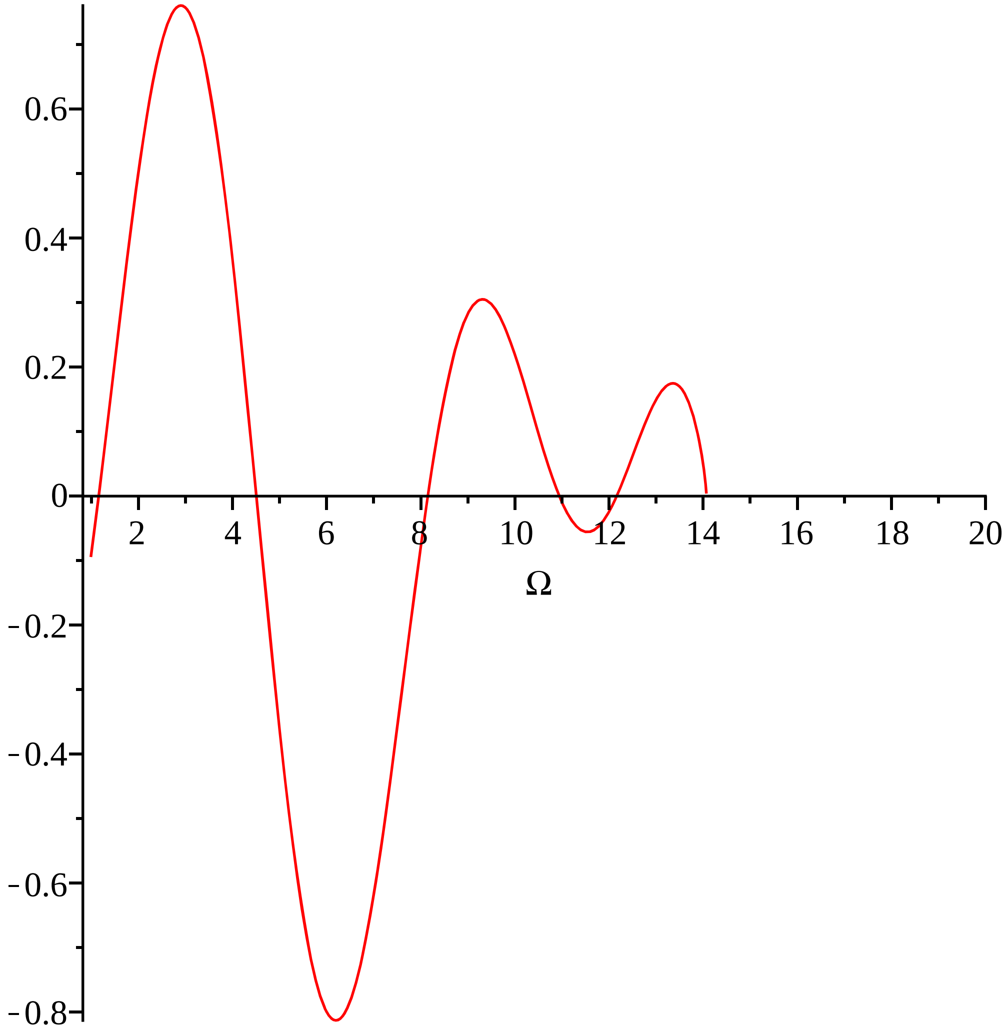

> $mode_1[99] := fsolve(B = 0, \text{Omega}, L\,..2)$:

> $mode_2[99] := fsolve(B = 0, \text{Omega}, 3\,..6)$:

> $mode_3[99] := fsolve(B = 0, \text{Omega}, 6\,..9)$:

> xi := $ran[100]$;

$$\xi := 1 \tag{11}$$

> #$plot(B, \text{Omega} = L\,..20)$;

> $mode_1[100] := fsolve(B = 0, \text{Omega}, L\,..5)$:

> $mode_2[100] := fsolve(B = 0, \text{Omega}, 3\,..6)$:

> $mode_3[100] := fsolve(B = 0, \text{Omega}, 6\,..9)$:

> $print(ran)$

(12)

$$\begin{bmatrix} \text{1 .. 100 } Vector_{row} \\ \text{Data Type: anything} \\ \text{Storage: rectangular} \\ \text{Order: Fortran\_order} \end{bmatrix} \tag{12}$$

> $print(mode_1)$

$$\begin{bmatrix} \text{1 .. 100 } Vector_{row} \\ \text{Data Type: anything} \\ \text{Storage: rectangular} \\ \text{Order: Fortran\_order} \end{bmatrix} \tag{13}$$

> $print(mode_2)$

$$\begin{bmatrix} \text{1 .. 100 } Vector_{row} \\ \text{Data Type: anything} \\ \text{Storage: rectangular} \\ \text{Order: Fortran\_order} \end{bmatrix} \tag{14}$$

> $print(mode_3)$

$$\begin{bmatrix} \text{1 .. 100 } Vector_{row} \\ \text{Data Type: anything} \\ \text{Storage: rectangular} \\ \text{Order: Fortran\_order} \end{bmatrix} \tag{15}$$

APPENDIX C

MATLAB Script Sample

```
%Michael Dean
%Torsion Wave Dispersion in Composite Cylinder with Functionally Graded
%Core and Imperfect Interface - Dispersion Curves - 3-8-13
%Ohio State University
%Spring 2013

close all
clear all
clc
format long

%%%%%%%%%%%%%%%%%%%%%%%%%%%COMPLETE%%%%%%%%%%%%%%%%%%%%%%%%%%%%%%%%%%%%%%%%%%%


%THIS DOCUMENT IS FOR ALPHA=0.1, PSI=2, ETA=1.8, LAMBDA=0.01

psi2=xlsread('psi2.xlsx');


%% F=0
wavenumber0=psi2(1,:);
mode1_0=psi2(2,:);
mode2_0=psi2(3,:);
mode3_0=psi2(4,:);

%% F=1
wavenumber1=psi2(7,:);
mode1_1=psi2(8,:);
mode2_1=psi2(9,:);
mode3_1=psi2(10,:);

%% F=10
wavenumber10=psi2(14,:);
mode1_10=psi2(15,:);
mode2_10=psi2(16,:);
mode3_10=psi2(17,:);

%% F=100
wavenumber100_1=psi2(21,:);
wavenumber100_23=psi2(24,:);
mode1_100=psi2(22,:);
mode2_100=psi2(25,:);
mode3_100=psi2(26,:);

%% Plot Modes Together for Increasing Damage
%Mode 1
figure(1)
hold on
plot(wavenumber0,mode1_0,'c','LineWidth',1)
plot(wavenumber1,mode1_1,'m','LineWidth',1)
plot(wavenumber10,mode1_10,'r','LineWidth',1)
plot(wavenumber100_1,mode1_100,'g','LineWidth',1)
legend('F=0','F=1','F=10','F=100','Location','SouthEast')
title('\lambda=0.01, \psi=2, \eta=1.8, \alpha=0.1','fontsize',10)
xlabel('\xi','fontsize',16)
```

```
ylabel('\Omega','fontsize',16)
axis([0 1 0 1.25])
%Mode 2
figure(2)
hold on
plot(wavenumber0,mode2_0,'c','LineWidth',1)
plot(wavenumber1,mode2_1,'m','LineWidth',1)
plot(wavenumber10,mode2_10,'r','LineWidth',1)
plot(wavenumber100_23,mode2_100,'g','LineWidth',1)
legend('F=0','F=1','F=10','F=100','Location','SouthEast')
title('\lambda=0.01, \psi=2, \eta=1.8, \alpha=0.1','fontsize',10)
xlabel('\xi','fontsize',16)
ylabel('\Omega','fontsize',16)
axis([0 1 0.5 5])

%Mode 3
figure(3)
hold on
plot(wavenumber0,mode3_0,'c','LineWidth',1)
plot(wavenumber1,mode3_1,'m','LineWidth',1)
plot(wavenumber10,mode3_10,'r','LineWidth',1)
plot(wavenumber100_23,mode3_100,'g','LineWidth',1)
legend('F=0','F=1','F=10','F=100','Location','SouthEast')
title('\lambda=0.01, \psi=2, \eta=1.8, \alpha=0.1','fontsize',10)
xlabel('\xi','fontsize',16)
ylabel('\Omega','fontsize',16)
axis([0 1 3.5 8.5])
```